Aus dem Medizinischen Zentrum für Innere Medizin, Schwerpunkt
Gastroenterologie und Stoffwechsel
Direktor: Prof. Dr. med. Thomas Gress
des Fachbereichs Medizin in Zusammenarbeit mit dem Universitätsklinikum Gießen
und Marburg GmbH, Standort Marburg

Molecular Characterization of Zoledronic acid Induced Growth Inhibition in Cancer

Inaugural-Dissertation zur Erlangung des Doktorgrades der gesamten Humanmedizin
dem Fachbereich Medizin der Philipps-Universität Marburg
vorgelegt von

Shiv Kishor Singh

aus Gorakhpur, India

Marburg, 2010

Angenommen vom Fachbereich Medizin der Philipps-Universität Marburg am
15.04.2010
Gedruckt mit Genehmigung des Fachbereichs
Dekan: Prof. Dr. med. Matthias Rothmund
Referent: Prof. Dr. Volker Ellenrieder
Korreferent: Prof. Dr. Rolf Müller

I dedicate my thesis to my wife Garima and my parents

Table of contents

SUMMARY I

ZUSAMMENFASSUNG III

1 INTRODUCTION 1

1.1 BISPHOSPHONATES 1

1.1.1 Background *1*

1.2 CHEMISTRY AND STRUCTURE OF BISPHOSPHONATES 2

1.3 MOLECULAR MECHANISMS OF ACTION OF NITROGEN-CONTAINING BISPHOSPHONATES 4

1.4 ANTI-TUMORIGENIC FUNCTIONS OF ZOLEDRONIC ACID 6

1.5 ZOLEDRONIC ACID AND THE CELL CYCLE MACHINERY 8

1.6 THE NFAT FAMILY OF TRANSCRIPTION FACTORS 10

2 AIMS OF THE STUDY 13

3 MATERIALS AND METHODS 14

3.1 MATERIALS 14

3.1.1 Mice *14*

3.1.2 Cell lines *14*

3.1.3 General Materials *14*

3.1.3.1 Chemicals and Reagents 15

3.1.3.2 Instruments 18

3.1.3.3 Kits 19

3.1.3.4 General materials and reagents for PCR, siRNA and site directed mutagenesis 19

3.1.3.5 Antibodies 22

3.1.4 Mediums and buffer solutions *23*

3.1.4.1 Cell biological *23*

3.1.4.2 Biochemical 24

3.1.4.3 Morphological 27

3.1.4.4 Molecular biological 27

3.2 METHODS 28

3.2.1 Cell Culture *28*

3.2.2 Plasmid constructs and transient transfection *28*

3.2.3 siRNA *29*

3.2.4 Preparation of whole protein extract from mammalian cells *29*

3.2.5 Preparation of nuclear and cytoplasmic protein extracts from mammalian cells *29*

3.2.6 Protein determination *30*

3.2.7 SDS-polyacrylamide gel electrophoresis *31*

3.2.8 Western blotting *31*

3.2.9 Proliferation Assay and Cell Cycle Analysis *32*

3.2.10 In vivo Tumor Xenograft Studies *32*
3.2.11 Real-Time PCR *33*
3.2.12 Co-Immunoprecipitation *33*
3.2.13 Immunofluorescence *34*
3.2.14 Immunohistochemistry with ABC-peroxidase method *34*
3.2.15 Ubiquitination Assays *35*
3.2.16 Luciferase Reporter Assays *35*
3.2.17 Statistical analysis *36*

4 RESULTS **37**

4.1 ZOLEDRONIC ACID INHIBITS CANCER CELL PROLIFERATION BY INDUCING G1/S PHASE ARREST 37
4.2 EFFECTS OF ZOLEDRONIC ACID, ON THE GROWTH OF IMIM-PC-1 TUMORS IN ATHYMIC NUDE MICE ... 40
4.3 NFATC2 PROMOTES G1/S-PHASE TRANSITION IN CANCER CELLS 41
4.4 ZOLEDRONIC ACID SUPPRESSES NFATC2 ACTIVITY THROUGH ENHANCED PROTEASOMAL DEGRADATION 44
4.5 HDM2 IS REQUIRED FOR ZOLEDRONIC ACID MEDIATED PROTEASOMAL DEGRADATION OF NFATC2 48
4.6 ZOLEDRONIC ACID INHIBITS GSK3β KINASE ACTIVITY AND INDUCES NUCLEAR ACCUMULATION OF HDM2 TO DEGRADE NFATC2 53
4.7 GSK3β PHOSPHORYLATION AT THREE KEY RESIDUES ELEVATES CELLULAR NFATC2 LEVELS AND RESCUES IT FROM ZOLEDRONIC ACID MEDIATED PROTEASOMAL DEGRADATION 59
4.8 THE LYSINES 684 AND 897 OF NFATC2-SPECIFIC C-TERMINUS ARE POTENT UBIQUITINATION SITES 66

5 DISCUSSION **74**

5.1 ZOLEDRONIC ACID EXERTS STRONG ANTITUMORIGENIC ACTIVITIES IN BREAST AND PANCREATIC CANCER 74
5.2 ZOLEDRONIC ACID TARGETS NFATC2 TO MEDIATE GROWTH SUPPRESSION IN CANCER 76
5.3 ZOLEDRONIC ACID DISRUPTS A NUCLEAR GSK3β NFAT STABILIZATION PATHWAY IN CANCER 78
5.4 EXISTENCE AND TARGETING OF A NUCLEAR GSK3β-NFATC2 STABILIZATION PATHWAY IN CANCER 79
5.5 CHARACTERIZATION OF ZOLEDRONIC ACID MEDIATED NFATC2 UBIQUITINATION IN CANCER 82
5.6 SIGNIFICANCE AND CONCLUSION OF THIS DISSERTATION 84

6 REFERENCES **87**

7 ABBREVIATIONS **103**

8 ACKNOWLEDGMENTS **106**

9 CURRICULUM VITAE **109**

SUMMARY

Zoledronic acid is a nitrogen-containing bisphosphonate widely used in the treatment of bone metastasis secondary to breast cancer. In addition, current clinical trials suggest direct antitumor effects, which may reduce the risk of overall disease progression in breast cancer patients. Consistently, recent experimental approaches have demonstrated strong antiproliferative and apoptotic effects in various human cancer cells, although the molecular mechanisms remained elusive.

This study was conducted to identify key mechanisms underlying the growth suppressor activity of zoledronic acid in epithelial cancer. For this purpose, we employed an extensive series of cellular, molecular as well as biochemical studies and uncovered the existence of a nuclear GSK3β-NFATc2 stabilization pathway that is target for inactivation by zoledronic acid during growth suppression. GSK3β labels nuclear NFAT through phosphorylation of three phosphoserines (Ser 215, Ser 219 and Ser 223) residues located within the N-terminal SP2 motif of the factor, and this post-translational modification protects the factor from ubiquitination and degradation. The phosphoserine sequences are highly conserved among species and are identical to the previously reported “phospho-degron” elements through which GSK3β labels other key cell cycle regulators for subsequent ubiquitination and proteasomal degradation.

Here, we show that GSK3β can make use of the “phospho-degron” elements to stabilize rather than proteolyse mitogenic transcription factors, and thus GSK3β exerts pro-proliferative functions through stabilization of NFATc2 levels in cancer. Treatment with zoledronic acid, however, inhibits GSK3β kinase activity, thus disrupts NFATc2 phosphorylation and stabilization in the nucleus, and finally allows the 26S

proteasomal machinery to target NFATc2 for degradation. Mechanistically, HDM2, the human homologue of the E3-ligase MDM2, accumulates in the nucleus upon treatment binds to NFATc2 and transfers ubiquitin to lysines K-684 and K-897. Ubiquitination of K-684 and K-897 requires an unphosphorylated status of NFATc2 in the nucleus and is key for the subsequent recognition and degradation by the 26S proteasome. The net cellular outcome of GSK3β -NFATc2 pathway disruption and degradation of the transcription factor is a progredient halt of cancer cells at the G1 cell cycle phase. Together, this study uncovers a key pathway in cancer growth control that is aimed for inactivation by zoledronic acid. From the medical point of view, we believe that these findings significantly contribute to a better understanding of the biochemical basis underlying one of the most promising and exciting new treatment for malignant disease.

ZUSAMMENFASSUNG

Bisphosphonate gehören zur Standardtherapie verschiedener Erkrankungen, die mit einem gesteigerten Osteoklasten-Stoffwechsel und einem Abbau der Matrix einhergehen. Hierzu zählen neben der Behandlung einer Osteoporose, des Morbus Paget und des malignen Myeloms v.a. osteolytische Metastasen des Brustdrüsenkrebses und anderer epithelialer Tumore. Darüber hinaus belegen Arbeiten der letzten Jahre eine starke anti-tumoröse Wirkung v.a. neuer Bisphosphonate wie z.B. Zoledronsäure, die auf einer direkten Beeinflussung der Tumorzellen beruhen. *In vitro* und *in vivo* Studien belegen eine ausgeprägte antiproliferative Funktion von Zoledronsäure in verschiedenen Tumormodellen, obgleich die zugrundeliegenden Mechanismen nur unzureichend verstanden sind. Im Rahmen der vorliegenden Untersuchung wurden in einem kombinierten *in vitro/ in vivo* Modell die molekularen Mechanismen der Zoledronsäure vermittelten Tumorsuppression im Pankreas- und Mammakarzinom analysiert. Dabei konnten wir einen interessanten Wirkmechanismus identifizieren und zeigen, dass Zoledronsäure durch Inaktivierung einer GSK3β-abhängigen NFATc2 Stabilisierung dessen proteasomalen Abbau induziert. NFATc2 ist ein zentraler Regulator der Zellzykluskontrolle und stimuliert durch transkriptionelle Regulation von Zyklinen und deren Aktivatoren die G1-Zyklus Progression in Tumorzellen. Aktives NFATc2 wird entsprechend unserer Ergebnisse im Zellkern von Tumorzellen durch GSK3β phosphoryliert und vor einer Ubiquitinylierung und Degradation geschützt. Dabei erkennt und phosphoryliert GSK3β drei Serinstellen innerhalb der N-terminalen SP2-Domäne. Zoledronsäure führt zur Hemmung von GSK3β im Zellkern und verhindert somit die schützende Phosphorylierung von NFATc2. Darüber hinaus induziert Zoledronsäure die nukleäre Akkumulation der E3-Ligase HDM2, welche unphosphoryliertes NFATc2 an

dessen C-Terminus (K-684 und K-897) ubiquitinyliert und für die nachfolgende proteasomale Degradation markiert. Zusammenfassend führten diese Untersuchungen zur erfolgreichen Identifikation eines zentralen Mechanismus der Zoledronsäure induzierten Wachstumshemmung, die auf der Inaktivierung eines wichtigen onkogenen Signalweges (GSK3β-NFATc2) beruht. Aus molekularer Sicht sind diese Ergebnisse von groβem Interesse, da sie einen bislang unbekannten Regulationsmechanismus der NFAT-Transkriptionsfaktoren beschreiben und zu einem besseren Verständnis dieser onkogenen Transkriptionsfaktoren in der Tumorbiologie beitragen. Noch relevanter dürften unsere Erkenntnisse allerdings aus medizinischer Sicht sein, da sie den Nutzen von Zoledronsäure in der Tumortherapie epithelialer Krebserkrankungen unterstützen und deren Wirksamkeit durch Identifikation eines wichtigen molekularen Ansatzes belegen.

1 INTRODUCTION

1.1 BISPHOSPHONATES

1.1.1 Background

The potential to inactivate osteoclastic bone resorption makes the third generation bisphosphonate zoledronic acid an attractive agent in the treatment of benign and malignant skeletal diseases related with increased bone loss, e.g. Paget' disease, osteoporosis and metastasis related osteolysis (Rodan et al., 2002; Russell et al., 1999). The beneficial effect of zoledronic acid in the treatment of advanced cancer diseases with osteolytic bone metastasis has extensively been demonstrated and led to a widespread use of the compound in those patients (Hughes et al., 1995). Over the past decade, zoledronic acid has become the standard therapy for breast cancer patients with established metastasis in the bone (Costa et al., 2007; Body et al., 2003). In addition to its well characterized effects on skeletal metastasis, increasing evidence from preclinical and clinical trials emphasize strong anti-tumor functions of the drug that work outside the bone and directly target the tumor cells, resulting in inhibition of tumor outgrowth, reduced incidence of visceral metastasis, and increased overall survival (Boissier et al., 2000; Pluijm et al., 1996).

A new milestone in breast cancer therapy was recently achieved by an international multi-center study in early stage cancer patients, reporting a dramatic reduction of local tumor recurrence after surgery, when endocrine therapy was combined with zoledronic acid (Gnant et al., 2009). Consistent with the clinical data, *in vitro* and *in vivo* studies identified substantial growth suppression activities of zoledronic acid in breast and other tumors of epithelial origins.

1.2 CHEMISTRY AND STRUCTURE OF BISPHOSPHONATES

Bisphosphonates (BPs) are synthetic nonhydrolyzable analogues of the naturally occurring pyrophosphate molecule. Pyrophosphate (PP_i) is produced by many anabolic processes and rapidly hydrolysed to its two constituent phosphate groups. A bisphosphonate is formed when the linking oxygen atom in the pyrophosphate molecule is replaced by a carbon atom. Therefore, these analogues are completely resistant to hydrolysis and are chemically extremely stable for binding to the hydroxyapatite crystals of bone and prevent both their growth and their dissolution.

The biological activity of the bisphosphonates can be modified by altering the structure of the two side chains on the carbon atom and those two chains (referred to as R_1 and R_2) are covalently bound to the carbon atom of the common P–C–P structure. In addition, binding to bone mineral depends upon the P-C-P structure and is enhanced by including a hydroxyl group at R_1, allow BPs to bind to bone mineral.

The structure and three-dimensional configuration of the R_2 side chain determines the cellular effects of bisphosphonates (Fig. 1), and their relative efficacies as inhibitors of bone resorption as well as that imparts the ability to bind divalent metal ions, such as Ca^{2+}. For this cause, BPs are rapidly cleared from the circulation (Russell et al., 1999). BPs, such as etidronate, clodronate or tiludronate, which lack a nitrogen functional group in R_2 chain, inhibit essential ATP-dependent intracellular enzymes which leads to an intracellular accumulation of cytotoxic ATP-analogues (Rogers et al., 2003).

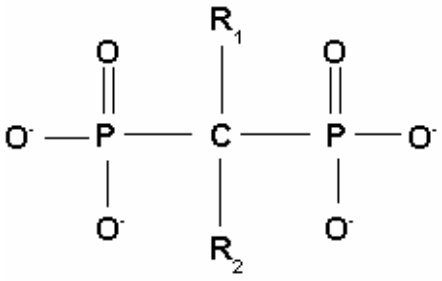

Fig. 1. Basic chemical structure of Bisphosphonates. The two phosphonate (PO_3) groups covalently linked to carbon determine both the name "bisphosphonate" and the function of the drugs. The long side chain (R_2 in the diagram) determines the chemical properties, the mode of action and the strength of bisphosphonate drugs. The short side chain (R_1), often called the 'hook', mainly influences chemical properties and pharmacokinetics.

Nitrogen-containing bisphosphonates or amino bisphosphonates, such as zoledronic acid are more potent at inhibiting bone resorption *in vivo*. The increased inhibitory potency of N-BPs results from structural differences that affect anti-resorptive capacities of the drug (e.g., pamidronate, risedronate, alendronate, minodronate, ibandronate and zoledronate or zoledronic acid). The most potent bisphosphonates are those containing a tertiary amine within a ring structure, such as zoledronic acid (Fig. 2).

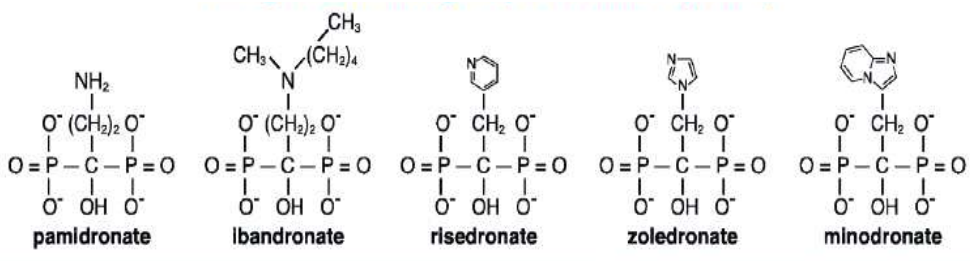

Fig. 2. Chemical structures of Nitrogen-containing bisphosphonates. Structure and conformation of the R^2 side chain of Nitrogen-containing bisphosphonates (adapted from Clezardin et al., 2005)

1.3 MOLECULAR MECHANISMS OF ACTION OF NITROGEN-CONTAINING BISPHOSPHONATES

Nitrogen-containing bisphosphonates act by inhibiting farnesyl pyrophosphate synthase (FPPS). Among these BPs, zoledronic acid and the structurally similar minodronate are extremely potent inhibitors of FPPS and inhibit the enzyme even at picomolar concentrations in osteoclasts (Dunford et al., 2001) (Fig. 3). FPPS is a key regulatory enzyme in the mevalonate pathway. This pathway, ubiquitous in mammalian cells, provides essential lipid molecules, such as cholesterol and isoprenoids, with the later necessary for post-translational prenylation of small GTPases, such as those of the Ras, Rho, Rac, Rab and Cdc42 (Rogers et al., 2003; Dunford et al., 2001; Coxon et al., 2003). These proteins are major players in a variety of cellular processes that are required for osteoclast functions.

Blocking this pathway by using N-BPs, induce severe morphologic changes in osteoclasts and interfere with various intracellular processes such as cytoskeleton reorganization, vesicle transport, exocytosis and ultimately leading to apoptosis (Coxon et al., 2003). Inhibition of the mevalonate pathway and loss of prenylated proteins, particularly geranylgeranylated small GTPases, seem to be the major mechanism of action of N-BPs in osteoclasts because bypassing inhibition of FPP synthase and replenishing cells with an isoprenoid lipid substrate that restores geranylgeranylation can overcome the effects of N-BPs on osteoclast formation, apoptosis, and bone resorption (Reszka et al., 1999; Fisher et al., 1999; van Beek et al., 2003). The blockade of this pathway is a concept that has found widespread clinical use, with statins as drugs that inhibit HMG-CoA reductase (HMGCR) and reduce cholesterol biosynthesis, and nitrogen-containing bisphosphonates (N-BPs) as drugs for osteoporosis therapy that target FPPS and inhibit protein prenylation.

FPP synthase inhibition in osteoclast might also play a central role in bone metastasis (Clezardin et al., 2005; Dunford et al., 2001). Infact, several reports suggest that FPPS inactivation probably via modification of the bone matrix affect the ability of tumor cells to infiltrate the bone and to establish metastasis (Sasaki et al., 1998; Sasaki et al., 1999; Green et al., 2000). In contrast, only very scarce information is available in the literature showing how bisphosphonates affect the tumor cells (see detailed information below). The current literature however, suggest that BPs such as zoledronic acid primarily target signaling and transcription pathways other than the FPPS system outside the bone metabolism.

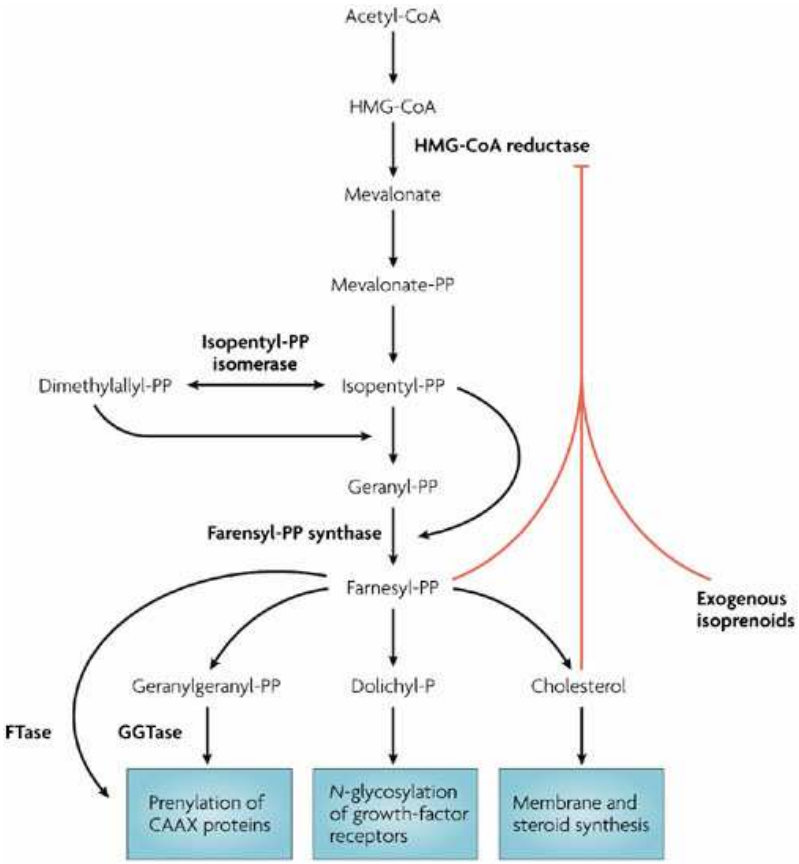

Fig. 3. Mechanisms of action of Nitrogen-containing bisphosphonates. 3-hydroxy 3-methylglutaryl-CoA (HMG-CoA) is converted to mevalonate by HMG-CoA reductase, the rate-limiting enzyme at the apex of the mevalonate pathway. Mevalonate is then converted to isopentyl pyrophosphate (isopentyl-PP; the 5-carbon basic isoprene unit), which is subsequently converted to farsenyl pyrophosphate (farsenyl-PP; a 15-carbon isoprenoid) through a series of enzymatic reactions. After addition of isopentyl-PP,

farsenyl-PP can be converted to geranylgeranyl pyrophosphate (geranylgernayl-PP; a 20-carbon isoprenoid), or alternatively farsenyl-PP can be converted to cholesterol or dolichol phosphate (dolichol-P), which is used for N-glycosylation of growth factor receptors such as insulin-like growth factor receptor. HMG-CoA reductase is the target of the cholesterol-lowering statins, whereas isopentenyl-PP isomerase and farsenyl-PP synthase are targets of bisphosphonates (adapted from Panagiotis et al., 2005)

1.4 ANTI-TUMORIGENIC FUNCTIONS OF ZOLEDRONIC ACID

Numerous approaches using diverse tumor types and models have been used to elucidate the effects of zoledronic acid, and other N-BPs, on tumor cells and their interaction with surrounding structures, apart from those mediated by osteoclast activity. Increasing evidence is accumulating that N-BPs are able to directly affect tumor cells. For instance, it has been shown that N-BP inhibit cell proliferation in myeloma, breast, prostate, skin and pancreatic cancer, in a concentration- and time-dependent manner (Shipman et al., 1997; Tassone et al., 2002; Clezardin et al., 2005 et al., Ying-Ying Lia et al., 2008; Sewing et al., 2008; Rachner et al., 2009).

The pioneering studies by Shipman et al. were the first to demonstrate direct antitumor activity of bisphosphonate in myeloma cell lines (Shipman et al., 1997; Shipman et al., 1998) and these promising studies were subsequently confirmed and extended by other groups using different models and different members of the bisphosphonate family (Aparicio et al., 1998). Overall the results clearly demonstrated that zoledronic acid reduces cell proliferation in epithelial tumors through induction of a cell cycle arrest and initiation of programmed cell death, called apoptosis. In some tumor cells, the growth inhibiting effect of bisphosphonates can partially be rescued through adding of geranylgeraniol and farsenyl, two intermediates of the mevalonate pathway (Shipman et al., 1998), although recent studies emphasize the presence of FPPS independent signaling

pathways that confer growth inhibition upon treatment with bisphosphonates. Similar to the situation in melanoma cells, BPs have been shown to block proliferation in breast and pancreatic cancer *in vitro* (Senaratne et al., 2000; Tassone et al., 2002), through aiming on the cell cycle machinery (Benassi et al., 2007; Sewing et al., 2008; Romani et al., 2009). The third generation nitrogen containing BPs, zoledronic acid has proven to be the most attractive and potent inhibitor of tumor cell proliferation. In addition, it also affects tumor cell migration and invasion in different systems (Magnetto et al., 1999; Boissier et al., 2000; Virtanen et al., 2002).

Recently, considerable progress have been made in elucidating the anti-tumorigenic functions of N-BPs in animal models. The potent N-BPs have been shown to inhibit skeletal metastasis and reduce tumor burden in animal models of breast, lung and prostate cancer (Green et al., 2004; Giraudo et al., 2004; Croucher et al., 2003; Santini et al., 2003; Santini et al., 2006). In addition, it also decreases the release of tumor-promoting growth factors from bone by inhibiting osteoclast-mediated bone resorption (Hall et al., 1994; Alvarez et al., 2000; Duivenvoorden et al., 2007; Florence et al., 2007; Ottewell et al., 2008; Lia et al., *2007;* Stearns et al., 1996; Pollar et al., 1985; Corey et al., 2001).

A separate but equally important phenotype in carcinoma progression is invasive migration, a process which eventually leads to metastatic dissemination of tumor cells to distant organs. Recent studies suggested that, zoledronic acid blocks tumor cell proliferation and migration of breast cancer cells in immunocompromised mice (Green et al., 2004; Giraudo et al., 2004; Croucher et al., 2003; Santini et al., 2003; Santini et al., 2006; Holen et al., 2009; Clezardin et al., 2005; Korpal et al., 2009). Recently, it has also been shown that zoledronic acid inhibits tumor growth and induces apoptosis in prostate cancer following inoculation of tumor cell in

a xenograft mice model (Caraglia et al., 2006). Importantly, several new studies provide evidence for additive or synergistic apoptotic effects of zoledronic acid in combination with a variety of standard anti-neoplastic agents, including paclitaxel, gemcitabine and doxorubicin (Jagdev et al., 2001; Ullen et al., 2003; Neville et al., 2005; Vogt et al., 2004; Matsumoto et al., 2005). For instance, sequential treatment with doxorubicin followed by zoledronic acid inhibited the growth of subcutaneous breast tumors *in vivo* (Ottewell et al., 2009). It has also been shown that zoledronic acid possess synergistic anti tumorogenic activity in combination with imanitib and paclitaxel by substantially improving the survival of mice bearing prostate and breast cancer cells (Kim et al., 2005).

Together, there is now growing evidence indicating that bisphosphonate and particularly zoledronic acid can directly target the tumor cell to suppress cancer growth, alone or in combination with chemotherapy.

1.5 ZOLEDRONIC ACID AND THE CELL CYCLE MACHINERY

Depending on the tumor type, zoledronic acid has been shown to disrupt cell cycle progression in tumor cells at various stages. The mammalian cell cycle consists of four phases, designated G1, S, G2 and M phase (Norbury et al., 1992). During each cell cycle, the complete genome is duplicated in S phase (the synthetic phase), and subsequently the two copies divided over two daughter cells in M phase (mitotic phase). Authorization for DNA synthesis and chromosomes segregation is tightly controlled by cyclins and their associated kinase activities that become active during the gap-phases G1 and G2, proceeding S and M phase, respectively (Fig. 4) (Nurse et al., 1999). D-type cyclins and their partners kinases CDK4 and CDK6 are key regulators in G1/S transition, while cyclin A and cyclin B1 activity is

essential for entry from G2 into M phase. These cyclins are well known targets of mitogenic and anti-mitogenic input signals, which can stimulate or block cell cycle progression. An important barrier to limitless proliferation is raised by a cell cycle control mechanism that prevents G1/S transition (heart of the cell cycle machinery) in response to growth-inhibiting stimuli like differentiation, DNA damage, oncogene, oncogene activation, loss of anchorage, confluency or mitogen deprivation. Loss of G1/ S control clearly is a mandatory step in tumor development and is associated with imbalanced and uncontrolled cell proliferation (Dannenberg et al., 2004). Recently, It has been also suggested that zoledronic acid can act at different levels and cell cycle stages. For instance, a profound cell cycle arrest in G2 phase was seen in osteosarcoma cells after exposure of zoledronic acid (Benassi et al., 2007).

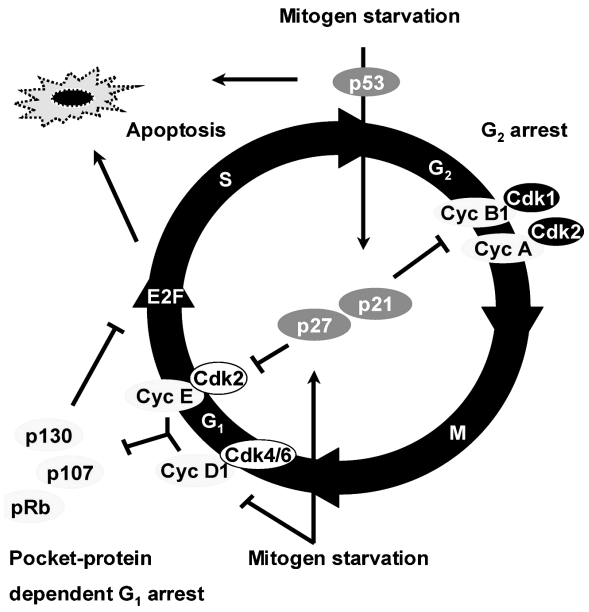

Fig. 4. Schematic representation of cell cycle. This simplified schematic representation of the cell cycle includes the main molecular participants that are involved in cell-cycle progression (adapted from Dannenberg et al., 2004)

However, most recent evidence also suggests that zoledronic acid particularly affects the G1 cell cycle phase and impairs progression to the DNA replicating S-phase in epithelial cancer (Fromigue et al., 2000; Jonathan et al., 2003). In fact, it has been shown that zoledronic acid targets colon cancer cells at G1 and blocks progression of the cell cycle (Sewing et al., 2008). Together, the current literature is not yet conclusive and therefore, detailed analysis are required to elucidate how zoledronic acid targets the cell cycle in a tumor specific manner.

1.6 THE NFAT FAMILY OF TRANSCRIPTION FACTORS

Cell cycle progression is tightly controlled by the action of mitogenic and anti-proliferative signaling and transcription pathways. Among others, the NFAT transcription factor family has key functions in cell cycle stimulation and not surprisingly exerts pro-proliferative activities in a variety of cancers. The nuclear factor of activated T cells (NFAT) signaling axis is a vertebrate-specific signaling and transcription pathway that controls various vital cellular functions through its ability to regulate gene expression (Crabtree et al., 2002; Im et al., 2004). The canonical NFAT pathway, first elucidated in immune cells, is activated through a raise in intracellular calcium through either increased flux from endoplasmic reticulum stores or activation of store-operated channels in the plasma membrane (Crabtree et al., 1999; Crabtree et al., 2002). In the basal state, NFATs are hyper-phosphorylated in the cytoplasm. Subsequent to cell stimulation and calcium release, NFATs are dephosphorylated by the phosphatase calcineurin and translocate to the nucleus (Luo et al., 1996), where they co-operate with other factors and co-activators to promote *de novo* gene transcription.

The foundation of the NFAT research field was based on the original discovery that NFATs are inducible nuclear factors bound to the

interleukin-2 (IL-2) promoter during the activation of T cells (Shaw et al., 1988). The importance of NFAT signaling is also highlighted by the fact that immunosuppressants such as cyclosporin A (CsA) and FK506, which specifically inactivate the canonical NFAT pathway, are widely used in the clinic to prevent organ transplant rejection. Since their discovery two decades ago, it has become increasingly clear that NFAT transcription factors are expressed not only in immune cells but in all cells and tissues (Crabtree et al., 2002; Im et al., 2004). In this context, several recent key findings have pointed to important roles for NFATs in modulating phenotypes associated with malignancy and tumor progression (Jauliac et al., 2002; Yoeli-lerner et al., 2005). NFAT isoforms are overexpressed in human solid tumors and haematological malignancies and seem to have roles in cancer cell-autonomous functions such as proliferation, invasive migration, differentiation and the survival of cells in the tumor and its microenvironment (Jauliac et al., 2002; Buchholz et al., 2006). It is thought that understanding the parts played by NFATs in tumor progression will help the development of effective therapeutics that target the NFAT pathway in cancer progression and metastasis. In fact, overexpression of NFAT have been described in various human breast, colon and pancreatic cancers and cell lines, and in particular in those with a aggressively growing phenotype (Jauliac et al., 2002; Chen et al., 2005; Yiu et al., 2006; Buchholz et al., 2006). NFATc1 and NFATc2 regulate the expression of cell cycle promoting genes as well genes that stimulate angiogenesis, migration and invasion, and thus targeting of these factors might be a promising new strategy in cancer (Caetano et al., 2002; Baksh et al., 2002; Graef et al., 2003; Buchholz et al., 2006).

Based on these findings in tumor diseases, one would predict that as potent calcineurin–NFAT inhibitors, both CsA and FK506 could be effective cancer therapeutics. Somewhat paradoxically, there is actually a significant increase in cancer incidence in patients on long-term immunosuppressive

treatments (Dantal et al, NEJM 2005). The explanation for this observation is twofold: first, the increased cancer incidence is probably due to decreased immune surveillance; second, other targets of calcineurin exist that function to modulate phenotypes associated with cancer, such as proliferation and survival. Moreover systemic administration of CsA and FK506 would affect the entire milieu of the tumor microenvironment, with pleiotropic effects on cellular pathophysiology. It is more reasonable to assume that effective NFAT therapy in cancer will have to come from targeted therapy for the tumor endothelium or the tumor cells themselves, as these are the primary compartments in which attenuation of NFAT activity is predicted to block or even reverse the tumorigenic phenotype.

2 AIMS OF THE STUDY

Bisphosphonates are proven to be effective in the treatment of benign or malignant skeletal diseases characterized by enhanced osteoclastic bone resorption. Nitrogen-containing bisphosphonates have also been demonstrated to exhibit direct anti-tumor effects. They not only inhibit proliferation and induce apoptosis in cultured cancer cells, but also additionally interfere with adhesion of cancer cells to the bone matrix and inhibit cell migration and invasion. Zoledronic acid is a highly potent N-BP that has been particularly well investigated, preclinical and in clinical practice. Growing preclinical evidence shows that zoledronic acid also exhibits direct anti-tumor activity in breast and other tumor of epithelial origins.

The overall effects on tumor cells appear to be mediated via diverse pathways, such as growth inhibition, cell cycle arrest and apoptosis. However, the molecular mechanisms underlying zoledronic acid mediated anti-tumor effects are only partially understood.

In previous work, we have demonstrated the pro-proliferative functions of NFAT transcription factors in cancer. Here, we questioned whether and how zoledronic acid targets the NFAT signaling and transcription pathway to mediate its growth suppressor function in breast and pancreatic cancer.

In particular, we addressed the following questions:

1. Does zoledronic acid suppress tumor growth *in vitro* and *in vivo*?
2. Does zoledronic acid target the oncogenic NFATc2 pathway in cancer cells?
3. Does zoledronic acid interfere with NFAT activity, distribution and stability in cancer?

3 MATERIALS AND METHODS

3.1 MATERIALS

3.1.1 Mice

6 to 8 weeks old pathogen-free female athymic nu/nu mice were obtained from Harlan Winkelman (Harlan Winkelman GmbH, Borchen, Germany). They were kept in the animal care facility of University hospital of Marburg, institutional guidelines were followed in handling mice throughout the course of the study.

3.1.2 Cell lines

The list of cell lines used in this study:

1. MDA-MB-231 (Breast cancer cell line)
2. MDA-MB-435 (Breast cancer cell line)
3. MDA-MB-468 (Breast cancer cell line)
4. IMIM-PC-1 (Pancreatic cancer cell line)
5. PaTu8988t (Pancreatic cancer cell line)

3.1.3 General Materials

Reagent	**Source**
Cell strainer (70 µl)	Greiner bio-one
2 ml cryotubes	Greiner bio-one
Disposable needles, cuvettes & syringes	Greiner bio-one

Glassware	Schott
Nitrocellulose membrane	Schleicher & Schuell
Polypropylene tubes	Greiner bio-one
Parafilm	Greiner bio-one
Pipette tips	Eppendorf
Pipettes	Sarstedt
Röntgen film (13x18 cm, BioMax)	Kodak
Sterile filters (0.2 µM/ 0.45 µM)	Schleicher & Schuell
Tissue culture plates	Greiner bio-one
Tissue culture flask (50, 250, 500 ml)	Greiner bio-one
Tissue culture dish (60 mm, 90 mm)	Greiner bio-one
Tubes (1.5 & 2 ml)	Eppendorf
Whatmann paper	Schleicher & Schuell
12 well cell culture plates	Cellstar
6 & 24 well cell culture plates	Cellstar
6 mm Petri dishes	Cellstar
T-25, T-75 & T-250 tissue culture flasks	Nunc

3.1.3.1 Chemicals and Reagents

Name of the chemical s	**Source**
Acetone	Carl Roth
Acrylamid solution	Carl Roth
Agar-Agar	Carl Roth
Agarose	Sigma-Aldrich
Ampicillin	Hoechst
APS Merck	Eurolab
β-mercaptoethanol	Carl Roth
BioRad protein assay	BioRad
Bromophenol blue	Eurolab
Bovine serum albumin (BSA)	Sigma

Calcium chloride	Carl Roth
Complete protease inhibitor	Roche
ECL chemiluminescence kit	Pierce
dNTPs	MBI-Fermentas
DTT	Carl Roth
ECL Chemiluminiscence Kit	Roche
EDTA	Carl Roth
EGTA	Sigma-Aldrich
Ethanol	Carl Roth
Ethidium bromide	Sigma-Aldrich
Formaldehyde	Carl Roth
Forskolin	Calbiochem
ECL chemiluminescence kit	Pierce
Gene Ruler™ 100bp ladder	MBI Fermentas
Glycerin (87%)	Carl Roth
Glycine	Carl Roth
Hepes	Carl Roth
Hydrochloric acid	Merck
Isoamylalcohol	Carl Roth
Isopropanol	Carl Roth
Leupeptin hydrochloride	Roche
Milk powder	Sigma
Magnesium acetate	Sigma-Aldrich
Magnesium chloride	Carl Roth
Magnesium sulfate	Carl Roth
Manganese chloride	Fluka
Methanol	Carl Roth
PCR purification kit	Qiagen
Phenol [C_6H_6O, TE equilibrated]	Carl Roth
Plasmid-DNA isolation kit (Maxi)	Qiagen
PMSF	Serva

Proteinase K	SIGMA-Aldrich
Protein A sepharose	Upstate
Protein G sepharose	Upstate
Polyacrylamide	Applichem
Ponceau Red	Sigma Aldrich
Potassium acetate	Carl Roth
Potassium chloride	Sigma-Aldrich
Potassium dihydrogen phosphate	Sigma-Aldrich
Potassium hydrogen phosphate	Sigma-Aldrich
Potassium hydroxide	Carl Roth
Propidiumiodide	Sigma Aldrich
Protease inhibitor tablet (complete mini)	Roche
Sodium azide	Sigma
Sodium citrate	Sigma
Sodium chloride	Roth
Sodiumdodecyl sulfate (SDS)	Roth
Sodium acetate	Merck Eurolab
Sodium carbonate	Carl Roth
Sodium chloride	Carl Roth
Sodium fluoride	Sigma-Aldrich
Sodium hydrogen phosphate	Merck Eurolab
Sodium hydroxide	Carl Roth
TEMED	Carl Roth
Tris	Carl Roth
Triton X-100	Aldrich
Tween 20	Carl Roth
Western blotting substrate (Lumi light)	Bio-Rad

Drug	Source
Zoledronic acid (ZOL) [2-(imidazol-1-yl)-hydroxy-ethylidene-1, 1-bisphosphonic acid, disodium salt, 4.75 hydrate]	Novartis-Pharma

Radioactive chemical	Source
[methyl-^{3}H] Thymidine 50Ci/mmol 1mCi/ml	Amersham Biosciences

3.1.3.2 Instruments

Hardware	Manufacturer
Autoclave	Stiefenhofer
Bacterial shaker	New Brunswick scientific
Balance machine	Sartorius
Cold centrifuge	Eppendorf
FACS Calibur	Becton Dickinson
Gel camera	Stratagene
Heating blocks	Eppendorf
Ice machines	Genheimer
Laminar hoods	Heraeus
Liquid nitrogen tank	Tec-lab
Luminometer	Berthold
Micro liter pipettes	Eppendorf
Microcentrifuge	Eppendorf
Microscope	Ziess
pH meter	Ingold

Refrigerators (-20°C; -80°C)	Privileg and Bosch
Ro shaking incubator	Eppendorf
Spectrophotometer	Amersham Pharmacia
Vortexer	Eppendorf
Water bath	Eppendorf
Western blot apparatus	Hoefer
Real-Time RCR machine	ABI Prism 7000
DL Ready™ Luminometer	Berthold Technologies

3.1.3.3 Kits

Qiagen RNA isolation Kit	Qiagen
Luciferase assay kit	Promega
Site-directed mutagenesis kit	Strategene
Qiagen Miniprep kit	Qiagen
Qiagen Gel Extraction Kit	Qiagen
Qiagen PCR purification kit	Qiagen
cDNA synthesis kit	Invitrogen

3.1.3.4 General materials and reagents for PCR, siRNA and site directed mutagenesis

Primers for real-time PCR

NFATc2:

Forward 5'-gttcctaccccacagtcattcag-3'

Reverse 5'-cccgcaggtaatacttccttttg-3'

XS-13:

Forward 5`-gtcggaggagtcggacgag-3'

Reverse 5`-gcctttatttccttgttttgcaaa-3`

Cyclophilin A:

Forward 5’-caccgtgttcttcgacatca3’

Reverse 5’-agca tttgccatggacaagat3’

PCR reagents

dNTPs	MBI Fermentas
MgCl2	MBI Fermentas
10x buffer	MBI Fermentas
Taq polymerase	MBI Fermentas

Transfection Reagent	**Source**
Transfast for plasmid transfection	Promega
Effectene for plasmid transfection	Qiagen
Transmessenger for siRNA transfection	Qiagen
Lipofectamine for siRNA transfection	Invitrogen
SilentFect for siRNA transfection	Bio-Rad

siRNAs applied in this dissertation

NFATc2

#2- 5’gcugaugagcggauccuuatt3’

#3- 5’ccauuaaacaggagcagaatt3’

HDM2

#1- 5’ ccacaaaucugauaguauuu 3’,

#2- 5’gaugagguauaucaaguuauu 3’

GSK3β - (SMARTpool siRNA)

Expression vectors applied in this dissertation

Mammalian expression vectors	**Epitope tags**
wt-NFATc2 (pcDNA3.1)	HA
NFATc2- ΔSP-2 (pcDNA3.1)	HA
NFATc2- pSP-2 (pcDNA3.1)	HA
NFATc2- K684R (pcDNA3.1)	HA
NFATc2- K684/897R (pcDNA3.1)	HA
NFATc2- ΔSP-2 – K684/897R (pcDNA3.1)	HA
NFATc2 –1-460 (pcDNA3.1)	HA
c.a. GSK3β (pcDNA3.1)	HA
Sumo-1 (pcDNA3.1)	Flag
Ubc-9 (pcDNA3.1)	Flag
HDM2 (pcDNA3.1)	Flag
pcDNA 3.1 (control vector)	HA
GFP (control vector)	GFP

Site-directed mutagenesis primers used in this work

Mutation of Lysine 684 to Arginine

For. 5’-cctgccatcaggacagagcccagc-3’

Rev. 5’- gctgggctctgtcctgatggcagggac-3’

Mutation of Lysine 897 to Arginine

For. 5’ -ggagtgaccgtcagacaggaacag-3’

Rev. 5’-ctgttcctgtctgacggtcactcc-3’

Mutation of Ser215 and Ser219 to Alanine

For. 5’-gctcattatgcccccagaaccgctccaataatg-3’

Rev. 5’-cgagtaatacgggggtcttggcgaggttattac-3'

Mutation of Ser223 in Alanine in existing mutant S 215/219 A

For. 5'-ccgctccaataatggcacctcgaaccagcc-3'

Rev. 5'-ggctggttcgaggtgccattattggagcgg-3'

Mutation of ΔSP2 mutant (S 215/219 A) to Aspartic acid

For. 5'-gctcattatgaccccagaaccgatccaataatg-3'

Rev. 5'-cattattggatcggttctggggtcataatgagc-3'

Mutation of Ser223 to Aspartic acid in existing mutant ΔSP2 (S 215/219 E)

For. 5'-ccgatccaataatggaacctcgaaccagcc-3'

Rev. 5'-ggctggttcgaggttccattattggatcgg-3'

C-terminus deletion of NFATc2 (NFATc2-1-460)

For. 5'- gag aac aag cct ctg ggg ctt tag atc ttc 3'

Rev. 5' gaa gat cta aag ccc cag agg ctt gtt ctc 3'

3.1.3.5 Antibodies

List of antibodies used in various methods: Co-immunoprecipitation, immunofluroscence, and Western blots

Antibodies	Dilutions	Source
Mouse anti-mouse NFATc2	1:500	Santa Cruz
Mouse anti-mouse HDM2	1:500	Santa Cruz
Mouse anti-mouse Sumo-1	1:500	Santa Cruz
Mouse anti-mouse p53	1:500	Santa Cruz
Mouse anti-mouse CycninD1	1:1000	Cell Signaling
Mouse anti-mouse CDK4	1:1,000	Cell Signaling
Mouse anti-mouse CDK6	1:1,000	Cell Signaling

Mouse anti-mouse β-actin	1:10,000	Cell Signaling
Rabbit anti-mouse Lamin A/C	1:1,000	Cell Signaling
Rabbit anti-mouse GSK3β	1:1,000	Cell Signaling
Rabbit anti-mouse phopho--Glycogen synthase	1:1,000	Cell Signaling
Mouse anti-mouse HA	1:1,000	Cell Signaling
Mouse anti-mouse FLAG	1:1,000	Roche
Mouse anti-mouse GFP	1:1,000	Roche
Rabbit anti-mouse Ubiquitin	1:1,000	Biomol
Rabbit anti-mouse ORC	1:1,000	Upstate

3.1.4 Mediums and buffer solutions

All chemicals of molecular biology research grade were procured from respective manufacturers and all solutions were prepared using pure distilled (Milli-Q grade) autoclaved water. Wherever necessary, solutions were sterile filtered or autoclaved.

3.1.4.1 Cell biological

PBS (Phosphate buffered saline)

8 g	NaCl
0.2 g	KCl
1.44 g	Na_2HPO_4
0.24 g	KH_2PO_4

Dissolve in 800 ml dH_2O, adjust pH to 7.4 with HCl

Volume adjust to 1 L, autoclave and stored at RT

Reagents	**Source**
DMEM medium	Invitrogen

L-Glutamin (0.07%)	GIBCO
Na-Pyruvat (1 mM)	GIBCO
β-Mercaptoethanol (0.05 mM)	GIBCO
MEM (non-essential amino acids) (1%)	GIBCO
Penicillin (100 U/ml)	GIBCO
Streptomycin (100 U/ml)	Fatol
FCS (fetal calf serum) (1-10%)	GIBC0

3.1.4.2 Biochemical

SDS-PAGE

Composition of SDS-Polyacrylamide gels: Resolving Gel

Component volumes (ml) per 10 ml gel mix for 8% to 12%

H_2O 3.3 - 4.6 ml

30% acrylamide mix 2.7 ml - 4.0 ml

1.5 M Tris (pH 8.8) 2.5 ml

10% SDS 0.1 ml

10% ammonium persulfate 0.1 ml

TEMED 0.004 ml

Stacking Gel

Component volumes (ml) per 3 ml gel mix for 10% to 15%

H_2O 2.1 ml

30% acrylamide mix 0.5 ml

1.0 M Tris (pH 6.8) 0.38 ml

10% SDS 0.03 ml

10% ammonium persulfate 0.03 ml

TEMED 0.003 ml

Protein Loading Buffer (1X SDS gel loading buffer)

50 mM Tris-Cl (pH 6.8)

100 mM Dithiothreitol

2% SDS

0.1% Bromophenol blue

10% Glycerol

Gel Running Buffer: (10X)

144.13 g Glycine

30.3 g Tris

100 ml 10% SDS

Volume adjusted to 1 L with dH_2O

Protein transfer buffer: (10X)

145 g Glycine

29 g Tris

volume adjusted to 1 L with dH_2O

Blocking Solution

5% (w/v) nonfat dried milk in TBS/0.1% Tween

Agarose gel electrophoresis

TBE buffer (1x):

10.8 g	Tris
5.5 g	Boric acid
0.37 g	EDTA
add	1 L H_2O

DNA Loading Buffer

0.25% Bromophenol blue

0.25% Xylene Cyanol FF

30% Glycerol in water

1% Agarose Gel:

1.5 g Agarose

150 ml 1x TBE buffer

Boil and add 4 µl Ethidium bromide (10 mg/ml)

Cell extract preparation

Whole cell extract (WCE) buffer:

5mM Tris HCL, pH7.4

150 mM NaCl

1 mM EDTA

1% Triton X-100

Protease inhibitor cocktail was added immediately before use

.

Cellular Fractionation Buffer

For cytoplasmic protein:

10 mM Hepes, pH 7.9

10 mM KCl

0.1 mM EDTA

0.1 mM EGTA

0.1 M DTT

For nuclear protein

20 mM Hepes, pH 7.9

0.4 M NaCl

1 mM EDTA

1 mM EGTA

0.1 M DTT

Protease inhibitor cocktail was added immediately before use

Cell lysis buffer for IP

5 mM Tris HCL, pH7.4

150 mM NaCl

1 mM EDTA

1% Triton X-100

(10X) wash buffer for IP

0.5 M Tris HCL, pH 7.4, 1.5 M NaCl

Protease inhibitor cocktail was added immediately before use

3.1.4.3 Morphological

Buffers for immunofluorescence

Fixing solution

4% formaldehyde in PBS

Permeabilization solution

0.2% Triton X-100 in PBS

Blocking solution

10% FCS in PBS (1:20)

3.1.4.4 Molecular biological

Restriction enzymes and buffers

Reagent	**Source**
Bam HI	BioLabs
EcoRI	BioLabs
Hind III-	BioLabs
Not I	BioLabs
Xho I	BioLabs
Ligase, T4	BioLabs
DNA polymerase, T4	BioLabs
DNA polymerase, Klenow	BioLabs
DNA Ladder, 1 kb	BioLabs
DNA Ladder, 100 bp	BioLabs
Phosphatase, calf intestinal (CIP)	BioLabs
Phosphatase, shrimp alkaline (SAP)	Promega
TAE buffer, 10X	Sigma

3.2 METHODS

3.2.1 Cell Culture

MDA-MB-231, MDA-MB-435, MDA-MB-468, PaTu8988t, and IMIM-PC-1 cell lines were purchased from ATCC (Manassas, Virginia, USA) and supplemented with 10% FCS in DMEM (Invitrogen, Karlsruhe, Germany). Cells were treated with 10-25 µM of zoledronic acid and harvested at indicated time points. All cell lines were found to be free of mycoplasma infection on repeated PCR screens.

3.2.2 Plasmid constructs and transient transfection

Flag-Sumo-1 and Ubc-9 expression constructs were provided by Dr. Guntrum Suske (Institute of Molecular and Tumor Biology, Marburg, Germany). Mouse NFATc2 and HDM2 constructs were generated in pcDNA3.1 (+) by sequential sub cloning of the HA-NFATc2 and HDM2 open reading frame into HindIII–XbaI and BamHI-XhoI. All mutations and deletions in NFATc2 were generated by site-directed mutagenesis and verified by DNA sequencing. The ΔSP2 (S 215/219/223 A) mutation was produced by mutating Serine 215, 219 and 223 to Alanine residues. The phospho mimicking (pSP2) mutation was produced by mutating existing mutant ΔSP-2 Alanine 215, 219, 223 to Aspartic acid. The K684/897R mutation was produced by mutating Lysine 684 and 897 to Arginine. For transient transfection MDA-MB-231, MDA-MB-435, cells were transfected by using the effectene transfection reagent (Qiagen) and PaTu8988 and IMIM-PC-1 cells were transfected with Transfast (Promega) according to the manufacturer's instructions.

3.2.3 siRNA

Small interfering RNA (siRNA) was transfected using the Lipofectamine (Invitrogen) in MDA-MB-435 and MDA-MB-231 cells and TransmessengerTM reagent (Qiagen) in PaTu8988 and IMIM-PC-1 cells according to the manufacturer's instructions. The specific siRNAs were purchased from Ambion Applied Biosystems (Austin, TX, USA) with the following sequences. siRNA against HDM2 and the SMARTpool siRNA against GSK3β was purchased from Dharmacon. As a negative control, the silencer negative control was purchased from Ambion.

3.2.4 Preparation of whole protein extract from mammalian cells

Cells were washed with ice cold PBS and then scraped in whole cell extract buffer. Then transferred them into 1.5 ml tubes. Kept on ice for 30 min to 1 h. Cells were disrupted by two times freezing and thawing on dry ice or passing the cell suspension through 26 gauge needle 10 times and incubated for further 10 min. The cell suspension was centrifuged at 15,000 rpm for 30 min at 4°C and supernatant was saved as whole cell extract in another 1.5 ml tube, which was stored for future use at -20°C. The protein concentration of the supernatant was determined by Bio-Rad protein assay.

3.2.5 Preparation of nuclear and cytoplasmic protein extracts from mammalian cells

Cells were washed and scraped in cold PBS. Transferred them into 1.5 ml tube and centrifuge at 1500 rpm for 5 min at 4°C to remove the

supernatant. The pellet was resuspended in 200 µl to 1 ml of extraction buffer A (100 µl per $1x10^7$ cells) and incubated for 20-30 min at 4°C or on ice. Extraction buffer A is a low salt buffer (indicates that DTT and PMSF were added to buffer A), which allowed the cells to swell. To destroy the swollen cells, the solution was passed 10 times through 1 ml syringe with 26 gauge needle and centrifuged at 3,600 rpm for 20 min at 4°C. The supernatant contained cytosolic fraction and the pellet, which appeared transparent, containing nuclear fraction. The supernatant was transferred to a fresh 1.5 ml tube and kept on ice. The pellet was resuspended with 200 µl extraction buffer C (leupeptin was added in addition to DTT and PMSF) by pipetting and vigorously mixing with force, followed by vortexing the nuclear extract vigorously for 30 min and incubate on ice for 30 min. Now the suspension was centrifuged at 15,000 rpm for 30 min at 4°C and supernatant containing nuclear proteins was frozen in –20°C. The protein concentration of the supernatant was determined by Bio-Rad protein assay.

3.2.6 Protein determination

The Bio-Rad protein assay is based on the observation that when Coomassie brilliant blue G-250 binds to the protein, the absorbency maximum shifts from 450 nm to 595 nm. Equal volumes of cell lysate containing 1-20 µg of protein was added to diluted dye reagent and mixed well (1:5 dilution of dye reagent concentrate in dH_2O). After 5-10 min, the absorption at wavelength at 595 nm was measured versus reagent blank (which contains only the lysis buffer).

3.2.7 SDS-polyacrylamide gel electrophoresis

SDS-polyacrylamide gels were prepared in 8 cm x 10 cm x 1.5 mm mini gel format according to the standard Laemmli method. Separating or lower gel mix was prepared according to the volume required, poured in the gel apparatus, overlaid gently with 0.1% SDS and before the separating gel polymerized, immediately poured the stacking gel, the comb was inserted and allowed to polymerize at RT for 1 h to 2 h. Requisite concentrations of protein samples were mixed with 4x Laemmli buffer and denatured by heating at 95°C for 5 min, loaded in the wells, (one well was loaded with protein marker) of polymerized gel and electrophoresed at constant current initially at 120 V and when the marker start separating current increased up to 160 V per gel in 1X SDS-PAGE running buffer.

3.2.8 Western blotting

SDS-PAGE gel was electrotransferred onto nitrocellulose membrane at 300-400 mA for 90 min at 4°C. The air dried membrane was incubated in a blocking solution (5% fat free milk in 1X TBS-Tween) for 1 h at RT. Membrane was directly incubated in primary antibodies against cyclinD1, CDK4, CDK6, GSK3β, HA, Lamin a/c, HDM2, p53, NFATc2, Ubiquitin and β-actin antibodies over night at 4°C. After incubation, the membrane was washed in 1X TBS-Tween for 3 X 10 min each. Now membrane was incubated in secondary antibodies conjugated with peroxidase against mouse or rabbit antibody for 1-2 h at room temperature and washed in 1 X TBS-Tween for 3 X 10 min each. Proteins were visualized and developed with ECL developing solution according to the manufacturer's instructions.

3.2.9 Proliferation Assay and Cell Cycle Analysis

MDA-MB-231, MDA-MB-435, PaTu8988t, IMIM-PC-1 cells were seeded in 12-well plates and cultured in medium containing 10% FCS. Cells were kept in the presence of 10 or 25 µM zoledronic acid for indicated time periods. [^{3}H] thymidine (0.5mCi/well) was added during the last 6 h of incubation. Incorporated [^{3}H] thymidine was quantified as described previously. Cell cycle analysis was performed by flow cytometry. Cells were treated with 10 µM zoledronic acid for 72 h, trypsinized, washed with PBS and fixed in 70% ethanol. After washing with PBS, cells were incubated with 20 µg/ml RNase, DNase-free water with 50µg/ml propidium iodide for 3 h at RT under light protection. The DNA content of 10^6 cells was analyzed on a Becton Dickinson FACS Calibur flow cytometer (San Jose, CA, USA). The fractions of cells in the G0/G1, S and G2/M phases were calculated using Cell Quest software from Becton Dickinson (Topsham, ME, USA).

3.2.10 *In vivo* Tumor Xenograft Studies

6-8 weeks old female athymic nu/nu mice were obtained from Harlan Laboratories (San Diego, CA, USA) and housed in the animal care facility of University hospital of Marburg, under pathogen-free conditions. IMIM-PC-1 cells were detached from the culture dishes by trypsinization and then collected, washed, and resuspended in DMEM. To establish IMIM-PC-1 tumor xenografts, mice were injected s.c. with 1×10^6 IMIM-PC-1 cells mixed with 50 µL DMEM + 50 µL Matrigel (BD Biosciences) in the right and left flanks of each mouse. One week after injection, tumors were size matched and mice were randomized into two treatment groups: animals in group I (control) received 10% DMSO; and group II received 1 mg/kg zoledronic acid, i.p., 3 days per week. Once xenografts started growing, their sizes were measured with caliper twice in a week. Tumor volume was

calculated using the formula for volume of an ellipsoid: $4/3\pi \times (L / 2) \times (W / 2) \times (H / 2)$, where *L* is the length, *W* is the width, and *H* is the height. Protocols for animal handling and experimentation were approved by the animal research facility of the University hospital of Marburg.

3.2.11 Real-Time PCR

RNA was extracted using the RNeasy Mini Kit (Qiagen) and first-strand cDNA was synthesized from 1 µg total RNA using random primers (Superscript first-strand synthesis kit). The RT-PCR was performed using a 7500 Fast-Real-Time-PCR-System from Applied Biosystems. Specific primer pairs were designed with the Primer Expresss 3.0 (Applied Biosystems).

3.2.12 Co-Immunoprecipitation

Cells were lysed in either RIPA buffer (50 mM Tris HCL, pH 7.5, 150 mM NaCl, 1% NP40, 0.5% sodium deoxycholate, 0.1% SDS, 0.2 mM PMSF, 2 mM orthovanadate and 20 mM N-ethylmaleimide) supplemented with protease inhibitor cocktail or lysis buffer (50 mM Tris HCl, pH 7.4, 150 mM NaCl, 1 mM EDTA, 1% Triton X-100, and 20 mM N-ethylmaleimide) supplemented with protease inhibitor cocktail. For immunoprecipitaion, lysates were incubated overnight at 4°C with the relevant antibodies (3 µg anti-NFATc2, 3 µg anti-HDM2 or 3 µg of anti-HA; anti-Flag) followed by a 2 h incubation with protein A or G agarose beads at 4°C (Upstate, USA). The beads were then washed three times with washing buffer (50 mM Tris HCl, pH 7.4, 150 mM NaCl) or PBS, supplemented with protease inhibitor cocktail. Than precipitates input control lystae were prepared for western blot.

3.2.13 Immunofluorescence

Cells were grown on chambered cover slips and they were washed three times with PBS and then fixed in 4% paraformaldehyde for 10 min at RT. After fixation, cells were washed two times in PBS and permeabilized in PBS containing 0.2% Triton X-100 for 20 min. Cells were blocked in PBS containing 10% FCS at RT for 1 h and incubated with anti-HA in blocking solution. Cells were washed three times with PBS and incubated for 1 h at RT Cy3-conjugated goat-anti-mouse secondary antibody (Dianova, Jackson ImmunoResearch Laboratories, USA) in blocking solution and nuclei counterstained with DAPI (containing 1.5 µg/ml). Cover slips were mounted on glass slides and preparations were observed with a fluorescence microscope (Carl Zeiss, Göttingen, Germany).

3.2.14 Immunohistochemistry with ABC-peroxidase method

Paraffin embedded sections of human pancreatic and breast cancer tissues of 2-3 µm were deparaffinized with xylene (3 x 5 min) followed by rehydration in a series of ethanol (2 x 99%, 96%, 80%, 70%, 50% ETOH, 1.5 min each step). For antigen retrieval and improved accessibility of epitopes, rehydrated sections were subjected to 0.01% trypsin digestion for 10 min at 37°C and additional irradiation for 3 x 5 min in a microwave oven (850 W, in citrate buffer, pH 6) with subsequent cooling 1 h at RT. Blocking of endogenous peroxidase was done by incubating the sections for 5 min with 3% H_2O_2 (Merck, Darmstadt, Germany) in a moist chamber at RT. Non-specific protein binding sites and endogenous biotinylated proteins in these sections were blocked for 2 h with 10% FCS in PBS pH 7.4) containing avidin (Avidin/Biotin blocking kit, Vector, Burlingame, CA). Washing steps were performed between all following steps with PBS for 5 min. After washing, sections were incubated overnight with primary

antibodies in 10% FCS at 4°C, including free biotin to saturate the bound avidin (Avidin/Biotin blocking kit. For detection of antigen-antibody complexes the sections were incubated with a biotinylated secondary antibody for 1 h at RT. The bound secondary antibody was detected with peroxidase-coupled extravidin system and visualized by histochemical staining. This reaction was stopped with H_2O and the sections were counterstained with hematoxylin for 10 min. Negative controls were incubated in parallel without primary antibody. These sections were analyzed by a photo microscope (Zeiss).

3.2.15 Ubiquitination Assays

Cells were treated with ZOL (10 µM) for 32 h followed by MG132 (10 µM) for at least 12 h. After that cells were lysed and subjected to immunoprecipitation. Anti-NFATc2 immunoprecipitates or anti-HA or anti-HDM2 immunoprecipitates were immunoblotted against anti-ubiquitin (BioMol).

3.2.16 Luciferase Reporter Assays

For luciferase reporter gene assays, 10^6 cells were seeded onto 12-well tissue culture dishes and transfected after 24 h with the above indicated constructs. Cells were treated for 72 h in the presence of zoledronic acid (10 µM) then luciferase assays were performed with a luminometer and the Dual-Luciferase®-Reporter Assay System (Promega). Firefly luciferase values were normalized to Renilla luciferase activity and were either expressed as relative luciferase activity (RLA) or as mean 'fold induction' with respect to empty vector control. Mean values are displayed +/- standard deviations.

3.2.17 Statistical analysis

Each experiment was reproduced at least three times. Values were expressed as the mean ± SD of triplicate measurements unless otherwise stated. Student's paired *t*-test was used to analyze differences between the sample of interest and its control. Time courses and dose responses were compared by multiple measurements ANOVA and corrected by Student-Newman–Keul's test for differences between groups. A *p* value of less than 0.05 was considered statistically significant by this test.

4 RESULTS

4.1 ZOLEDRONIC ACID INHIBITS CANCER CELL PROLIFERATION BY INDUCING G1/S PHASE ARREST

To investigate the effect of zoledronic acid on tumor cell proliferation, we performed proliferation assays by measuring ^{3}H-thymidine incorporation in MDA-MB-435, MDA-MB-231, IMIM-PC-1, PaTu8988t and MDA-MB-468 cells. Treatment with zoledronic acid led to a dramatic reduction in proliferation rates of MDA-MB-435, MDA-MB-231, IMIM-PC-1 and 8988t cells respectively (Fig. 5A). In contrast, cell growth remained unaffected in MDA-MB-468 cells (Fig. 5C). Reduction of cell proliferation occurred in a time-dependent manner and became significant after 48 h in zoledronic acid responsive cancer cell lines. Maximal growth suppression was reached 72 h after treatment with zoledronic acid (Fig. 5B).

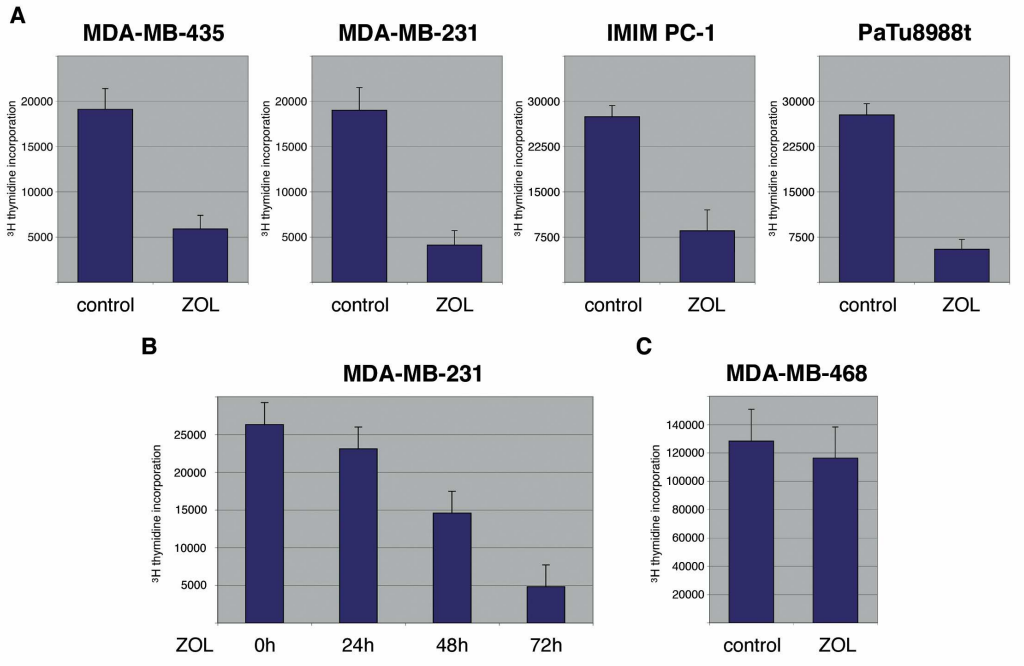

Fig. 5. Zoledronic acid inhibits cancer cell proliferation. (A) MDA-MB-435, MDA-MB-231, IMIM-PC-1, 8998t cells were treated with zoledronic acid (10 µM) in serum condition. 72 h after treatment, cells were subjected to a proliferation assay by incorporation of ^{3}H thymidine. (B) MDA-MB-435 cells were treated with zoledronic acid (10 µM) with the indicated time points (C) Zoledronic acid non-responsive MDA-MB-468 cells were treated with the zoledronic acid (10 µM) in serum condition. 72 h after treatment, cells were subjected to a proliferation assay by incorporation of ^{3}H thymidine. Data are representative of triplicate experiments and are displayed as bars ± SD.

To determine whether zoledronic acid mediates growth inhibition, which could be due to cell cycle inhibition, therefore we assessed the effect of zoledronic acid on cell cycle regulation by using flow cytometry analysis. Zoledronic acid treated and untreated cancer cells revealed that this effect was most likely due to induction of cell cycle arrest, as evidenced by the shift of cells in G1 phase and synchronization of cells in phase in corresponding MDA-MB-435 and MDA-MB-231 cells (Fig. 6). Time course analysis after treatment with 10 µM zoledronic acid in MDA-MB-435 and MDA-MB-231 cells revealed decreased expression of cyclin D1 and its corresponding kinases CDK4 and CDK6 over time, reflecting cell cycle inhibition. Maximal inhibition was seen after 72 h consistently in both cell lines (Fig. 7). Thus, zoledronic acid suppresses proliferation of cancer cells through induction of a G1-S phase arrest of cell cycle.

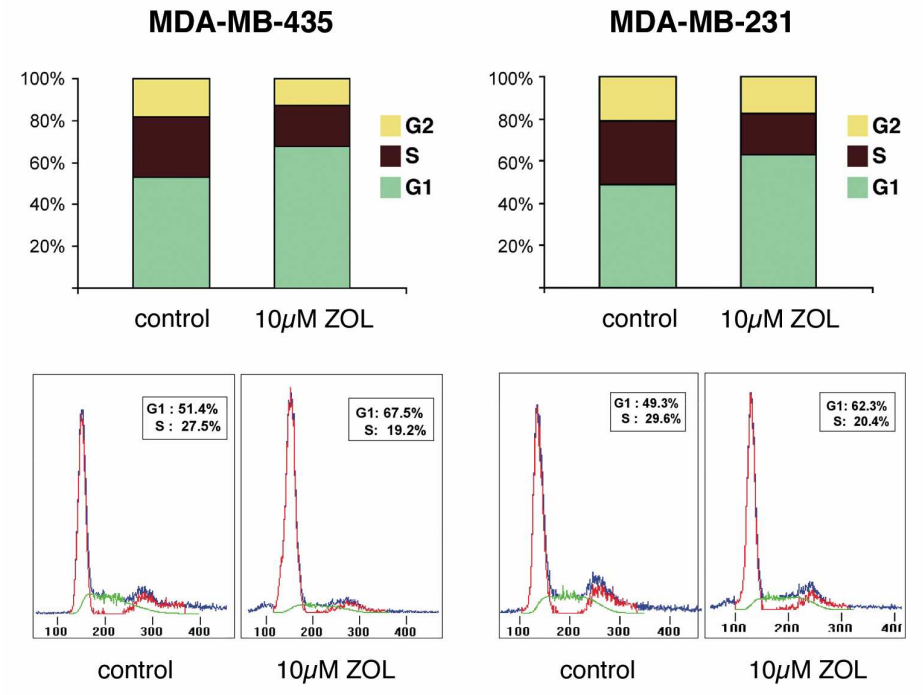

Fig. 6. Zoledronic acid induces G1/S phase arrest in cancer cells. MDA-MB-435 and MDA-MB-231 cells were treated with zoledronic acid (10 μM) in serum containing medium. After 72 h of treatment with zoledronic acid, flow cytometry analysis was performed after propidium iodide (PI) staining. Cell cycle stages are illustrated in different colors: G2 (yellow), S (brown), and G1 (green). Bars indicate mean values ± SD of three independent experiments.

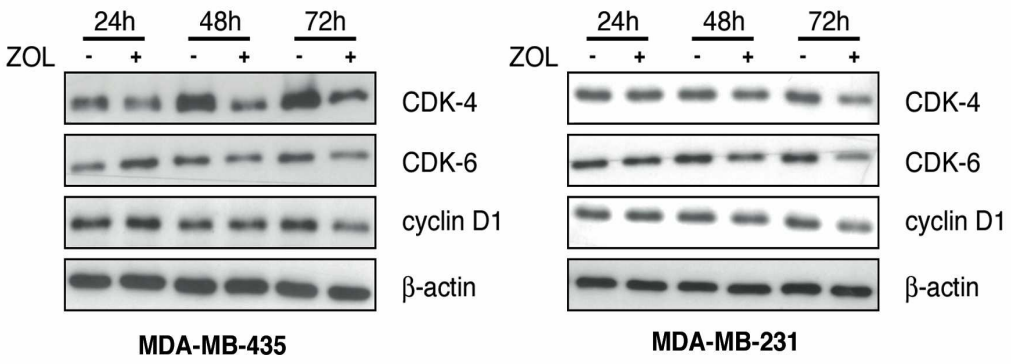

Fig.7. Zoledronic acid down regulates G1/S phase regulatory proteins in a time dependent fashion. Western blot analysis to examine the effect of zoledronic acid on the expression of cell cycle regulatory genes in growth promoted cell lines. Cells were treated with 10 μM zoledronic acid in indicated time points. Total cell lysates were then analyzed for expression of D-type cyclins and their kinase partners (CDKs). Protein loading was controlled using β-actin antibodies.

4.2 EFFECTS OF ZOLEDRONIC ACID, ON THE GROWTH OF IMIM-PC-1 TUMORS IN ATHYMIC NUDE MICE

To determine the *in vivo* relevance of our *in vitro* findings, we selected athymic nude mice and injected pancreatic cancer cells (IMIM-PC-1) subcutaneously. Mice were treated with a sterile i.p. injection of 10% DMSO in 0.9% NaCl. To determine the effect of zoledronic acid treatment on the growth of tumors in this xenograft mouse model, we compared treatment with zoledronic acid 1 mg/kg intraperitoneal (i.p). 3 days per week, (n = 7) with a control group (n = 7). We observed that zoledronic acid significantly reduces the growth of tumors compared to the control group ($p < 0.05$; Fig. 8).

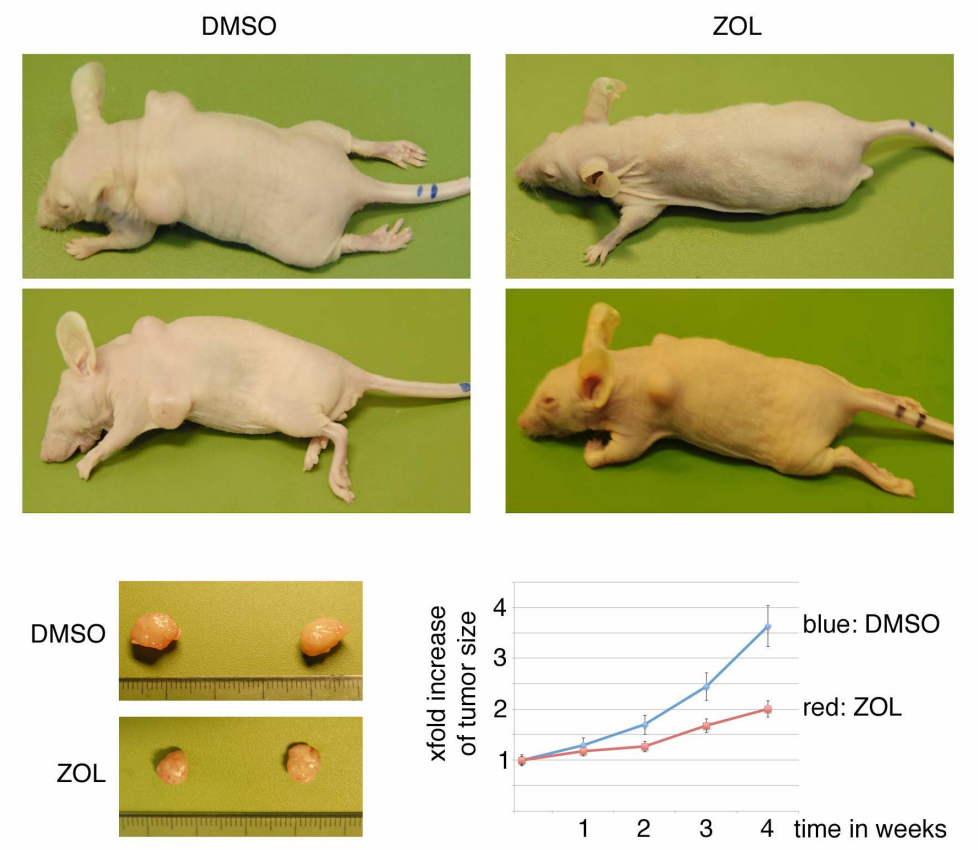

Fig. 8**. Antitumor effects of zoledronic acid inhibition *in vivo.*** IMIM-PC-1 tumor xenografts mice were injected subcutaneously (s.c.). with 1×10^6 IMIM-PC-1 cells mixed

with 50 µL DMEM + 50 µL matrigel in the right and left flanks of each mouse. One week after injection, tumors were size matched and mice were randomized into two treatment groups: animals in group I (control) received 10% DMSO in 0.9% NaCl; and group II received 1 mg/kg zoledronic acid, i.p., 3 days per week. Photographs of representative mice with tumors from each group (upper panel). Photographs of excised tumors from each group (lower-left panel). Average tumor volume of DMSO control and zoledronic acid treated mice plotted over days after tumor cell inoculation (lower-right panel). Once tumors started growing, their sizes were measured with calipers in three dimensions two times weekly. Tumor volume was calculated using the formula for volume of an ellipsoid: $4/3\pi \times (\boldsymbol{L} / 2) \times (\boldsymbol{W} / 2) \times (\boldsymbol{H} / 2)$, where ***L*** is the length, ***W*** is the width, and ***H*** is the height points mean of seven animals; bars, SD.; $\boldsymbol{P} < 0.05$. Results were analyzed using student's paired *t*- test, and $p< 0.05$ was considered significant.

4.3 NFATc2 PROMOTES G1/S-PHASE TRANSITION IN CANCER CELLS

NFATc2 exerts strong oncogenic properties through its ability to promote cancer cell growth and migration. We observed the localization and expression of NFATc2 in a series of breast and pancreatic cancer tissues (Fig. 9) and also in all investigated cancer cell lines (Fig. 10).

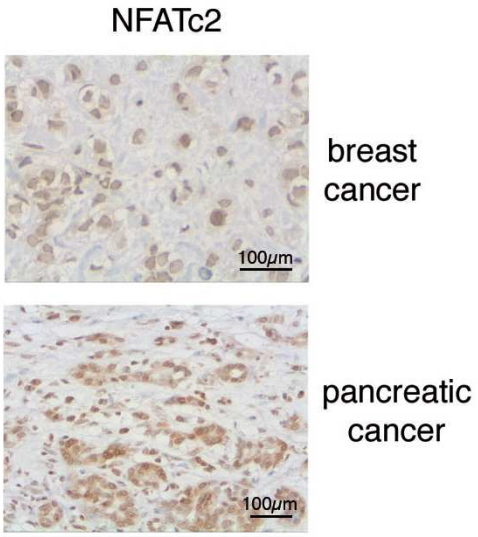

Fig. 9. NFATc2 expression in human breast and pancreatic cancer tissues. Immunohistochemical analysis of NFATc2 expression and localization in human breast cancer tissue (upper panel) and pancreatic cancer tissue (lower panel). Scale bars, 100 µm.

To investigate the role of NFATc2 in cancer cell proliferation, we first used MDA-MB-231 and MDA-MB-435 cells and performed proliferation assays by measuring ^{3}H-thymidine incorporation in the presence or absence of NFATc2. For this purpose, we transiently knocked down NFATc2 expression in MDA-MB-435 and MDA-MB-231 cells by using RNAi technology, illustrating successful silencing of NFATc2 in MDA-MB-231 cells upon transfection of siRNA #2 and #3 (Fig. 10).

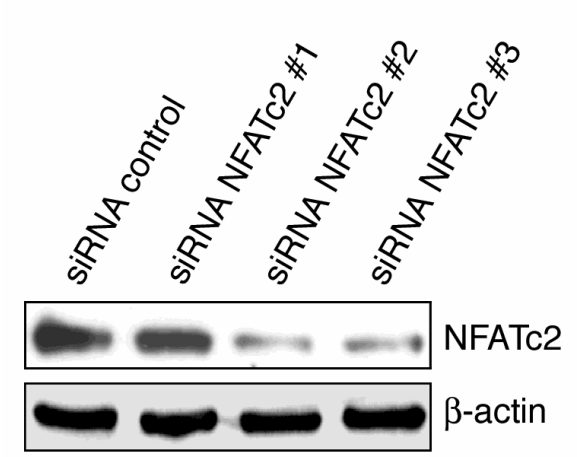

Fig. 10. Transient knock down of NFATc2 by using siRNA. MDA-MB-231 cells were transiently transfected with three different oligonucleotide sequences of NFATc2 or control siRNA. After 24 h of transfection cell were then analyzed for expression of NFATc2 or β-actin antibody.

We then used oligonucleotide sequence #3 or control siRNA for further analysis to examine the effects of NFATc2 knockdown on cell growth in MDA-MB-435 and MDA-MB-231 cells. In both conditions, NFATc2 expression was dramatically reduced compared to control cells (Fig. 11, upper panel). We next assessed the effect of NFATc2 silencing on cell proliferation using ^{3}H thymidine incorporation. In both cell lines, silencing of NFATc2 resulted in a potent inhibition of cell proliferation compared to cell transfected with control siRNA, (Fig. 11, lower panel), and this is equivalent to cell growth inhibition imposed by zoledronic acid.

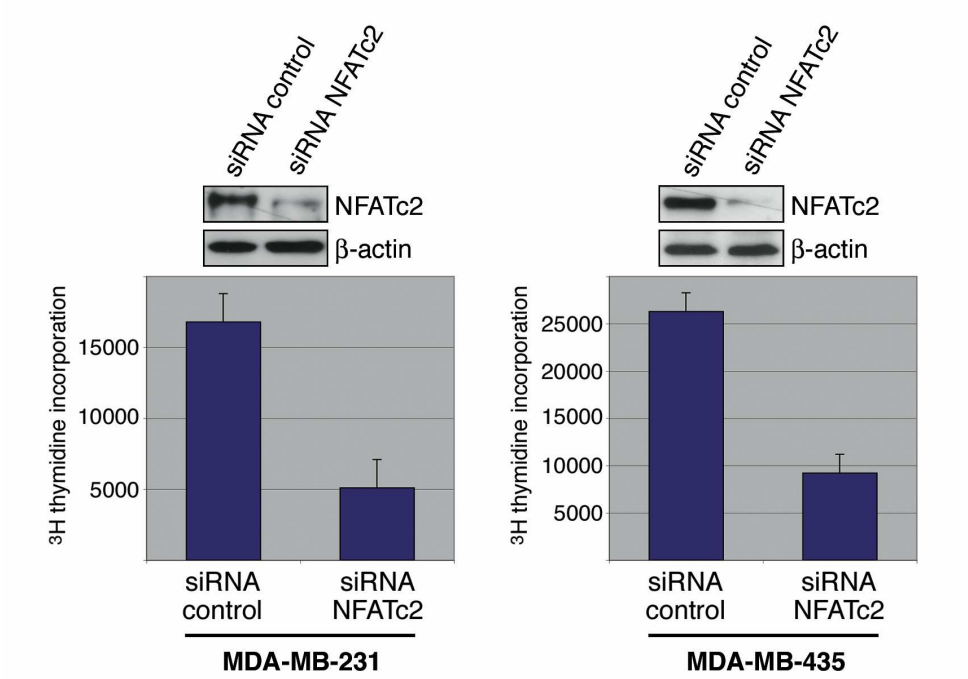

Fig. 11. NFATc2 is required for cancer cell proliferation. MDA-MB-231 and MDA-MB-435 cells were transiently transfected with NFATc2 siRNA (NFATc2 siRNA #3) or control siRNA (upper panel). After transfection, cells were subjected to a proliferation assay by incorporation of ^{3}H thymidine (lower panel). Data are representative of triplicate experiments and are displayed as bars ± SD. In the upper panel, NFATc2 expression levels were determined by immunoblotting with NFATc2 and β-actin as loading control.

In addition, expression analysis revealed that analogy to the effects of zoledronic acid treatment, in the NFATc2 knock-down cells showed a cell cycle arrest caused by reduced levels of cyclin D1 and its partner kinase CDK6 (Fig. 12). Thus, NFATc2 activity is required for the proliferative capacity of cancer cells, and reduction of NFATc2 activity results in near complete loss of the G1/S phase regulatory cyclins and their kinases, which reduces proliferation.

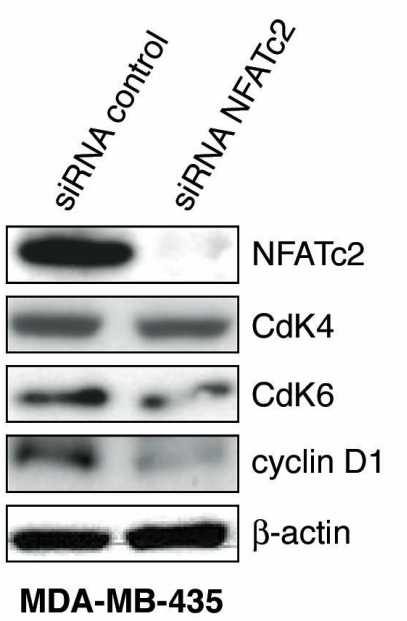

Fig. 12. NFATc2 targets G1/S phase genes to induce tumor cell proliferation. MDA-MB-435 cells were transiently transfected with NFATc2 siRNA (NFATc2 siRNA #3) or control siRNA. After transfection, lysates were immunoblotted with anti-NFATc2, D-type cyclins and their kinase partners (CDKs). Protein loading was controlled by using β-actin antibody.

4.4 ZOLEDRONIC ACID SUPPRESSES NFATc2 ACTIVITY THROUGH ENHANCED PROTEASOMAL DEGRADATION

We next investigated the mechanism by which zoledronic acid could block cell proliferation. We sought to implicate zoledronic acid in the modulation of growth control through NFATc2 in cancer cells. To test this hypothesis, we first evaluated NFATc2 transcriptional activity by reporter gene assays using a NFAT responsive promoter reporter construct (cisNFAT) bearing GGAAA NFAT concensus binding sites obtained from the IL-2 promoter. Upon introduction of NFATc2 caused a six-fold induction of the cis-NFAT reporter construct. However, treatment of cells with zoledronic acid leads to a complete loss of NFATc2 mediated promoter transactivation

suggesting that zoledronic acid treatment antagonizes the transcription activity of NFATc2 in cancer cells (Fig. 13).

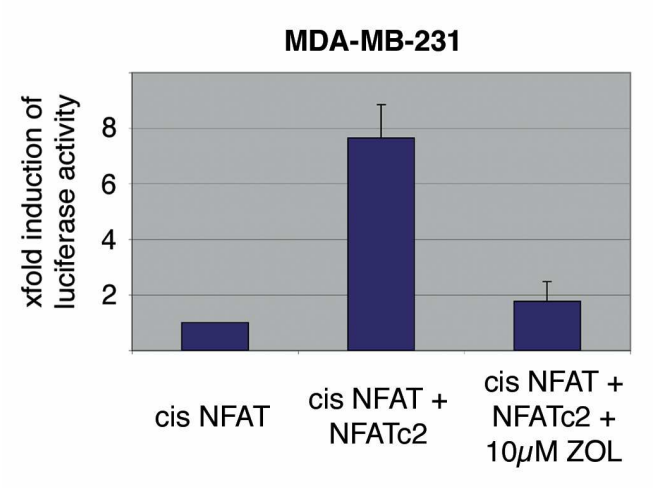

Fig. 13. Zoledronic acid blunts NFATc2 transactivation. MDA-MB-231 cells were transiently transfected with the cis-NFAT luciferase reporter plasmid and the indicated NFATc2 plasmids, or empty vector control. After transfection, cells were treated with zoledronic acid (10 µM) for 48 h, then lysed and luciferase assays were performed. Data are representative of triplicate experiments and are displayed as bars ± SD.

In fact, western blot analysis revealed a significant reduction of endogenous NFATc2 expression levels in MDA-MB-435, MDA-MB-231 and IMIM-PC-1 cells after 72 h of zoledronic acid treatment (Fig. 14) Interestingly, the level of NFATc2 remained unaffected in MDA-MB-468 cells (Fig. 14). Time dependent experiments showed that NFATc2 protein expression in MDA-MB-435 cells was abolished after 48 h (Fig. 15).

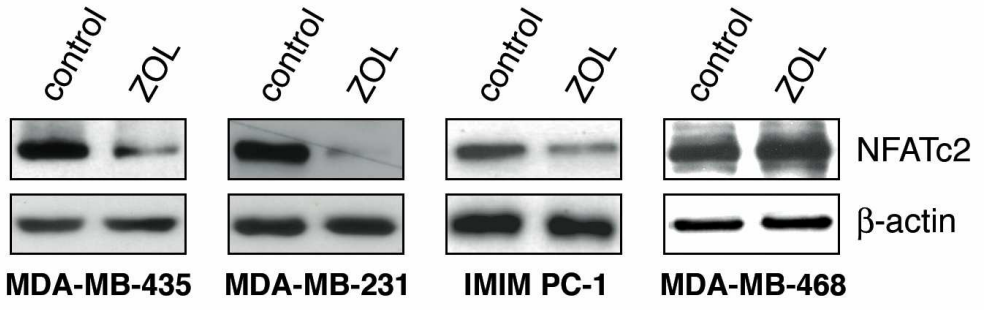

Fig. 14. Zoledronic acid reduces NFATc2 protein expression. Expression level of NFATc2 in MDA-MB-435, MDA-MB-231, IMIM PC-1 and MDA-MB-468 cells after treatment with

zoledronic acid (10 µM), 72 h after treatment protein levels of NFATc2 in the cells were determined by immunoblotting.

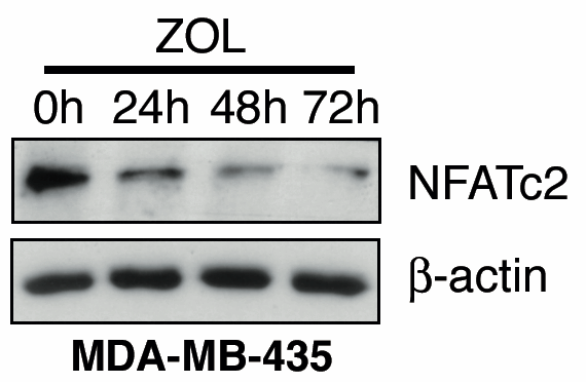

Fig. 15. Zoledronic acid reduces NFATc2 protein expression in a time dependent manner. In MDA-MB-435 cells, time course experiment showing NFATc2 protein expression in indicated time points after zoledronic acid treatment.

Furthermore, inhibition of NFATc2 protein expression in MDA-MB-435 and MDA-MB-231 did not result from disrupted mRNA expression (Fig. 16), but was the consequence of increased protein turnover and degradation. While zoledronic acid did not affect the level of NFATc2 mRNA expression, it dramatically lowered NFATc2 protein levels in all responsive cell lines.

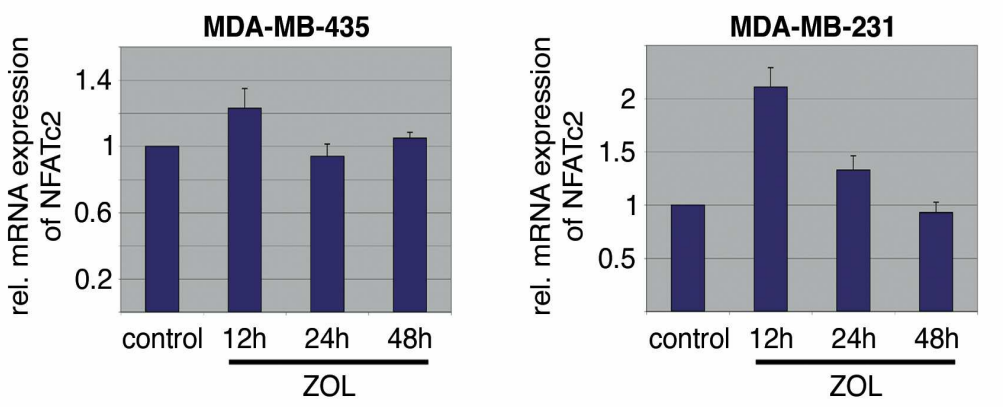

Fig. 16. Zoledronic acid does not alter NFATc2 mRNA expression. MDA-MB-231 and MDA-MB-435 cells were treated with zoledronic acid (10 µM) for indicated time points. Bars are showing NFATc2 mRNA expression was measured by real-time PCR using NFATc2 and XS-13 oligonucleotides. Data are representative of triplicate experiments and are displayed as bars ± SD.

Moreover, zoledronic acid induced loss of NFATc2 expression was completely rescued by pre-treatment of cells with MG-132, a cell-permeable and reversible proteasome inhibitor that allows ubiquitination but reduces the subsequent degradation of ubiquitin-conjugated proteins by the 26S proteasome complex (Fig. 17). Indeed, immunoprecipitation from zoledronic acid treated cells showed a strong ubiquitination signal upon administration of zoledronic acid with a characteristic ladder, indicative for polyubiquitination. Noteworthy, the ubiquitination signal was weakly detectable in cells without zoledronic acid, indicating that a basal turnover of NFATc2 also exists in the absence of zoledronic acid. Accordingly, we found increased expression levels of NFATc2 upon pretreatment of cells with MG-132 (Fig. 18). Taken together, these results show that zoledronic acid targets the mitogenic transcription factor NFATc2 for ubiquitination and proteasomal degradation in growth inhibited cancer cells.

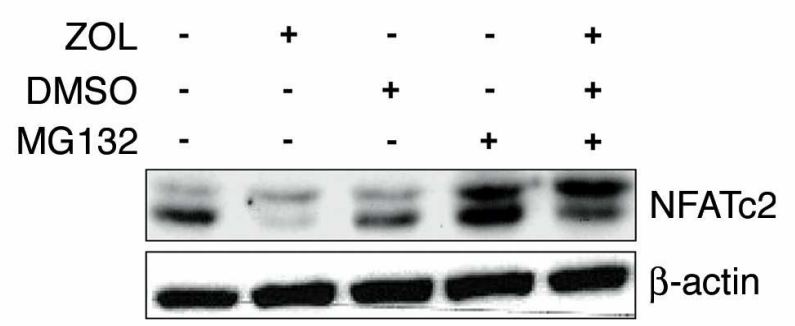

Fig. 17. Zoledronic acid promotes NFATc2 proteasomal degradation. MDA-MB-435 cells were treated with zoledronic acid (10 µM) for 32 h in complete media, then treated with MG132 (10 µM) or DMSO control for at least 12 h. After 48 h cells were lysed and total cell lysates were immunoblotted with NFATc2 antibodies. Protein loading was controlled by using β-actin antibody.

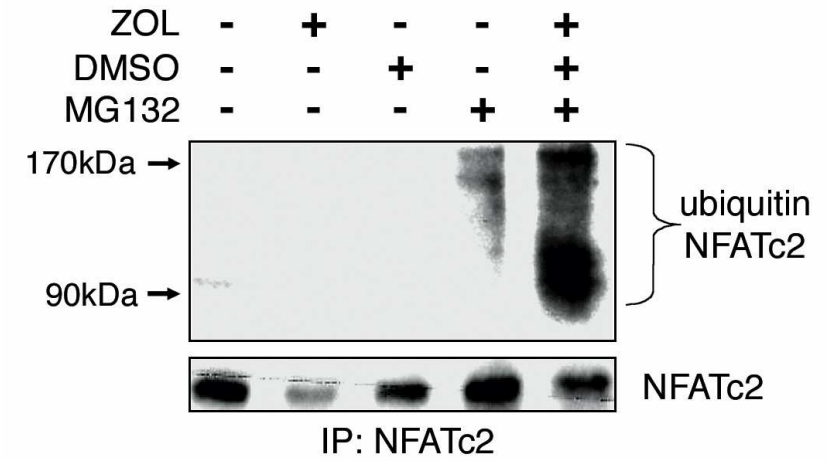

Fig. 18. Zoledronic acid induces NFATc2 ubiquitination and proteasomal degradation. MDA-MB-435 cells were treated with zoledronic acid (10 µM) for 32 h in complete media, then treated with MG132 (10 µM) or DMSO control for at least 12 h. After 48 h cells were lysed and NFATc2 immunoprecipitates were immunoblotted with ubiquitin and NFATc2 antibodies.

4.5 HDM2 IS REQUIRED FOR ZOLEDRONIC ACID MEDIATED PROTEASOMAL DEGRADATION OF NFATc2

Polyubiquitination is mediated by and required for E3-ligase induced substrate degradation. HDM2, the human homolog of the E3-ligase MDM2 (murine double minute 2), is a nucleoplasmic RING-finger protein interacting with several tumor suppressor proteins including p53, retinoblastoma protein, p14ARF and promyelocytic leukemia protein (PML). HDM2 controls the levels of p53 by acting as an E3 ubiquitin ligase initiating p53 proteasomal degradation. It has recently been shown that HDM2 is activated by the Pi3K-AKT pathway in breast cancer cells and this mechanism has been associated with inhibition of NFAT mediated cancer cell migration (Yoeli-Lerner et al., 2005). We therefore, tested whether HDM2 is involved in zoledronic acid mediated degradation of NFATc2. First, zoledronic acid treatment led to a significant increase of endogenous

cellular HDM2 and loss of NFATc2 in MDA-MB-435 and MDA-MB-231 cells (Fig. 19). We also found that zoledronic acid induced HDM2 expression and NFATc2 degradation in a dose dependent manner (Fig. 20). In addition, overexpression of HDM2 reduced endogenous NFATc2 protein levels in a dose dependent manner respectively (Fig. 21).

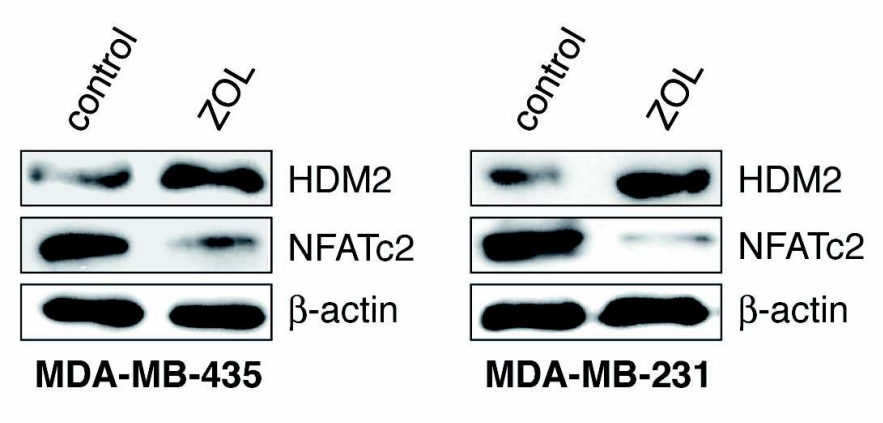

Fig. 19. Zoledronic acid induces E3-ligase HDM2 protein expression. MDA-MB-435 and MDA-MB-231 cells were treated with zoledronic acid (10 μM). After 72 h of treatment total cell lysates were subjected to analyze the expression of NFATc2 and HDM2. Protein loading was controlled by using β-actin antibody.

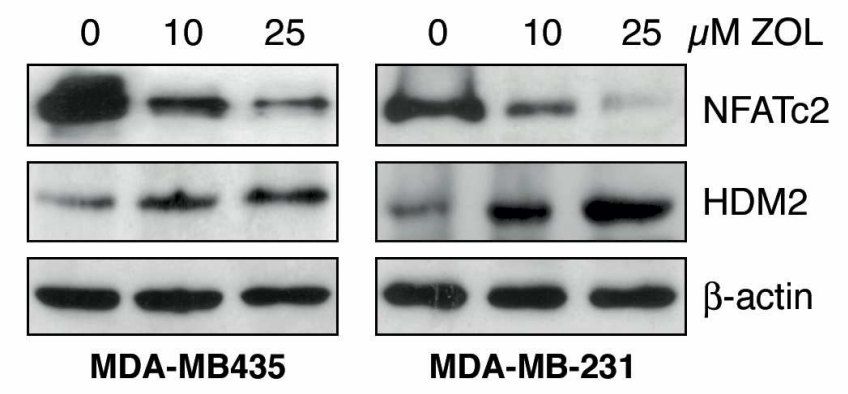

Fig. 20. Zoledronic acid induces E3-ligase HDM2 protein expression in a dose dependent manner. MDA-MB-435 and MDA-MB-231 cells were treated with zoledronic acid (10 or 25 μM). 72 h after treatment, total cell lysates were subjected to analyze the expression of NFATc2 and HDM2. Protein loading was controlled by using β-actin antibody.

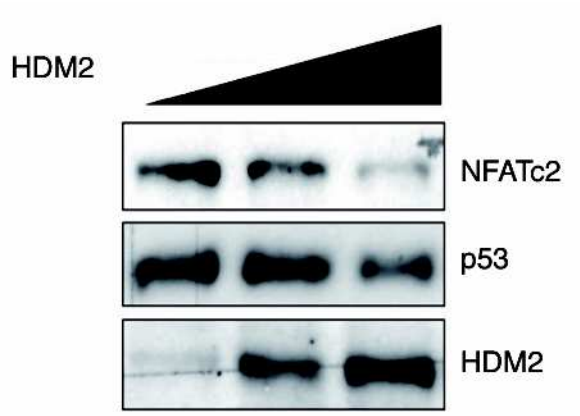

Fig. 21. Overexpression of HDM2 in MDA-MB-435 cells. MDA-MB-435 cells were transfected with different doses of HDM2. After 36 h of transfection, total cell extracts were immunoblotted with anti-NFATc2, anti-HDM2 and anti-p53.

Second, immunoprecipitation assays demonstrated physical interaction between HDM2 and NFATc2 in both cell lines. Thus, it appeared likely that HDM2 can promote NFATc2 degradation in response to zoledronic acid. We therefore assayed the ability of HDM2 to interact with and to induce ubiquitination and degradation of NFATc2. Co-immunoprecipitation studies showed that HDM2 readily interacts with endogenous NFATc2 in untreated cells which explains the low level of ubiquitination and degradation of NFATc2 in unstimulated cells (Fig. 22).

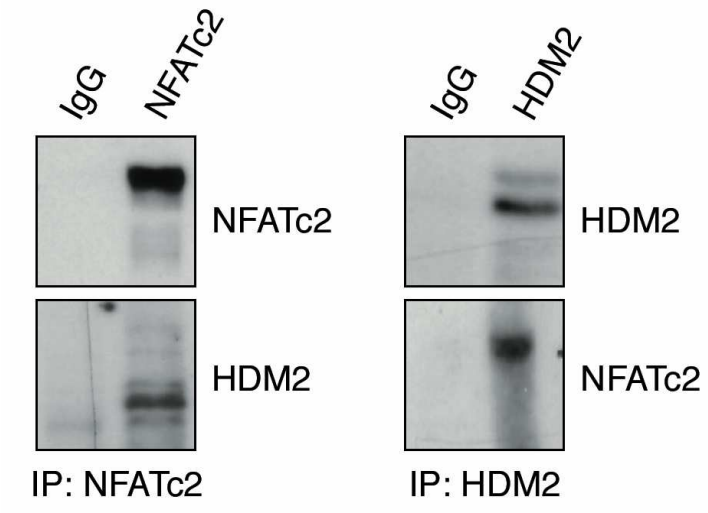

Fig. 22. E3 ligase HDM2 physically interacts with NFATc2. Total cell lysates from MDA-MB-231 cells were immunoprecipitated using anti-NFATc2 or anti-HDM2 and control (IgG) antibody and immunoblotted using the indicated antibodies.

Moreover, knockdown of HDM2 by RNA interference stabilized endogenous NFATc2 protein level and, in addition, prevented NFATc2 degradation and its downstream targets cyclin D1 and its kinases in response to zoledronic acid (Fig. 23). Surprisingly, silencing of HDM2 rescued cell proliferation in response to zoledronic acid (Fig. 24).

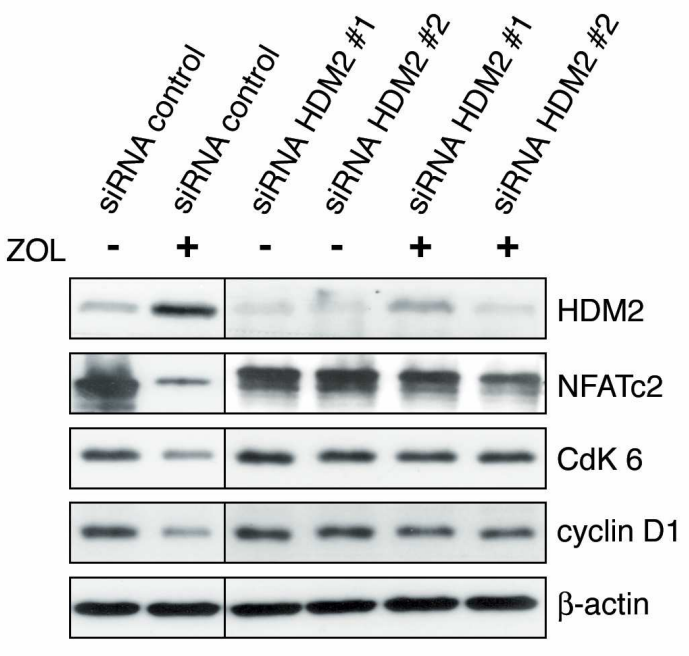

Fig. 23. E3-ligase HDM2 promotes NFATc2 degradation in response to zoledronic acid. MDA-MB-231 cells were transfected with HDM2 siRNA (HDM2 siRNA #1 and #2), or control siRNA. After transfection, cells were treated with zoledronic acid (10 μM) for 48 h in serum media then lysates were immunoblotted with NFATc2, HDM2, cyclin D1 and their kinase partners (CDK6). Protein loading was controlled using β-actin antibodies.

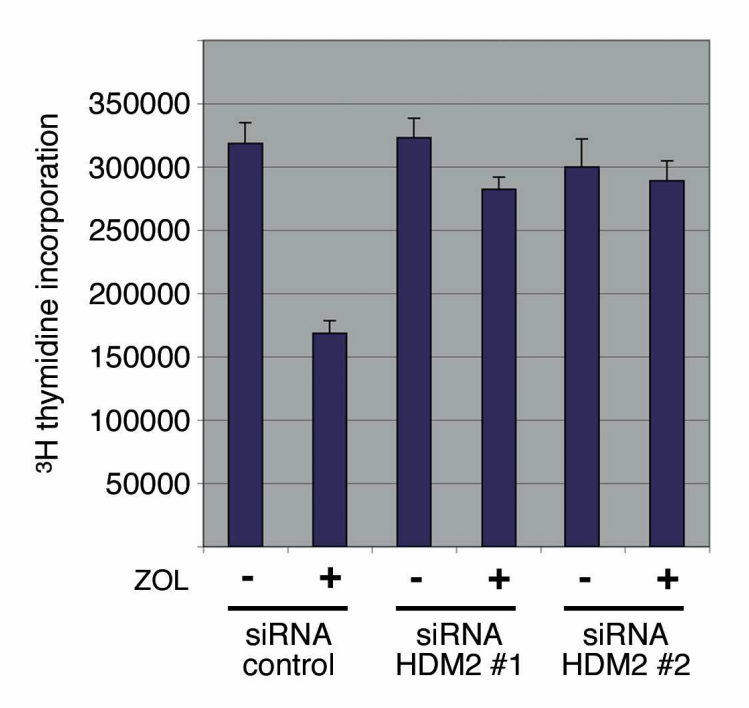

Fig. 24. Zoledronic acid inhibits cell proliferation through HDM2. MDA-MB-231 cells were transfected with HDM2 siRNA (HDM2 siRNA sequences #1 and #2), or control siRNA. 48 h after transfection, cells were subjected to a proliferation assay by incorporation of ^{3}H thymidine. Data are representative of triplicate experiments and are displayed as bars ± SD.

In addition, HDM2 was also responsible for mediating NFATc2 ubiquitination upon zoledronic acid, as NFATc2 ubiquitination was not detectable in HDM2 knockdown cells. Together, these results indicate that the E3 ubiquitin ligase HDM2 promotes NFATc2 degradation (Fig. 25).

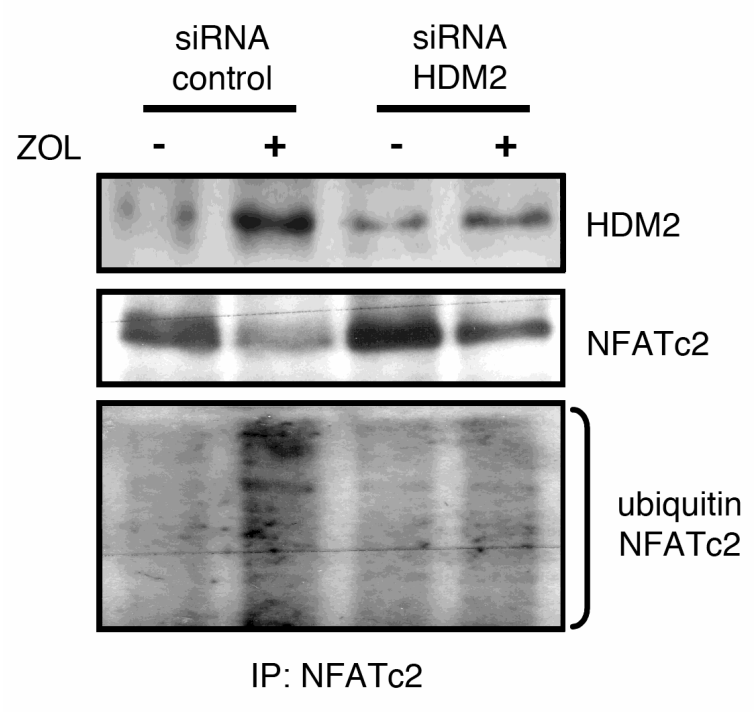

Fig. 25. E3-ligase HDM2 is required for ubiquitination followed proteasomal degradation of NFATc2 in response to zoledronic acid. MDA-MB-435 cells were transfected with HDM2 siRNA or control siRNA. After transfection, cells were treated with zoledronic acid (10 µM). After 48 h cells were lysed and NFATc2 immunoprecipitates were immunoblotted with ubiquitin and NFATc2 antibodies. Total lysates were immunoblotted to reveal expression of HDM2.

4.6 ZOLEDRONIC ACID INHIBITS GSK3β KINASE ACTIVITY AND INDUCES NUCLEAR ACCUMULATION OF HDM2 TO DEGRADE NFATc2

Nuclear translocation and accumulation of NFATc2 are prerequisites for transcriptional activity. We therefore evaluated whether zoledronic acid degrades NFATc2 in the nucleus or in the cytosol. After treatment with zoledronic acid (10 µM), nuclear and cytosolic extracts were immunoblotted for NFATc2 (Fig. 26). In untreated cells, NFATc2 was detected at equivalent levels in the cytosol (inactive) and nucleus (active). In untreated cells, the expression of nuclear NFATc2 was high, an there was

a striking reduction of NFATc2 protein in the nucleus following treatment with zoledronic acid. In the rescue experiment, nuclear NFATc2 levels were measurably increased in cells treated with MG-132 in combination with zoledronic acid (Fig. 27).

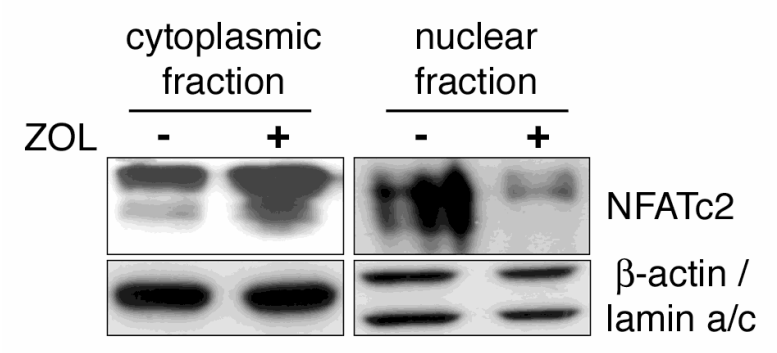

Fig. 26. Zoledronic acid targets NFATc2 in the nucleus. MDA-MB-435 cell were treated with zoledronic acid (10 μM) for 72 h. Nuclear and cytoplasmic fractions were then analysed by immunoblotting with the indicated antibodies. Protein loading was controlled using lamin a/c and β-actin antibodies.

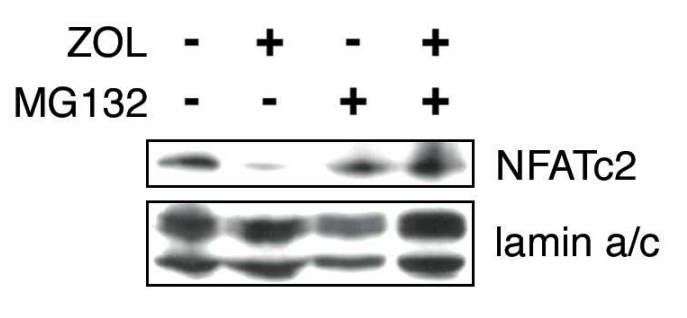

Fig. 27. Zoledronic acid induces NFATc2 degradation exclusively in the nucleus. Cells were treated with zoledronic acid (10 μM) for 32 h, then treated with MG132 (10 μM) or DMSO control, after 48 h cells were lysed and nuclear extracts were immunoblotted, NFATc2 antibodies were used. Protein loading was controlled using lamin a/c.

In the next experiment, subcellular fractionation further showed an inverse correlation between the level of nuclear HDM2 and NFATc2 upon zoledronic acid treatment. In fact, HDM2 strongly accumulated in the nuclei of zoledronic acid treated cells, in which NFATc2 expression declined. Moreover, HDM2 strongly accumulated in the nucleus upon treatment and most interestingly, nuclear fractionation also revealed that

reduction of NFATc2 mainly occurs in the nucleus, while cytoplasmic NFATc2 remained unaffected by zoledronic acid (Fig. 28).

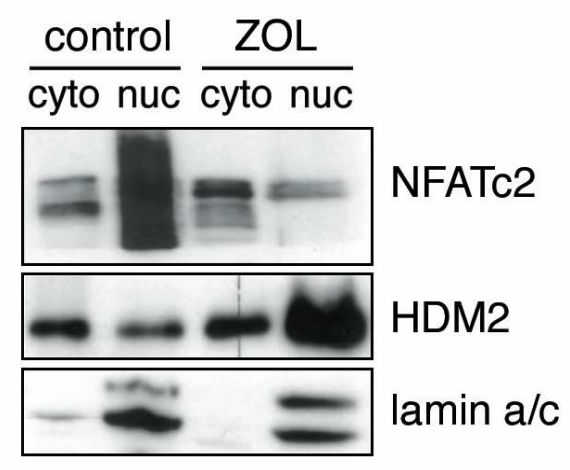

Fig. 28. Zoledronic acid induces HDM2 protein expression exclusively in the nucleus that leads to NFATc2 proteosomal degradation. MDA-MB-435 cells were treated with zoledronic acid (10 µM) for 72 h, nuclear and cytosolic extract were immunoblotted with NFATc2, HDM2 and lamin a/c as a nuclear loading control.

Several protein kinases that can phosphorylate NFAT and control its nuclear-cytoplasmic shuttling are known. We were especially interested in GSK3β, which is a substrate of Akt. Recently, It has been shown that Akt-signaling through inhibition of GSK3β induces NFATc2 turnover and blocks breast cancer cell migration (Yoeli-Lerner et al., 2009). Prompted by these recent findings, we investigated the role of GSK3β and NFATc2 stabilization pathways under the influence of zoledronic acid and sought to determine the expression pattern of GSK3β in human pancreatic cancer tissue. Using immunohistochemical staining, we found high levels of GSK3β and NFATc2 with in pancreatic cancer tissues and cell lines (Fig. 29, 31).

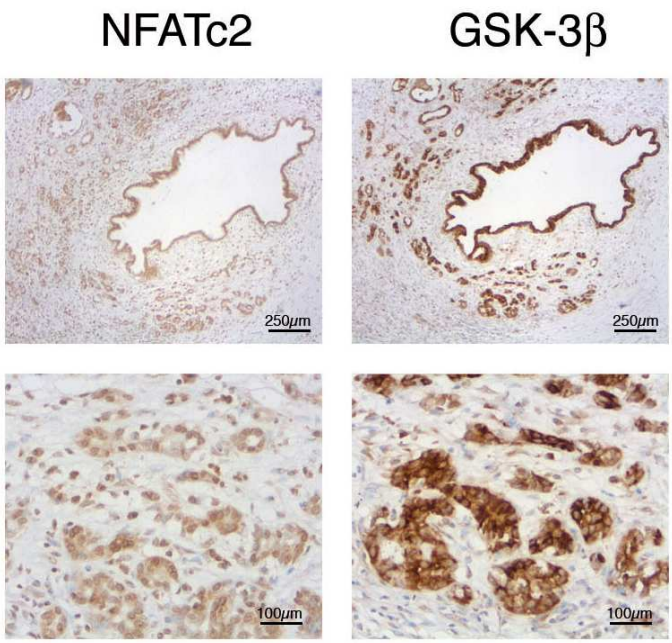

Fig. 29. NFATc2 and GSK3β expression in human pancreatic cancer tissue. Immunohistochemical analysis of NFATc2 (left panel) and GSK3β (right panel) expression and localization in human pancreatic cancer tissues. Scale bars, 250 µm and 100 µm.

However, treatment with zoledronic acid blunts GSK3β activity by its phosphorylation at Ser-9 residues, results in blocked activity of its substrate glycogen-synthase kinase. These findings were observed in all tested cancer cell lines (Fig. 32). After dose dependent treatment with zoledronic acid, nuclear fractionation revealed that zoledronic acid induces GSK3β phosphorylation which leads to nuclear NFAT inactivation by phosphorylation (Fig. 30 and 31).

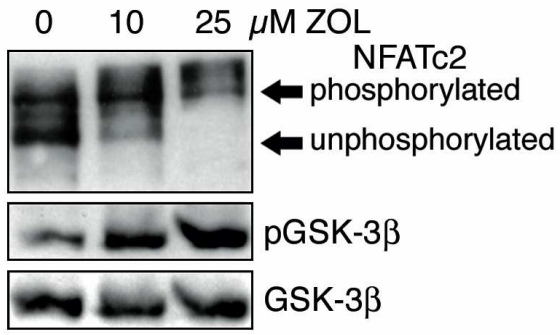

Fig. 30. Zoledronic acid blunts GSK-3β activity by Ser-9 phosphorylation. PaTu8988t cells were treated with zoledronic acid (10-25 µM) for 72 h, nuclear extracts were

immunoblotted with NFATc2, pGSK3β and GSK3β antibodies. Phosphorylated and unphophorylated forms of NFATc2 are indicated by arrows.

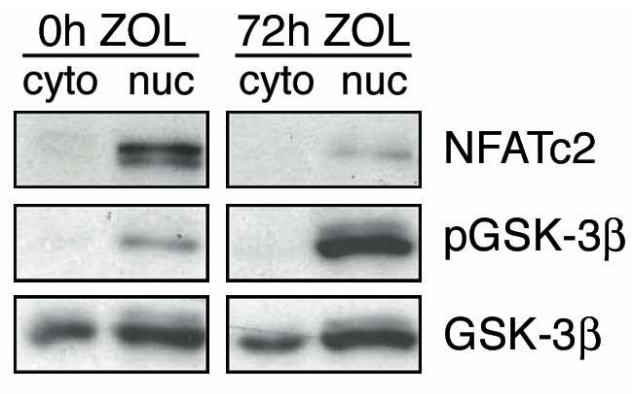

Fig. 31. Zoledronic acid inactivates GSK-3β exclusively in the nucleus. IMIM-PC-1 cells were treated with zoledronic acid (10 μM) for 72 h, nuclear and cytosolic extracts were immunoblotted with NFATc2, pGSK3β and GSK3β antibodies.

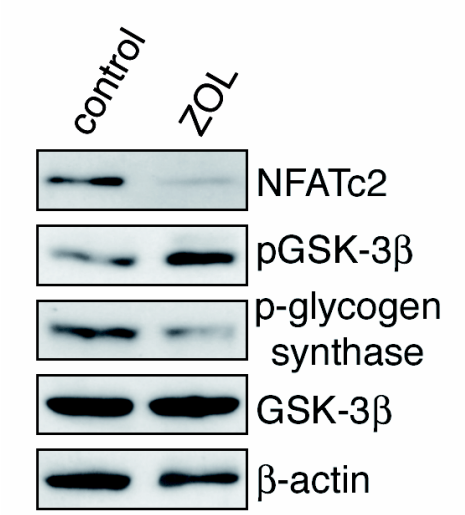

Fig. 32. Loss of GSK-3β activity reduces NFATc2 expression. MDA-MB-435 cells were treated with zoledronic acid (10 μM), after 72 h nuclear lysates were analyzed for expression of NFATc2, pGSK3β, p-glycogen synthase. Protein loading was controlled using β-actin antibodies.

These findings prompted us to investigate the role of GSK3β in NFATc2 stabilization. Therefore, we demonstrated that knockdown of GSK3β by siRNA in MDA-MB-435 cells resulted in a decreased level of NFATc2, as compared to controls (Fig. 33).

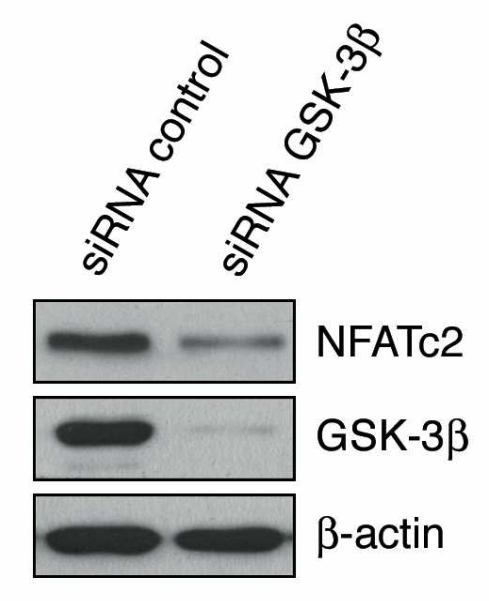

Fig. 33. GSK3β requires for NFATc2 stability. 8988t cells were transfected with GSK3β siRNA or control siRNA. After 24 h of transfection, lysates were immunoblotted with indicated antibodies. Protein loading was controlled by using β-actin antibodies.

To provide a causal and direct demonstration of the effect of GSK3β on NFATc2 stability, we used the GSK3β.S9A mutant which is Akt/PKB unresponsive. We transfected constitutively active (c.a.) GSK3β or vector control. Phophorylation of GSK3β at one key residue on serine 9 is required for its inactivation. Mutation of serine 9 to Alanine renders the GSK3β constitutively active. Upon zoledronic acid treatment, NFATc2 was totally rescued compared to control cells (Fig. 34). Taken together, these results show that phosphorylation of GSK3β at Ser9 by zoledronic acid, which inhibits GSK3β activity, is required for NFATc2 stability in the nucleus.

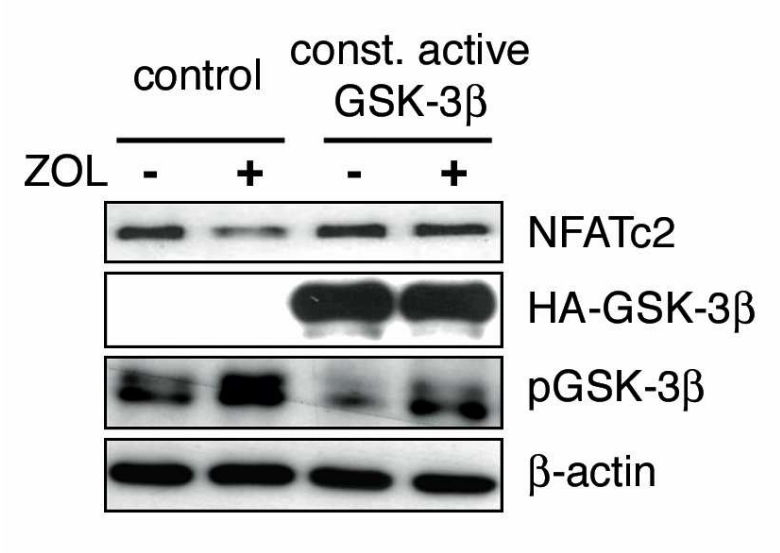

Fig. 34. Active GSK3β protects NFATc2 from zoledronic acid mediated proteasomal degradation. MDA-MB-435 cells were transfected with either vector control or constitutively active GSK3β (Ser 9 to Ala). After 18 h of transfection, cells were treated with zoledronic acid (10 μM) for 72 h in serum containing media. Total lysates were immunoblotted with NFATc2, HA-GSK3β or pGSK3β antibodies. Protein loading was controlled using β-actin antibodies.

4.7 GSK3β PHOSPHORYLATION AT THREE KEY RESIDUES ELEVATES CELLULAR NFATc2 LEVELS AND RESCUES IT FROM ZOLEDRONIC ACID MEDIATED PROTEASOMAL DEGRADATION

Finally, we investigated the mechanism by which zoledronic acid and GSK3β signaling attenuates NFATc2 degradation. Consistent with the results shown in Fig. 33, siRNA mediated silencing of GSK3β in MDA-MB-435 cells results in a marked reduction of NFATc2 protein. In contrast, using c.a. GSK3β mutants, rescued NFATc2 from being degraded under zoledronic acid treatment (Fig. 34).

Sequence analysis revealed that three key serine residues (Ser 213, Ser 217 and Ser 221) located within the N-terminal SP2 motif of NFATc2 and they are conserved in both human and mice (Kehlenbach et al., 2000; Beals et al., 1997) (Fig. 35). GSK3β is known to mediate NFATc2 phosphorylation at these sites (Beals et al., 1997). To further support the evidence that GSK3β mediated phosphorylation of NFATc2 alters its stability towards zoledronic acid mediated degradation, we investigated the effects of different doses of HDM2-mediated degradation of wild type (wt) NFATc2, NFATc2-pSP2, a phosphorylation-mimic mutant in which all three serine residues were substituted for Aspartic acid, and NFATc2-ΔSP2, a non-phosphorylation-mimic mutant in which all three serine residues were substituted for Alanine with two NFATc2 mutants. Interestingly, we could show that high doses of HDM2 declined protein level of wild type NFATc2 and notably, even more efficiently to NFATc2-ΔSP2 (Fig. 36B). However, high dose of HDM2 did not affect NFATc2-pSP2 on protein level. Together with the data shown in Fig. 36B, these results suggest that phosphorylation of NFATc2 at three key serine residues by GSk3β regulates NFATc2 protein stability as well as it keeps it away from HDM2 mediated degradation.

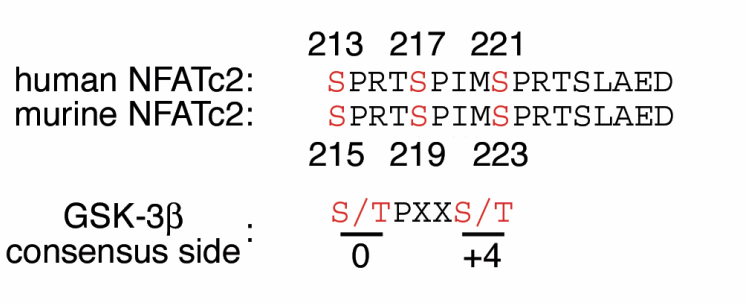

Fig. 35. GSK3β phosphorylation sites are conserved among human and mouse NFATc2. The putative GSK3β consensus sequences for possible phosphorylation sites on NFATc2 were P, proline; S, serine; T, threonine; and X, any amino acids.

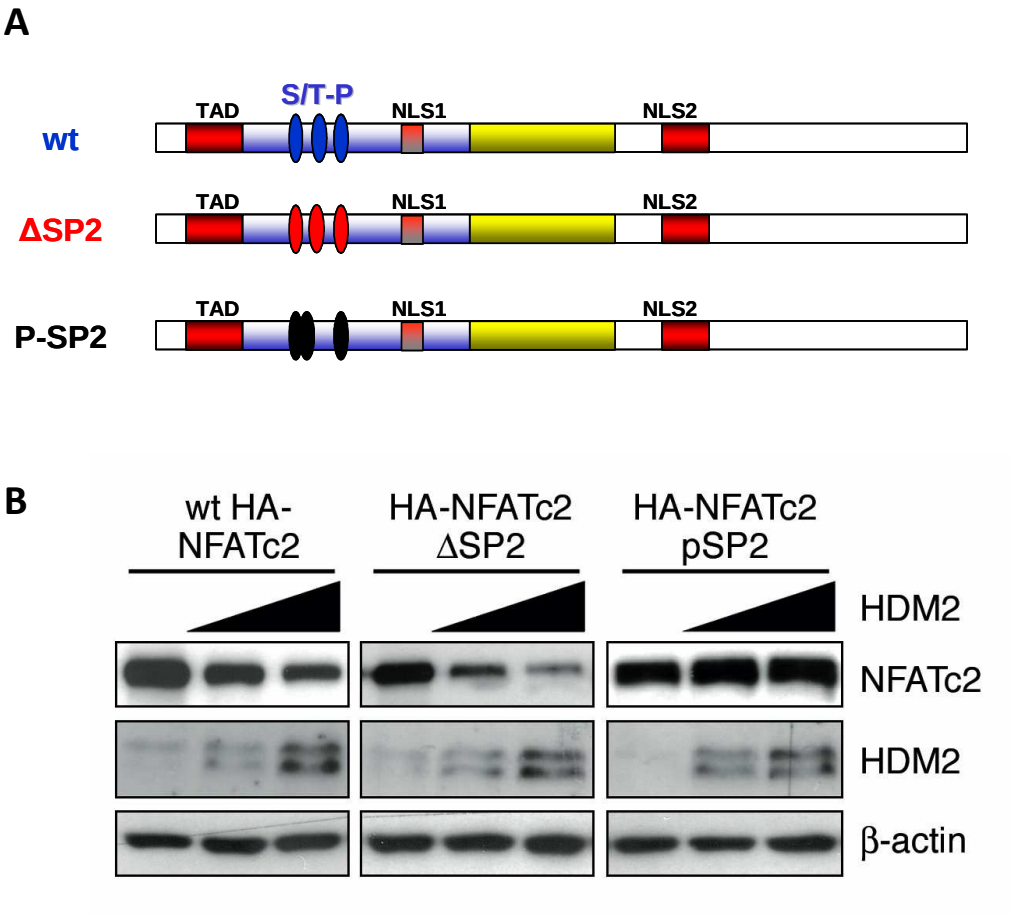

Fig. 36. Phosphorylation of S215/217/221 is crucial for NFATc2 stability. (A) Schematic representation of wild-type (WT) HA-NFATc2, NFATc2-ΔSP2 and NFATc2-pSP2 mutants, including the position of the putative NFATc2 phosphorylation (Ser 215, 217 and 219) sites. The described mutations in all three Ser are indicated in different colors. (B) MDA-MB-435 cells were co-transfected with the indicated wild-type (WT) HA-NFATc2 or mutants NFATc2-pSP2 and NFATc2-ΔSP2, either alone or in combination with different doses of HDM2, as indicated. Cell extracts were immunoblotted with either anti-HA or anti-HDM2.

To analyze the described effects of zoledronic acid on NFATc2 mutants in more detail, time kinetic experiments were conducted. Cells were exposed to 10 µM of zoledronic acid for up to 72 h and subcellular localization was analyzed by using immunofluorescence staining. As demonstrated in Fig. 37A, a dramatic down regulation or proteasomal degradation of NFATc2-ΔSP2 can be observed exclusively in the nucleus as early as after 24 h, whereas wild-type NFATc2 was degraded as early as 48 h after zoledronic

acid exposure. After 72 h of exposure, almost complete nuclear degradation of wild-type NFATc2 and NFATc2-ΔSP2 was detected. In contrast, phospho mimicking NFATc2-pSP2 mutants were widely expressed in the nucleus and were not degraded. This was consistent with our readout in context to dose dependent effects of HDM2. Therefore, in the next experiment, we examined the role of zoledronic acid mediated degradation of wild-type (wt) NFATc2 and the two NFATc2 mutants in the presence of MG132. Again, exposure of cells to zoledronic acid resulted in proteasomal degradation of wild-type NFATc2 and NFATc2-ΔSP2 protein, but this was completely reversed to control levels when cells were co-treated with MG132. As expected, the NFATc2-pSP2 mutant showed complete resistance against zoledronic acid mediated proteasomal degradation (Fig. 37B).

A

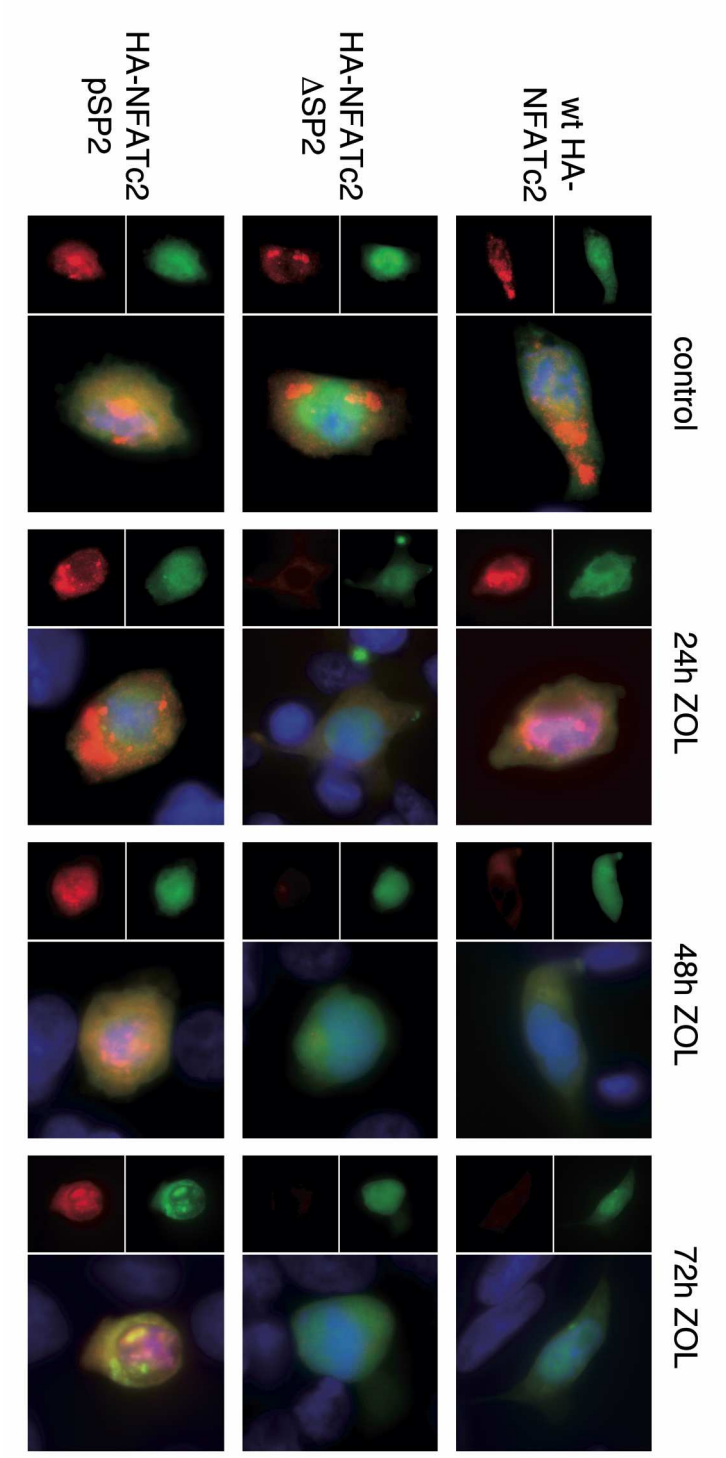
control
24h ZOL
48h ZOL
72h ZOL
wt HA-NFATc2
HA-NFATc2 ΔSP2
HA-NFATc2 pSP2

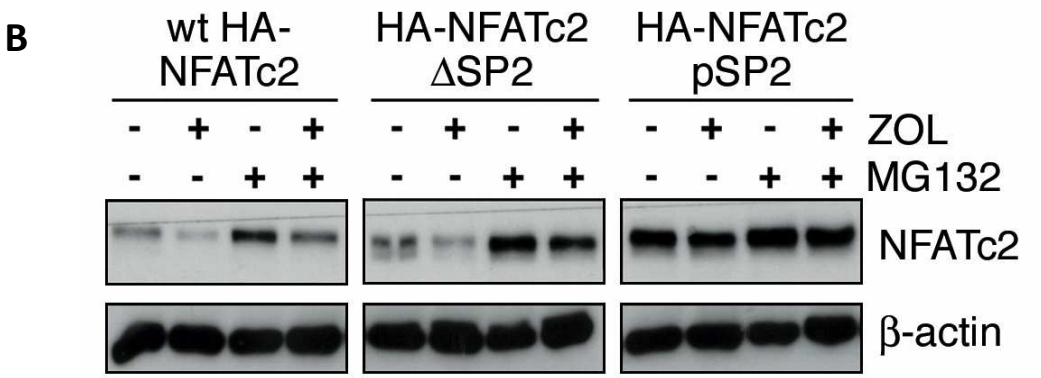

Fig. 37. NFATc2 phosphorylation on S215/217/221 renders NFATc2 resistant against zoledronic acid mediated proteasomal degradation. (A) Immunofluorescence detection of the indicated wild-type (WT) HA-NFATc2, NFATc2-ΔSP2, NFATc2-pSP2 and GFP control localization in MDA-MB-435 cells, after 18 h of transfection cells were treated with zoledronic acid (10 μM) at indicated time points. Cells were stained with anti-HA (red colour) and DAPI (blue) and GFP (green; original magnification for all: 63X). (B) MDA-MB-435 cells were transfected with the indicated wild-type (WT) HA-NFATc2 or mutants NFATc2-pSP2 and NFATc2-ΔSP2, after 18 h of transfection cells were treated with zoledronic acid (10 μM) for 32 h in complete media, then treated with MG132 (10 μM) for at least 12 h. After 72 h, cell lysates were immunoblotted with HA-antibodies.

We therefore assayed the ability of HDM2 to interact with and to induce ubiquitination and degradation of NFATc2. Co-immunoprecipitation studies showed that HDM2 readily interacts with endogenous NFATc2 exclusively in the nucleus in untreated cells (Fig. 38A). Therefore, we tested the association between HDM2 and NFATc2 mutants respectively. Surprisingly, all three NFATc2 constructs interacted with HDM2, even NFATc2-pSP2 interacted with HDM2 (Fig. 38B).

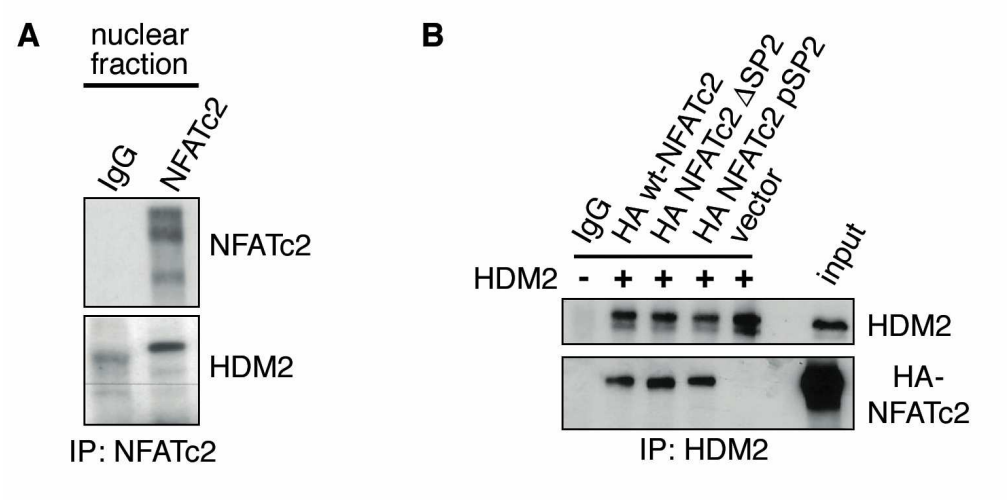

Fig. 38. E3 ligase HDM2 physically interacts with NFATc2 mutants exclusively in the nucleus. (A) Nuclear lysates from MDA-MB-435 cells were immunoprecipitated using endogenous anti-NFATc2 and control (IgG) antibodies, and immunoblotted using the indicated antibodies. (B) MDA-MB-435 cells were co-transfected with the indicated wild-type (WT) HA-NFATc2, NFATc2-ΔSP2, NFATc2-pSP2 and vector control in combination with HDM2, as indicated. After 24 h of transfection, nuclear lysates were immunoprecipitated using anti-HDM2 and control (IgG) antibodies, and immunoblotted using the indicated antibodies. Total cell lysates used as a input control to reveal the expression of HDM2 and HA-NFATc2.

However, to determine whether the interaction between NFATc2-pSP2, NFATc2-ΔSP2 and wt NFATc2 with HDM2, promotes NFATc2 ubiquitination dependent degradation, cells were transiently transfected with all three NFATc2 constructs and treated with zoledronic acid in the presence or absence of MG132. Ubiquitination of wild type NFATc2 and NFATc2 mutants was then examined. wt NFATc2 and NFATc2-ΔSP2 were heavily ubiquitinated, whereas NFATc2-pSP2 was resistant to zoledronic acid mediated ubiquitination and proteasomal degradation (Fig. 39). Taken together, these data show that the E3 ligase HDM2 serves for NFATc2 degradation, and the interaction between HDM2 and NFATc2 is independent from GSK3β kinase activity.

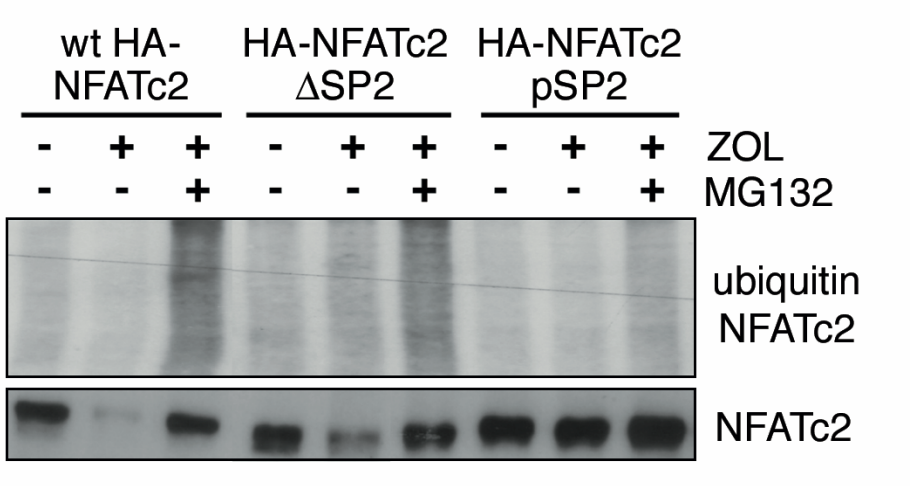

Fig. 39. NFATc2 phosphorylation on S215/217/221 is resistant against zoledronic acid mediated ubiquitination. MDA-MB-435 cells were transfected with the indicated wild-type (WT) HA-NFATc2 or mutants NFATc2-pSP2 and NFATc2-ΔSP2, after 18 h of transfection cells were treated with zoledronic acid (10 µM) for 32 h, then treated with MG132 (10 µM) for at least 12 h. After 48 h of treatment, nuclear HA-NFATc2 immunoprecipitates were immunoblotted with ubiquitin and HA-antibodies.

4.8 THE LYSINES 684 AND 897 OF NFATc2-SPECIFIC C-TERMINUS ARE POTENT UBIQUITINATION SITES

To assess the intracellular location of ubiquitination, we analyzed the individual ubiquitination sites within the N-terminus of NFATc2, we transfected constructs encoding HA-tagged NFATc2 or a deletion construct that covers the lysine rich N-terminus (NFATc2$^{1-460}$) and vector control in MDA-MB-231 cells. Notably, NFATc2$^{1-460}$ was not degraded, compared to wt NFATc2 after zoledronic acid treatment (Fig. 40B), suggesting that the C-terminus of NFATc2 is crucial for ubiquitination. For further confirmation, cells were transfected with constructs encoding HA-tagged NFATc2, either wild type (wt) or NFATc2$^{1-460}$. Interestingly, we found that wt-NFATc2 underwent ubiquitination, whereas NFATc2$^{1-460}$ did not show ubiquitination

in the presence of zoledronic acid and MG132, suggesting that the NFATc2 C-terminus contains ubiquitin binding sites (Fig. 40C).

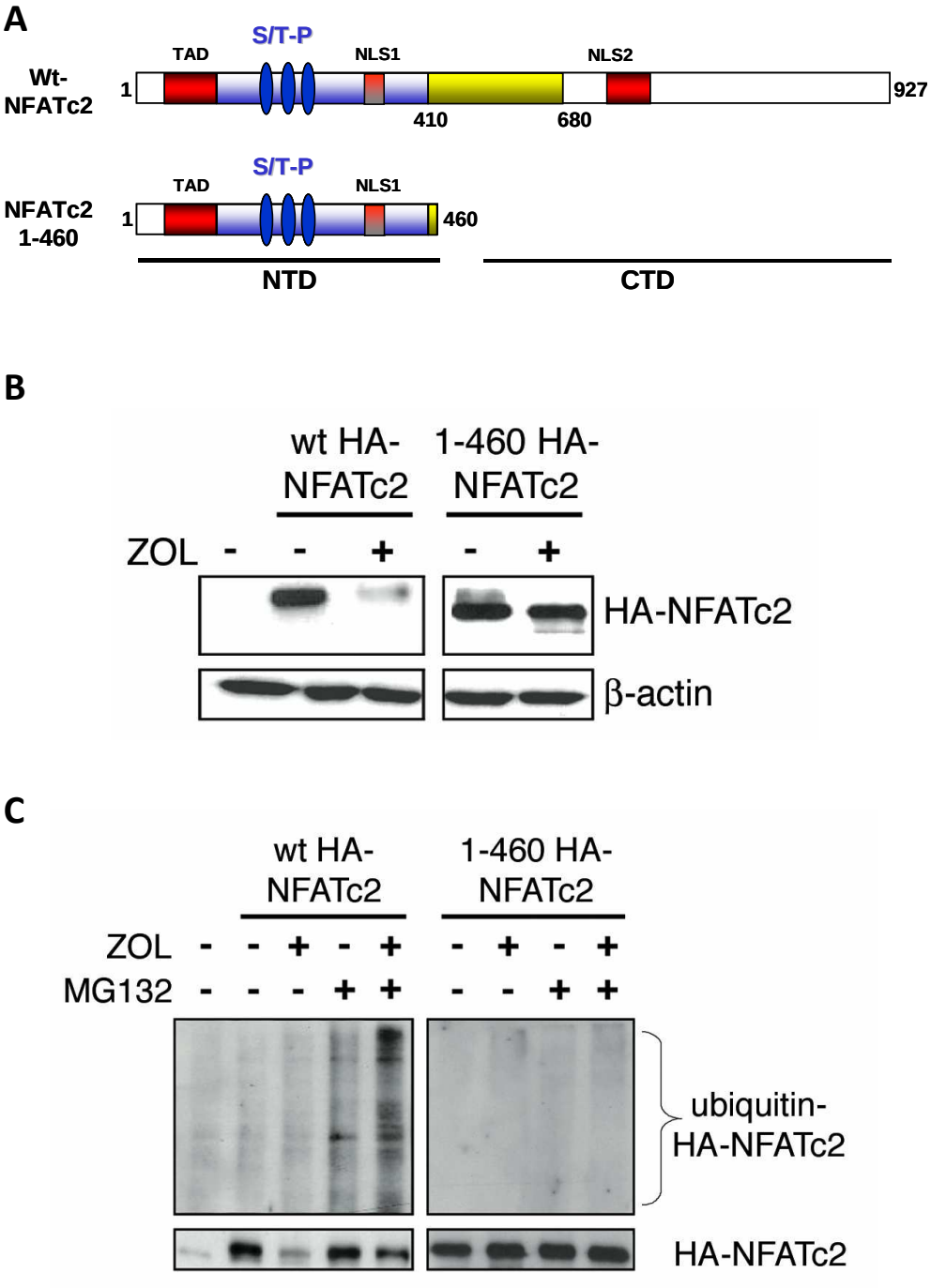

Fig. 40. C-terminal deletion of NFATc2 prevents zoledronic acid mediated ubiquitination and degradation of NFATc2. (A) Schematic representation of full length and C-terminus deletion of NFATc2 (B) MDA-MB-231 cells were transfected with either vector control or wild-type (WT) HA-NFATc2 and NFATc2$^{1-460}$. After transfection, cells were treated with zoledronic acid (10 μM) for 72 h in serum media. Total lysates were immunoblotted with HA- or β-actin antibodies (C) MDA-MB-231 cells were transfected with either vector

control or (WT) HA-NFATc2 or NFATc2$^{1-460}$. After 18 h of transfection cells were treated with zoledronic acid (10 µM) for 32 h in complete media, then treated with MG132 (10 µM) for at least 12 h. After 48 h cells were lysed and HA- or IgG immunoprecipitates were immunoblotted with ubiquitin and HA-antibodies.

However, despite the presence of multiple putative ubiquitin acceptor lysine residues, the NFATc2$^{1-460}$ mutant showed resistance to zoledronic acid induced ubiquitination and proteasomal degradation. The lysine-poor C-terminal domain of NFATc2 contains two previously reported lysine residues (K 684 and K 897), which have most recently been identified as target sites for the small ubiquitin-related modifier SUMO (Terui et al., 2004). Both lysines (K 684 and K 897) within the C-terminus region of NFATc2 fit to ubiquitination/sumoylation consensus sequences (ΦKXE: Φ, hydrophobic; K, lysine; X, any amino acid; E, glutamic acid) and are conserved in both humans and mice, respectively (Fig. 41A and 41B). To determine if the lysine residues of NFATc2 are serving as ubiquitination sites, we focused on Lys-684 and Lys-897. Therefore, we mutated the residue in each of these two sites to Arginine. Immunoblot was performed after transfecting MDA-MB-231 cells with constructs encoding HA-tagged NFATc2, either wild type (wt) or NFATc2^{K684} and NFATc2$^{K684/897R}$ in the presence of zoledronic acid. Interestingly, mutation of both the lysines in NFATc2$^{K684/897R}$ completely rescued from the proteasomal degradation compared to wt NFATc2 (Fig. 41C); the individual mutation of NFATc2^{K684} reduced proteasomal degradation.

A

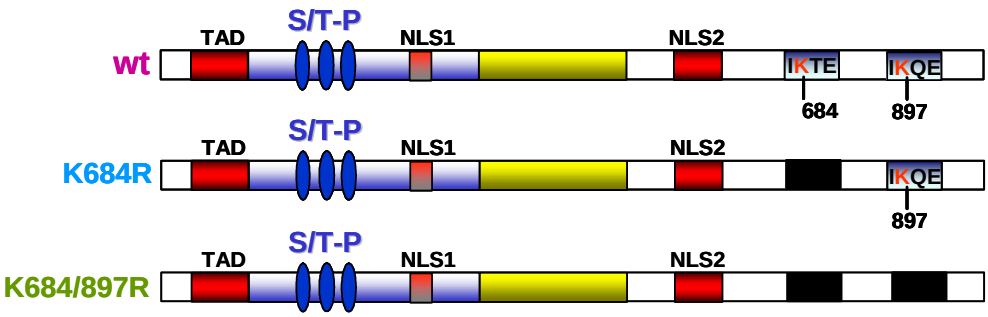

B

NFAC2_HUMAN 678 - PAI**K**TEPTDE 889 - PAGVTI**K**QEN

NFAC2_MOUSE 680 - PAI**K**TEPSDE 890 - PTGVTV**K**QEQ

Sumoylation consensus øKxE

C

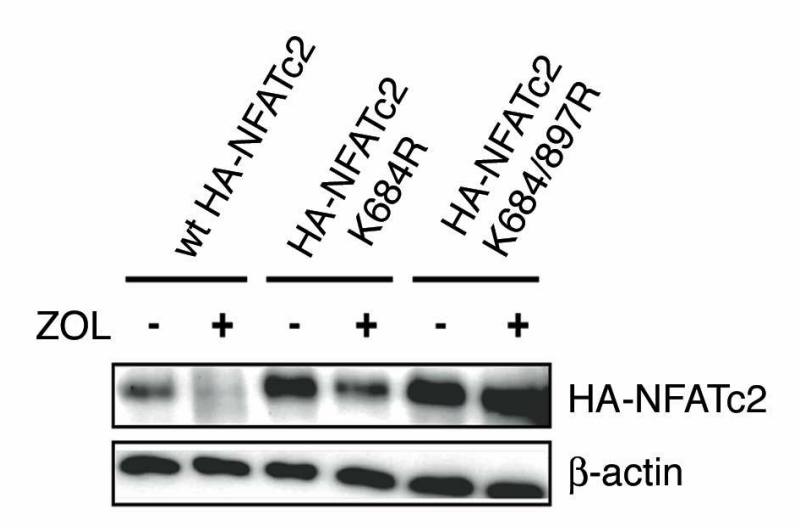

Fig. 41. The C-terminal domain of NFATc2 contains two putative ubiquitination/sumoylation sites. (A) Sequence analysis showed that C-terminus of NFATc2 contains two consensus sequences for priming ubiquitination/sumoylation sites (Φ KXE: Φ, hydrophobic; K, lysine; X, any amino acid; E, glutamic acid) on NFATc2 (B) Sumoylation/ubiquitination consensus sequences of NFATc2 are conserved in both human and mice (C) MDA-MB-231 cells were transfected with the indicated wild-type (WT) HA-NFATc2 or mutant NFATc2^{K684} and NFATc2$^{K684/897R}$ expression constructs, then treated with zoledronic acid (10 μM) for 72 h. Total lysates were immunoblotted with anti-HA or β-actin.

To further analyze the effects of zoledronic acid on subcellular localization of wild type (wt) or NFATc2$^{K684/897R}$ mutant by using immunofluorescence-staining, time kinetic experiments were performed as demonstrated in Fig. 42A. Consistently, we saw wild-type NFATc2 nuclear degradation, whereas NFATc2$^{K684/897R}$ mutant was widely expressed in the nucleus and not degraded. For further confirmation, IP experiments were performed after transfecting MDA-MB-231 cells with constructs encoding HA-tagged

NFATc2, either wild type (wt) or NFATc2$^{K684/897R}$ in the presence of zoledronic acid. As predicted, NFATc2$^{K684/897R}$ mutant significantly reduced NFATc2 ubiquitination and proteasomal degradation as compared to wt NFATc2, suggesting that both the C-terminus lysines (K-684 and K-897) are crucial for NFATc2 ubiquitination and proteasomal degradation (Fig. 42B).

A

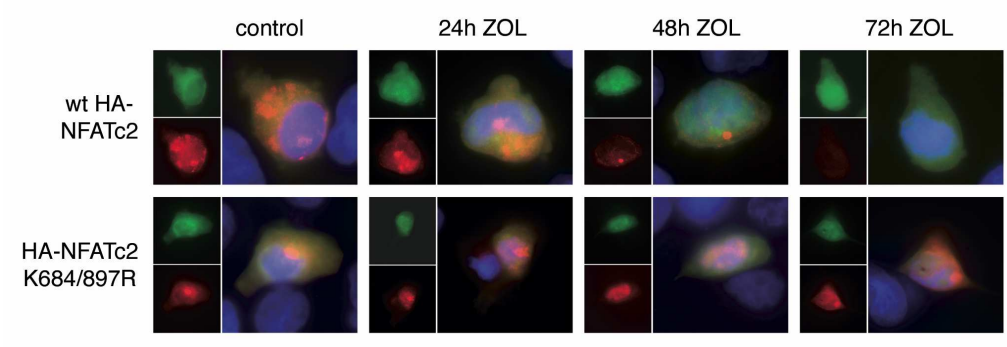

B

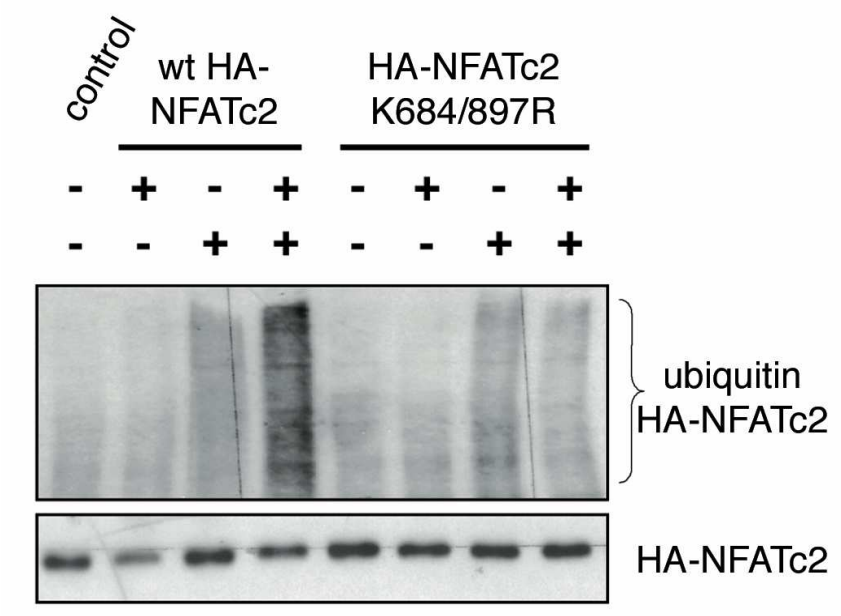

Fig. 42. Zoledronic acid induces NFATc2 ubiquitination and proteasomal degradation via two C-terminal lysines. (A) Immunocytological detection of the indicated wild-type (WT) HA-NFATc2, NFATc2$^{K684/897R}$ mutant and GFP control localization in MDA-MB-435 cells, after 18 h of transfection cells were treated with zoledronic acid (10 µM) in indicated time

points. Cells were stained with anti-HA (red) and DAPI (blue) and GFP (green; original magnification: 63X). (B) The indicated HA-NFATc2 constructs was transfected in MDA-MB-231 cells. After 18 h of transfection cells were treated with zoledronic acid (10 μM) for 32 h in complete media, then treated with MG132 (10 μM) for at least 12 h. After 48 h cells were lysed and NFATc2 immunoprecipitates were immunoblotted with ubiquitin and HA-antibodies.

To further determine the relevance of these two K-684 and K-897 lysines in the highly unstable NFATc2-ΔSP2 mutant, we mutated these two lysine residues to Arginine. Immunoblot was performed after transfecting MDA-MB-435 cells with constructs encoding HA-tagged NFATc2, either wild type (wt) or NFATc2-ΔSP2$^{K684/897R}$ in the presence of zoledronic acid. Interestingly, we found that NFATc2-ΔSP2$^{K684/897R}$ was resistant to proteasomal degradation by zoledronic acid compared with the NFATc2-ΔSP2 mutant (Fig. 43).

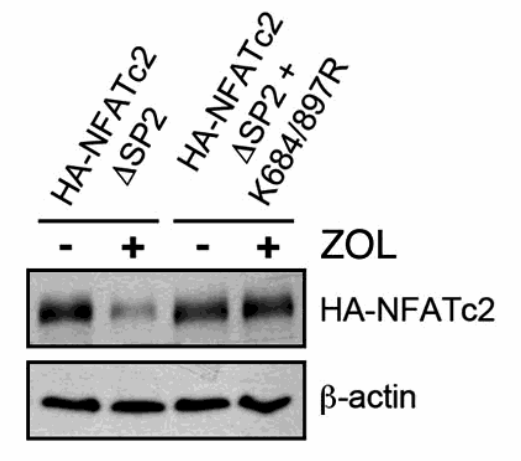

Fig. 43. The lysines K-684 and K-897 are crucial for zoledronic acid mediated proteasomal degradation. MDA-MB-435 cells were transfected with the indicated NFATc2-ΔSP2 and NFATc2-ΔSP2$^{K684/897R}$ constructs, then treated with zoledronic acid (10 μM) for 72 h. Total lysates were immunoblotted with anti-HA- or β-actin antibodies.

Next, we examined the effects of zoledronic acid on subcellular localization by using immunofluorescence staining. As demonstrated in Fig. 44, a clear proteasomal degradation of NFATc2-ΔSP2 can be observed exclusively in

the nucleus as early as 24h, and as expected, the NFATc2-ΔSP2$^{K684/897R}$ mutant was widely expressed in the nucleus and not degraded in comparison with the NFATc2-ΔSP2 mutant. Taken together, these data support that these two lysines (K-684 and K-897) residues are crucial for NFATc2 turnover.

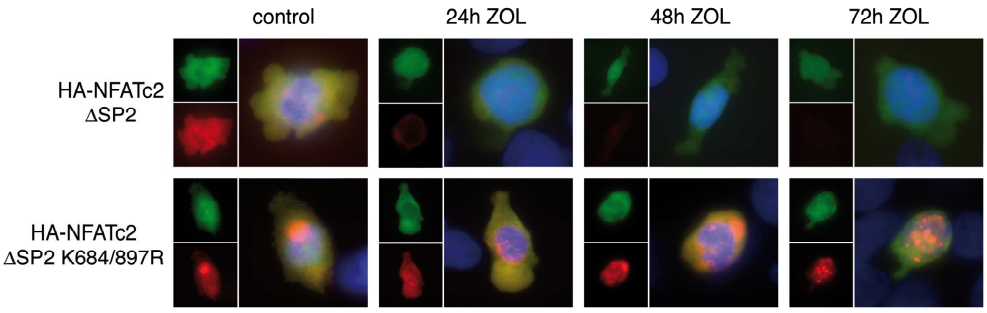

Fig. 44. Two lysine residues, K-684 and K-897, rescue the effect of zoledronic acid mediated degradation of NFATc2 (ΔSP2). Immunofluorescence detection of the indicated NFATc2-ΔSP2, NFATc2-ΔSP2$^{K684/897R}$ and GFP control localization in MDA-MB-435 cells, after 18 h of transfection cells were treated with zoledronic acid (10 μM) at indicated time points. Cells were stained with anti-HA (red) and DAPI (blue) and GFP (green; original magnification: 63X).

Recently, it has been shown that post-translational protein modification with small ubiquitin-related modifier (SUMO), triggers ubiquitin mediated proteasomal degradation (Breitenbach et al., 2008). To examine whether ubiquitination on NFATc2$^{K684/897R}$ mutant is sumoylation dependent, IP experiments were performed after transfecting MDA-MB-231 cells with constructs encoding HA-tagged NFATc2, either wild type (wt) or NFATc2$^{K684/897R}$, Flag-Sumo-1, E2 ligase Ubc-9 or vector control in the presence of zoledronic acid. Wt NFATc2 produced Sumo-specific bands in untreated cells whereas after treatment with zoledronic acid, Sumo-bands disappear. Significant ubiquitination on wt NFATc2 compare to untreated cells (Fig. 45) could be seen. Taken together, we neither see sumoylation nor does ubiquitination in NFATc2$^{K684/897R}$ mutants follow zoledronic acid treatment.

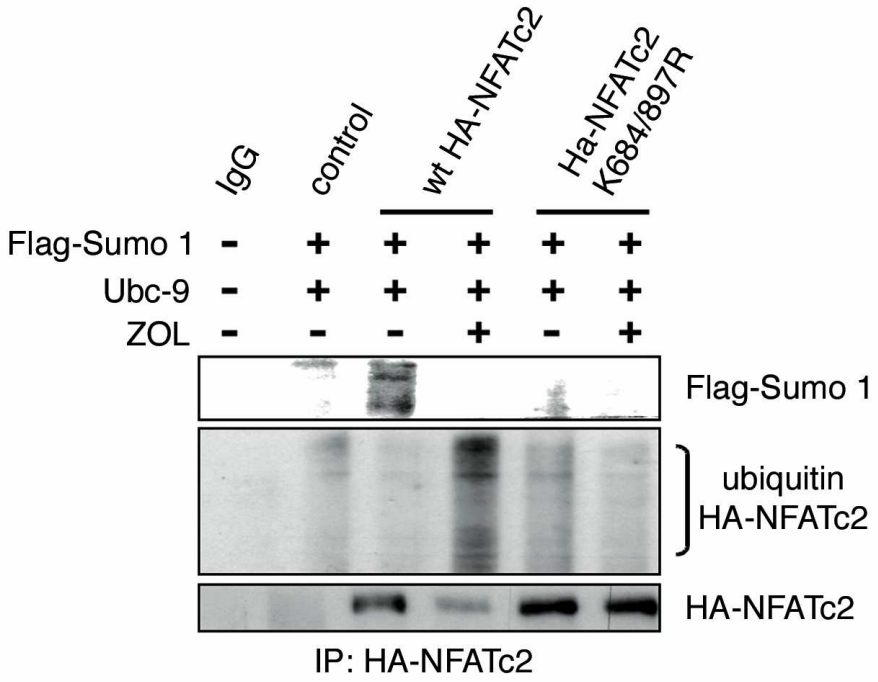

Fig. 45. Zoledronic acid induces NFATc2 ubiquitination and proteasomal degradation via two C-terminal lysines. MDA-MB-435 cells were co-transfected with the wild-type (WT) HA-NFATc2 or mutant NFATc2$^{K684/897R}$ or indicated Flag-Sumo-1 or Ubc-9 constructs. After 18 h of transfection cells were treated with zoledronic acid (10 µM) for 48 h in complete media, then lysates were analysed by HA-NFATc2 or IgG immunoprecipitates and immunoblotted with Flag-Sumo-1, ubiquitin and HA-antibodies.

5 DISCUSSION

5.1 ZOLEDRONIC ACID EXERTS STRONG ANTITUMORIGENIC ACTIVITIES IN BREAST AND PANCREATIC CANCER

Third generation nitrogen-containing bisphosphonates (N-BPs) such as zoledronic acid, are a class of antiresorptive drugs used to treat the benign and malignant skeletal diseases related with increased bone loss, e.g. Paget' disease, osteoporosis and metastasis related osteolysis (Rodan et al., 2002; Russell et al., 1999. After targeting the skeleton because of their high affinity for bone mineral, N-BPs primarily act by inhibiting osteoclastic bone resorption, thus alleviating the tumor-associated bone disease (Clezardin et al., 2005). However, in recent years, it has become clear from studies in preclinical models that these drugs also have potential antitumor activity.

In vitro and *in vivo* studies revealed inhibition of cancer cell proliferation, adhesion and invasion and demonstrated successful reduction of tumor outgrowth in mice bearing subcutaneous tumors derived from various epithelial tissues (Boissier et al., 2000; Pluijm et al., 1996). Concordantly, growing data from clinical trials emphasized strong tumor suppressor capacities of zoledronic acid and encourages its application in both adjuvant and palliative settings. A most recently published multi-center study supports application of the drug in an adjuvant setting and showed that zoledronic acid treatment most significantly reduces the risk of local

tumor recurrence and increases disease-free survival of patients with early breast cancer stages who underwent surgery (Gnant et al., 2009).

Though the therapeutic impact of zoledronic acid on cancer growth is now well established, it is still unclear, how these tumor suppressor activities are mediated in molecular level. We therefore conducted the presented study with the ambitious aim to identify signaling and transcription pathways with key roles in zoledronic acid growth suppression. We focused our attention on breast and pancreatic cancer and combined a battery of *in vitro* and *in vivo* approaches to address this issue.

As predicted from previous studies, we could show that zoledronic acid treatment indeed exerts strong growth suppressor functions in human cancer cell lines and in xenograft mice models as well. In detail, we observed that zoledronic acid effectively blocks cancer cell proliferation in most of the tested cell lines. Growth inhibition was apparent 24 h post treatment and reached a maximal effect 72 h following administration of the drug. Depending on the cell type, zoledronic acid applied at a dosage of 10 µM caused a 60-80% reduction of cell growth in most of the tested cancer cell lines, and this effect originated from a cell cycle arrest, as evidenced by a shift of cells from S to G1 phase of the cell cycle. Moreover, G1 arrest was paralleled by a reduction of cyclin D1 expression and its partner kinases CDK4 and CDK6, as evidenced by western blot analysis. We then analyzed whether the *in vitro* growth suppression also holds true in a biological system and assessed the therapeutic effect of the new generation bisphosphonate in a xenograft tumor mice model following subcutaneous injection of IMIM-PC1 pancreatic cancer cells. These experiments confirmed the *in vivo* potential of zoledronic acid to suppress cancer outgrowth and revealed a significant reduction in tumor mass over time.

5.2 ZOLEDRONIC ACID TARGETS NFATc2 TO MEDIATE GROWTH SUPPRESSION IN CANCER

NFATc2 belongs to the nuclear factor of activated T-cells (NFAT) family of transcription factors which are primarily recognized for their roles in T-lymphocyte activation (Crabtree et al., 1999; Crabtree et al., 2002; Rao et al.,1997). NFAT (nuclear factor of activated T cells) transcription factors were originally described as nuclear proteins that bind to and control the activity of the interleukin 2 (IL-2) promoter and further lymphokine promoters/ enhancers in T lymphocytes (Shaw et al., 1988),. Among the five members of the NFAT factor family the activity of four NFATc proteins (NFATc1, c2, c3 and c4) is controlled by the Ca++/calmodulin-dependent phosphatase calcineurin (CN) that, by dephosphorylating numerous sites within the regulatory region of NFAT, stimulates cytosolic-nuclear translocation.

In the nucleus, NFAT interacts with the A/TGGAAA consensus sequence of target gene promoters through a common DNA-binding domain (DBD) that has a moderate sequence similarity to the DBD of the Rel family of transcription factors (Hoey et al., 1995; Masuda et al., 1995; Rao et al., 1997). NFAT proteins can either activate or repress the transcription of their target genes, depending on the cell-type, the target promoter sequence they bind to, and the nuclear context at a given time (Macian et al., 2005; Rao et al., 1997). NFAT proteins also share a regulatory conserved N-terminal region called the NFAT homology region (NHR) that harbours multiple sites for post-translational modifications and serves as a structural platform for interaction with co-activators and repressor proteins such as p300/CBP, HDACs and other chromatin remodelling proteins (Clipstone et al., 1992; Shibasaki et al., 1996; Lopez-Rodriguez et al., 1999; Downes et al., 2000). Re-phosphorylation of nuclear NFATc2 also occurs at the N-

terminal region, and is achieved by the action of export kinases, including CK-2 and the GSK3β kinase (Kehlenbach et al., 2000; Beals et al., 1997). Thus, the activity of NFAT proteins is mainly regulated on the level of phosphorylation and subcellular distribution. However, although primarily identified and characterized in T-cells, NFAT proteins are by no means restricted to the immune system.

In fact, NFAT proteins participate in the regulation of genes influencing the development and differentiation of numerous mammalian cells and tissues. It has been shown, for instance, that NFAT proteins control multiple steps in myogenesis, chondrocyte differentiation and the development of the cardiovascular system (Crabtree et al., 2002; Im et al., 2004). Recent evidence also suggests that NFAT proteins, and in particular NFATc1 and NFATc2, control important aspects of carcinogenesis and influence cancer cell proliferation and apoptosis, and regulate peripheral vascular development during angiogenesis (Caetano et al., 2002; Baksh et al., 2002; Graef et al., 2003; Buchholz et al., 2006). Consistent with previous findings, we found overexpression of the factor in a series of breast and pancreatic cancer tissues and in all cancer cell lines. Our proliferation assays combined with knockdown approaches revealed strong growth promoting function of NFATc2 in these cancer types and demonstrated a profound block of cell proliferation and reduced expression of the G1-cell cycle promoting genes cyclin D1, CDK4 and CDK6 upon genetic silencing of the factor.

Most importantly and similar to our findings in animal studies, zoledronic acid treatment caused a dramatic reduction of NFATc2 expression and activity in cancer cells. The loss of NFATc2 was time-and dose-dependent and was exclusively found in cancer cells responsive to growth inhibition by this compound. Together, these observations accounted for the pro-

proliferative functions of NFATc2 and pointed at a potentially critical role of its silencing in zoledronic acid induced growth suppression.

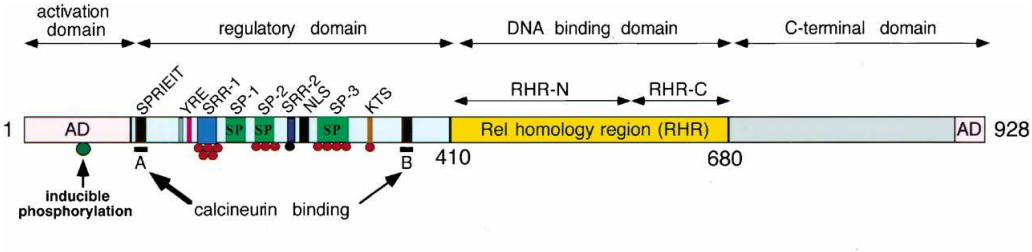

Fig. 46. Shematic representation of the NFAT domains. The regulatory domain is where calcineurin binding and dephosphorylation/phosphorylation occur. The red circles indicate phosphate groups that can be removed by calcineurin and the black circle on the SRR-2 domain indicates a phosphate group that can not be dephosphorylated by calcineurin. The A and B motifs indicate the calcineurin binding sites CnBP-A and CnBP-B (adapted from Hogan et al., 2003).

5.3 ZOLEDRONIC ACID DISRUPTS A NUCLEAR GSK3β NFAT STABILIZATION PATHWAY IN CANCER

Next, we performed an extensive series of cellular, biochemical and molecular studies to uncover the underlying mechanisms of NFATc2 inactivation by the bisphosphonate.

These studies revealed that decreased NFATc2 levels resulted from accelerated protein turnover rather than inhibition of gene expression. In fact, RT-PCR analyses showed unchanged level of mRNA expression upon treatment. However, application of MG-132, a cell-permeable and reversible inhibitor of proteasomal degradation, abolished NFATc2 down-regulation in cancer cells and this effect was paralleled by strong ubiquitination of NFATc2. We then performed subcellular fractionation

assays to control for the cellular distribution pattern of NFATc2 and to identify the cellular site of its degradation. In agreement with previous reports, we found NFATc2 distributed in both compartments and in different activation and phosphorylation status. Treatment with this compound, however, exclusively targeted NFATc2 when present in the nucleus and in its unphosphorylated, active form. Hyperphosphorylated NFATc2, on the other hand, was refractory to the bisphosphonate and thus remained stable, even after application of high doses. From these experiments reveal that the level of phosphorylation not only regulates NFATc2 activity and cellular localization (as described previously) but also determines its stability level and responsiveness to zoledronic acid.

5.4 EXISTENCE AND TARGETING OF A NUCLEAR GSK3β-NFATc2 STABILIZATION PATHWAY IN CANCER

The next step was to identify the NFATc2 kinase responsible for phosphorylation and stabilization of the transcription factor. We focused on glycogen synthase kinase 3β (GSK3β), which is a serine/threonine kinase with key functions in the regulation of various vital cellular processes ranging from glycogen metabolism and insulin signaling to embryonic development and carcinogenesis (Roberts et al., 2004; Henriksen et al., 2006; Lee et al., 2007). Depending on the tumor type, the subcellular distribution and the level of its activity, GSK3β can exert tumor suppressor activities as well as oncogenic functions. In pancreatic cancer, recent observations by Billadeau and coworkers suggested strong pro-proliferative functions of GSK3β (Ougolkov et al., 2006). Increased expression and nuclear localization levels were found in benign precursor lesions, termed

PanIN lesions, and with increased frequency and intensity in advanced cancers with a high proliferation rate.

Years ago, GSK3β was described as a nuclear export kinase that induces phosphorylation dependent nuclear-to-cytoplasmic translocation of NFATc2 in T-cells (Beals et al., 1997). In a very recent study, it has been postulated that GSK3β not only controls cellular shuttling but also the protein expression level of NFATc2 (Yoeli-lerner et al., 2009). It has been shown, for instance, that AKT-signaling through inhibition of GSK3β induces NFATc2 turnover in breast cancer cells, and this effect is ultimately linked to inhibition of tumor cell migration by activation of the Pi3K-AKT pathway (Yoeli-lerner et al., 2005). Prompted by these recent findings, we investigated whether GSK3β stabilizes NFATc2 in proliferating cancer cells and if so, whether this function is aimed by zoledronic acid.

We first analyzed the expression pattern of GSK3β in cancer and found high levels of the kinase in both pancreatic cancer and breast cancer tissues and cell lines and in co-localization with NFATc2. Like NFATc2, GSK3β was distributed throughout the cells with active fractions in the cytosolic and the nuclear compartment. Treatment with zoledronic, however, caused a dose-dependent inhibition of GSK3β kinase activity in the nucleus and this effect was paralleled by an accretive loss of NFATc2. Since introduction of a constitutive active GSK3β constructs antagonized NFATc2 degradation, we assumed the existence of a nuclear GSK3β-NFATc2 stabilization pathway that is disrupted by this compound. GSK3β phosphorylates its target substrates preferentially at the consensus sequence S/T-X-X-X-Phospho-S/T, where the first S/T residue is the target for GSK3β phosphorylation (Cohen et al., 2001, Harwood et al., 2001; Doble et al., 2003; Woodgett et al., 2003).

Sequence analysis of NFATc2 revealed the presence of three consensus GSK3β serine phosphorylation residues (S213, S217 and S221) located in the SP2 motif of the NFAT homology region. These phosphoserine residues are conserved among species and match with the previously characterized "phospho-degron" sequence through which GSK3β targets a subset of transcriptional regulators (e.g. c-Myc, SRC-3 and Notch-1) for phosphorylation dependent ubiquitination. The "phospho-degron" site is therefore recognized as a key identification code for GSK3β to label substrates for their subsequent turnover (Wu et al., 2007). For instance, phosphorylation of S505 by GSK3β marks the SRC-3 co-activator of STAT signaling for efficient ubiquitin transfer and rapid proteasomal degradation. Similarly, c-Myc phosphorylation by GSK3β at Threonine (58) provides the signal for its subsequent turnover by the proteasomal machinery (Gregory et al., 2003). We proposed that GSK3β also targets NFATc2 through the conserved "phospho-degron" sequence, in this case however, to protect the factor from ubiquitination and recognition by the 26S proteasome.

To verify our model, we generated NFATc2 mutations in which the "phospho-degron" elements were modified through substitution of S213/217/221 for either Alanine (NFATc2-ΔSP2) or Aspartic acid (NFATc2-pSP2). We then tested their remaining stability and responsiveness to zoledronic acid. These experiments performed in breast and pancreatic cancer cells confirmed the significance of the "phospho-degron" sites and demonstrated a high protein turnover of NFATc2 following mutational inactivation of the GSK3β phosphoserines. Moreover, introduction of GSK3β resistant mutations rendered NFATc2 highly unstable, led to reduced lifetime duration and caused accelerated degradation of the factor upon treatment with by zoledronic acid. The significance of phosphorylation by GSK3β was underscored by phospho-mimicking mutations which caused increased NFATc2 stabilization and fully protected

the transcription factor from nuclear ubiquitin transfer and degradation by the compound.

Taken together, these experiments identified the presence of a nuclear GSK3β-NFATc2 stabilization pathway that is aimed and disrupted by zoledronic acid to mediate anti-tumoral functions. Moreover, these findings contribute to a better understanding of how GSK3β and NFATc2 cooperate in tumor cell proliferation. It will be of great interest to identify under which conditions, GSK3β favors stabilization over degradation of key cell cycle regulators in cancer, and to verify whether this decision happens in a tumor-type dependent manner or is regulated by the nuclear context. It will also be of interest to investigate the anti-tumorigenic capacity of zoledronic acid in tumor types other than pancreatic and breast cancers, and to analyze whether the drug targets additional pro-proliferative pathways other than the GSK3β-NFAT signaling cascade to suppress tumor growth.

5.5 CHARACTERIZATION OF ZOLEDRONIC ACID MEDIATED NFATc2 UBIQUITINATION IN CANCER

To better understand the ubiquitination of NFATc2 which leads to degradation of this protein, we performed sequence analysis which revealed the presence of multiple putative ubiquitin acceptor lysine residues within the N-terminal domain.

Consequently, to determine whether the N-terminus is target for ubiquitination, we transfected cells with wt-NFATc2 or a deletion construct that encompasses the lysine rich N-terminus ($NFATc2^{1-460}$). Surprisingly, despite the presence of multiple putative ubiquitin acceptor sites,

treatment with the compound failed to induce ubiquitination and degradation of NFATc2$^{1-460}$. Analysis of the C-terminus, on the other hand, displayed two additional lysines residues (K-684 and K-897) which have most recently been identified as target sites for the small ubiquitin-related modifier SUMO (Terui et al., 2004). SUMO-1 shares similarity with ubiquitin and can be attached covalently to lysine residues in a process that is mechanically analogous to ubiquitination. Sumoylation involves the formation of an iso-peptide bond between the carboxy-terminal Gly of SUMO and the ε-amino group of a lysine side chain in the target protein (Hay et al., 2005).

Prompted by recent findings indicating that SUMO and ubiquitin can actually target the same lysine residues of common substrates, we tested the relevance of K-684 and K-897 in NFATc2 ubiquitination. Double mutation of both lysines (NFATc2$^{K684/897R}$) indeed prevented the transfer of ubiquitin and consequently abolished degradation upon treatment, indicating that K-684/897 ubiquitination is key for the NFATc2 turnover. In support of this conclusion, the highly unstable NFATc2-ΔSP2 mutant became fully resistant to zoledronic acid upon mutational disruption of the two ubiquitin acceptor sites (NFATc2-ΔSP2$^{K684/897R}$).

Ubiquitination is arranged through the action of E3 ligases which conjugate ubiquitin to target proteins and thus label them for subsequent degradation by the 26S proteasome. HDM2, the human homolog of the RING-finger ligase MDM2 (murine double minute 2) is often present at increased levels in tumors with wild-type p53 and likely serves as an alternate mechanism to disrupt the p53 pathway in developing cancer cells (Haupt et al., 1997; Fang et al., 2000). However, HDM2 also targets numerous other substrates, particularly in p53 mutant cancer cells and when present at elevated levels (Iwakuma et al., 2003; Lozano et al.,2003). Overexpression of HDM2 can result from gene amplification, increased transcription or enhanced translation and has been reported in

glioblastomas and malignant melanomas but also in pancreatic and breast cancer (Haupt et al., 1997; Kubbutat et al., 1997; Honda et al., 1997).

We questioned whether HDM2 is the E3-ligase responsible for zoledronic acid mediated NFATc2 ubiquitination and degradation. Weak to moderate HDM2 expression levels were found in all tested cell lines. Surprisingly, however, zoledronic acid dose-dependently enhanced the total amount and nuclear expression of endogenous HDM2 and this effect correlated inversely to the progredient loss of NFATc2. Moreover, we were able to demonstrate that HDM2 physically interacts with and induces degradation of NFATc2 in the nucleus and when present in its unphosphorylated version. Phosphorylated NFATc2, on the other hand, was proven to be resistant to HDM2 – as it is to zoledronic acid – and thus remains unaffected and stable. Finally, the crucial role of HDM2 in zoledronic acid mediated NFATc2 degradation and growth suppression is highlighted by HDM2 silencing experiments, demonstrating that HDM2 depletion not only obviates NFATc2 degradation and the consequent reduction of G1-phase promoting genes, but impairs growth retardation by the compound.

Therefore, this data identified HDM2 as the molecular machinery responsible for the ubiquitin transfer to unphosphorylated NFATc2 in response to zoledronic acid.

5.6 SIGNIFICANCE AND CONCLUSION OF THIS DISSERTATION

Taken together, this study identifies the pro-proliferative transcription factor NFATc2 as a master target of zoledronic acid in cancer. We show that proteasomal degradation of NFATc2 is a key event in zoledronic acid

mediated cancer growth suppression. Mechanistically, zoledronic acid inhibits nuclear GSK3β kinase and thereby impairs phosphorylation-dependent NFATc2 stabilization. In addition, bisphosphonate increases the accumulation of E3-ligase HDM2 in the nucleus of cancer cells to target unphosphorylated NFATc2 for ubiquitin transfers subsequent proteasomal degradation, resulting in a halt of cancer cells at the G1-cell cycle phase.

From the medical point of view, this work constitutes a highly descriptive molecular study on the mechanisms of action of zoledronic acid tumor suppression activity. Our study thus contributes to a better understanding at molecular and biochemical basis underlying one of the most promising and exciting new treatment for malignant disease. Biochemically, we outlined a defined pathway mediating the effects of zoledronic acid, discovering novel mechanisms for growth suppression that involucrate several molecules which can be potential additional targets for therapies which may complement zoledronic acid treatment. For instance, treatment with this drug lead to an accumulation of nuclear HDM2 and inhibition of GSK3β kinase in order to disrupt phosphorylation-dependent NFATc2 stabilization. HDM2 targets unphosphorylated NFATc2 for ubiquitin transfer and induces its proteasomal degradation, resulting in loss of NFAT transcriptional responses and a block of cancer cell growth.

Therefore, this study contributes to both the basic biochemical knowledge on cell cycle arrest but also reveals medical information of paramount importance to patients by providing a well-characterized example of pathways that mediate the beneficial effect of zoledronic acid.

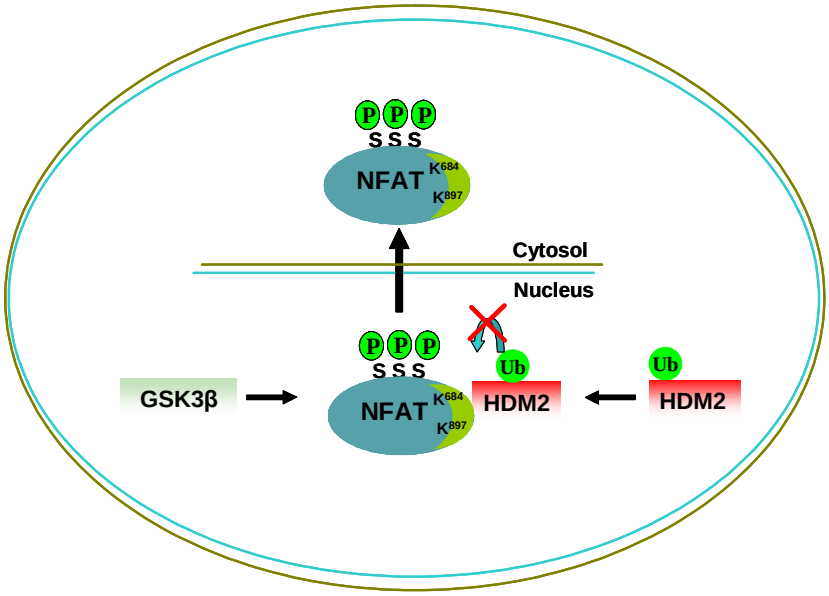

Fig. 47. Model showing NFATc2 stabilization in untreated cancer cells. GSK3β mediated phosphorylation of three serine residues protects NFATc2 from HDM2 mediated ubiquitination and proteosomal degradation.

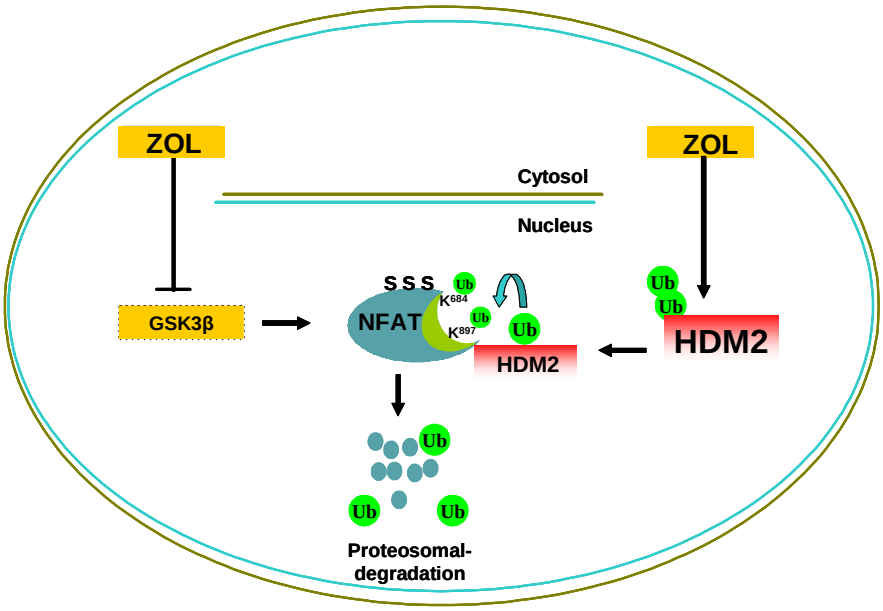

Fig. 48. Model showing the effect of zoledronic acid mediated ubiquitination and proteasomal degradation of NFATc2 in cancer cells. Loss of GSK3β activity by zoledronic acid, exposed two Lysines K-684 and K-897 of NFATc2 for ubiquitination and proteosomal degradation by HDM2.

6 REFERENCES

Alvarez E, Galbreath EJ, Westmore M. 2002. Properties of bisphosphonates in the 13762 syngeneic rat mammary carcinoma model of tumor induced bone resorption. Proc Am Ass Cancer Res. 43: 316.

Aparicio A, Gardner A, Tu Y, Savage A, Berenson J, Lichtenstein A. 1998. In vitro cytoreductive effects on multiple myeloma cells induced by bisphosphonates. Leukemia. 12: 220-229.

Bachelder RE. 2005. Glycogen synthase kinase-3 is an endogenous inhibitor of Snail transcription: implications for the epithelial-mesenchymal transition.The Journal of cell biology. 168: 29-33.

Benford HL, McGowan NW, Helfrich MH, Nuttall ME, Rogers MJ. 2001. Visualization of bisphosphonate-induced caspase-3 activity in apoptotic osteoclasts in vitro. Bone. 28: 465–473.

Body JJ, Diel IJ, Lichinitser MR, Kreuser ED, Dornoff W, Gorbunova VA, Budde M, Bergström B. 2003. Intravenous ibandronate reduces the incidence of skeletal complications in patients with breast cancer and bone metastases. Ann Oncol. 14: 1399-1405.

Boissier S, Ferreras M, Peyruchaud O, Magnetto S, Ebetino FH, Colombel M, Delmas P, Delaissé JM, Clézardin P. 2000. Bisphosphonates inhibit breast and prostate carcinoma cell invasion, an early event in the formation of bone metastases. Cancer Res. 60: 2949-2954.

Boissier S, Ferreras M, Peyruchaud O. 2000. Bisphosphonates inhibit breast and prostate carcinoma cell invasion, an early event in the formation of bone metastases. Cancer Res. 60: 2949-2954.

Boissier S, Magnetto S, Frappart L. 1997. Bisphosphonates inhibit prostate and breast carcinoma cell adhesion to unmineralized and mineralized bone extracellular matrices. Cancer Res. 57: 3890-3894.

Buchholz M, Schatz A, Wagner M, Michl P, Linhart T, Adler G, Gress TM, Ellenrieder V. 2006. Overexpression of c-myc in pancreatic cancer caused by ectopic activation of NFATc1 and the Ca2+/calcineurin signaling pathway. EMBO J. 25 (15):3714-3724.

Cadigan KM, Liu Y. 2006. Wnt signaling: complexity at the surface. J Cell Sci 119: 395–402.

Caraglia M, Marra M, Leonetti C, Meo G, D'Alessandro AM, Baldi A, Santini D, Tonini G, Bertieri R, Zupi G, Budillon A, Abbruzzese A. 2007. R115777 Zarnestra)/Zoledronic acid (Zometa) cooperation on inhibition of prostate cancer proliferation is paralleled by Erk/Akt inactivation and reduced Bcl-2 and bad phosphorylation. J Cell Physiol. 211: 533-43.

Clezardin P, Ebetino FH, Fournier PG. 2005. Bisphosphonates and cancer-induced bone disease: beyond their antiresorptive activity. Cancer Res 65: 4971–4974

Clipstone NA, Crabtree GR. 1992. Identification of calcineurin as a key signaling enzyme in T-lymphocyte activation. Nature. 357: 695-697.

Corey E, Brown LJ, Quinn JE, Poot M, Roudier MP, Higano CS. 2003. Zoledronic acid exhibits inhibitory effects on osteoblastic and osteolytic metastases of prostate cancer. Clin Cancer Res. 9: 295–306.

Corey E, Quinn JE, Brown LG, Roudier MPM, Higano C, Vessella RL. 2001. Examination of the effects of zoledronic acid on prostate cancer. J Bone Miner Res. 16: S192

Costa L. 2007. Bisphosphonates: Reducing the risk of skeletal complications from bone metastasis. Breast. 16: 16-20.

Coxon FP, Rogers MJ. 2003. The role of prenylated small GTP-binding proteins in the regulation of osteoclast function. Calcif Tissue Int. 72: 80–84.

Crabtree GR, Olson EN. 2002. NFAT signaling: choreographing the social lives of cells. Cell Suppl. 109: S67–S79

Croucher P, De Raeve H, Perry M. 2002. Zoledronic acid prevents the development of osteolytic bone disease and increases survival in a murine model of multiple myeloma. Bone. 30: 39S

Dannenberg L, Schuijff M, Dekker M, van der Valk, Riele T. 2004. Tissue-specific tumor suppressor activity of retinoblastoma gene homologs p107 and p130. Genes Dev. 18: 2952-62

Derenne S, Amiot M, Barillé S. 1999. Zoledronate is a potent inhibitor of myeloma cell growth and secretion of IL-6 and MMP-1 by the tumoral environment. J Bone Miner Res. 14: 2048-2056.

Doble BW, Woodgett JR. 2003. GSK-3: tricks of the trade for a multi-tasking kinase. J Cell Sci 116: 1175–1186.

Downes M, Ordentlich P, Kao HY, Alvarez JG, Evans RM. 2000. Identification of a nuclear domain with deacetylase activity. Proc. Natl. Acad. Sci. U. S. A. 97: 10330-10335

Duivenvoorden WCM, Vukmirović-Popović S, Kalina M, Seidlitz E, Singh G. 2007. Effect of zoledronic acid on the doxycycline-induced decrease in tumor burden in a bone. British J cancer. 96:1526–1531.

Dunford JE, Thompson K, Coxon FP, Luckman SP, Hahn FM, Poulter CD. 2001. Structure–activity relationships for inhibition of farnesyl diphosphate synthase in vitro and inhibition of bone resorption in vivo by nitrogen-containing bisphosphonates. J Pharmacol Exp Ther. 296: 235–242.

Fang S, Jensen JP, Ludwig RL, Vousden KH, Weissman AM. 2000. Mdm2 is a RING finger-dependent ubiquitin protein ligase for itself and p53. J. Biol. Chem. 275: 8945-8951

Frame S, Cohen P, Biondi RM. 2001. A common phosphate binding site explains the unique substrate specificity of GSK3 and its inactivation by phosphorylation. Mol Cell 7: 1321–1327.

Frame S, Cohen P. 2001. GSK3 takes centre stage more than 20 years after its discovery. Biochem J. 359: 1–16

Fromigue O, Lagneaux L, Body JJ. 2000. Bisphosphonates induce breast cancer cell death in vitro. J Bone Miner Res. 15: 2211-2221.

Fuchs SY, Adler V, Buschmann T, Wu X, Ronai Z. 1998. Mdm2 association with p53 targets its ubiquitination. Oncogene. 17: 2543-2547

Glickman MH, Ciechanover A. 2002. The ubiquitin-proteasome proteolytic pathway: Destruction for the sake of construction. Physiol Rev. 82: 373-428.

Gnant M, Mlineritsch B, Schippinger W, Luschin-Ebengreuth G, Pöstlberger C, Menzel C, Jakesz R, Seifert M, Hubalek M, Bjelic-Radisic V, Samonigg H, Tausch C, Eidtmann H, Steger G, Kwasny W, Dubsky P, Fridrik M, Fitzal F, Stierer M, Rücklinger E, Greil R, Marth C. 2009. Endocrine therapy plus zoledronic acid in premenopausal breast cancer. N Engl J Med. 360: 679-691.

Green J, Gschaidmeier H, Yoneda T, Mundy G. 2000. Zoledronic acid potently inhibits tumor-induced osteolysis in two models of breast cancer metastasis to bone. Ann Oncol. 11: 14.

Hall DG, Stoica G. 1994. Effect of the bisphosphonate risedronate on bone metastases in a rat mammary adenocarcinoma model system. J Bone Miner Res. 9: 221-230

Harwood AJ. 2001. Regulation of GSK-3: a cellular multiprocessor. Cell 105: 821–824.

Haupt Y, Maya R, Kazaz A, Oren M. 1997. Mdm2 promotes the rapid degradation of p53. Nature 387: 296-9.

Hay RT. 2005. SUMO: a history of modification. Mol. Cell 18: 1–12

Hay RT. 2007. SUMO-specific proteases: a twist in the tail. Trends Cell Biol. 17: 370–376.

Henriksen EJ, Dokken BB. 2006. Role of glycogen synthase kinase-3 in insulin resistance and type 2 diabetes. Curr Drug Targets 7: 1435–1441.

Hershko A, Ciechanover A. 1998. The ubiquitin system. Annu Rev Biochem 67: 425-79.

Hiraga T, Williams PJ, Ueda A, Tamura D, Yoneda T. 2004. Zoledronic acid inhibits visceral metastases in the 4T1/luc mouse breast cancer model. Clin Cancer Res. 10: 4559–4567.

Honda R, Tanaka H, Yasuda H. 1997. Oncoprotein MDM2 is a ubiquitin ligase E3 for tumor supressor p53. FEBS Lett. 420: 25-7.

Hughes DE, Wright KR, Uy HL, Sasaki A, Yoneda T, Roodman GD, Mundy GR, Boyce BF. 1995. Bisphosphonates promote apoptosis in murine osteoclasts in vitro and in vivo. J Bone Miner Res. 10: 1478-1487.

Ikeda F, Dikic I. 2008. Atypical ubiquitin chains: new molecular signals. 'Protein Modifications: Beyond the Usual Suspects' review series. EMBO Rep. 9: 536–542.

Jagdev RE, Coleman CM, Shipman HA, Rostami, Croucher PI. 2001. The bisphosphonate, zoledronic acid, induces apoptosis of breast cancer cells: evidence for synergy with paclitaxel. Br J Cancer 84: 1126–1134.

Kim SJ, Uehara H, Yazici S, He J, Langley RR, Mathew P. 2005. Modulation of bone microenvironment with zoledronate enhances the therapeutic effects of STI571 and paclitaxel against experimental bone metastasis of human prostate cancer. Cancer Res. 65: 3707–3715.

Kohno N, Aogi K, Minami H, Nakamura S, Asaga T, Iino Y, Watanabe T, Goessl C, Ohashi Y, Takashima S. 2005. Zoledronic acid significantly reduces skeletal complications compared with placebo in Japanese women with

bone metastases from breast cancer: a randomized, placebo-controlled trial. J. Clin. Oncol. 23: 3314–3321.

Korpal M, Yan J, Lu X, Xu S, Lerit DA, Kang Y. 2009. Imaging transforming growth factor-β signaling dynamics and therapeutic response in breast cancer bone metastasis. Nat Med. 15: 960-6.

Kubbutat MH, Jones SN, Vousden KH. 1997. Regulation of p53 stability by Lallemand-Breitenbach V. 2008. Arsenic degrades PML or PML–RARα through a SUMO-triggered RNF4/ubiquitin-mediated pathway. Nature Cell Biol. 10: 547–555.

Lee J, Kim MS. 2007. The role of GSK3 in glucose homeostasis and the development of insulin resistance. Diabetes Res Clin Pract. 77: 49–57.
Lee MV, Fong EM, Singer FR, Guenette RS. 2001. Bisphosphonate treatment inhibits the growth of prostrate cancer cells. Cancer Res. 61: 2602–2608.

Lee YP, Schwarz EM, Davies M, Jo M, Gates J, Zhang X. 2002. Use of zoledronate to treat osteoblastic versus osteolytic lesions in a severe-combined-immunodeficient mouse model. Cancer Res. 62: 5564–5570.

Lilian S, Florian S, Harald S, Lilian S, Rüdiger G. 2008. The bisphosphonate zoledronic acid inhibits the growth of HCT-116 colon carcinoma cells and induces tumor cell apoptosis. Apoptosis. 13:782-9.

Lowe LC, Senaratne SG, Colston KW. 2005. Induction of apoptosis in breast cancer cells by apomine is mediated by caspase and p38 mitogen activated protein kinase activation. Biochem Biophys Res Commun. 329: 772-779.

Luckman SP, Hughes DE, Coxon FP, Russell RJ, Rogers MJ. 1998. Nitrogen-containing bisphosphonates inhibit the mevalonate pathway and prevent post-translational prenylation of GTPbinding proteins, including Ras. J Bone Miner Res. 13: 581–589.

Luo C, Shaw KT, Raghavan A, Aramburu J, Garcia-Cozar F, Perrino BA, Hogan PG, Rao A. Interaction of calcineurin with a domain of the transcription factor NFAT1 that controls nuclear import. 1996. Proc Natl Acad Sci U S A. 20: 8907-12.

Macian F. 2005. NFAT proteins: key regulators of T-cell development and function. Nat Rev Immunol. 5: 472-484.

Magnetto S, Boissier S, Delmas PD, Clézardin P. 1999. Additive antitumor activities of taxoids in combination with the bisphosphonate ibandronate against invasion and adhesion of human breast carcinoma cells to bone. Int J Cancer. 83: 263-269.

Mahajan R, Delphin C, Guan T, Gerace L, Melchior F. 1997. A small ubiquitin-related polypeptide involved in targeting RanGAP1 to nuclear pore complex protein RanBP2. Cell 88: 97–107.

Martin TJ, Moseley JM. 2000. Mechanisms in the skeletal complications of breast cancer. Endocr Relat Cancer. 7: 271-284.

Matsumoto S, Kimura S, Segawa H, Kuroda J, Yuasa T, Sat K. 2005. Efficacy of the third-generation bisphosphonate, zoledronic acid alone and combined with anti-cancer agents against small cell lung cancer cell lines. Lung Cancer 47: 31–39.

Matunis MJ, Coutavas E, Blobel G. 1996. A novel ubiquitin-like modification modulates the partitioning of the Ran-GTPase-activating protein RanGAP1 between the cytosol and the nuclear pore complex. J. Cell Biol. 135: 1457–1470.

McCaffrey PG, Luo C, Kerppola TK, Jain J, Badalian TM, Ho AM, Burgeon E, Lane WS, Lambert JN, Curran T, Verdine GL, Rao A, Hogan PG. 1993. Isolation of the cyclosporin-sensitive T cell transcription factor NFATp. Science. 262: 750-754

Michigami T, Hiraga PJ, Williams M, Niewolna R, Nishimura, Mundy GR. 2002. The effect of the bisphosphonate ibandronate on breast cancer metastasis to visceral organs. Breast Cancer Res Treat. 75: 249-58.

Mönkkönen PP, Lehenkari, Kellinsalmi M. 2004. A new mechanism action for bisphosphonates: apppi dedicated cytotoxicity of N-BPs. Bone. 34: S66–S67.

Neville-Webbe HL, Rostami-Hodjegan, Evans CA, Coleman RE, Holen I. 2005. Sequence- and schedule-dependent enhancement of zoledronic acid induced apoptosis by doxorubicin in breast and prostate cancer cells. Int J Cancer 113: 364–371.

Nobuyuki H, Hiraga T, Williams PJ. 2001. The bisphosphonate zoledronic acid inhibits metastases to bone and liver with suppression of osteopontin production in mouse mammary tumor. J Bone Miner Res. 16: S191

Nurse P. 1990. Universal control mechanism regulating onset of M-phase. Nature. 344: 503–508.

Ottewell PD, Mönkkönen H, Jones M, Lefley DV, Coleman RE, Holen I. 2009. Antitumor effects of doxorubicin followed by zoledronic acid in a mouse model of breast cancer. J Natl Cancer Inst. 100: 1167-78.

Ougolkov AV, Fernandez-Zapico ME, Bilim VN, Smyrk TC, Chari ST, Billadeau DD. 2006. Aberrant nuclear accumulation of glycogen synthase kinase-3β in human pancreatic cancer: association with kinase activity and tumor dedifferentiation. Clin Cancer Res. 12: 5074-81

Ougolkov AV, Fernandez-Zapico ME, Bilim VN, Smyrk TC, Chari ST, Billadeau DD. 2006. Aberrant nuclear accumulation of glycogen synthase kinase-3β in human pancreatic cancer: association with kinase activity and tumor dedifferentiation. Clin Cancer Res. 12: 5074-81

Peyruchaud O, Winding B, Pécheur I, Serre CM, Delmas P, Clézardin P. 2001. Early detection of bone metastases in a murine model using fluorescent human breast cancer cells: application to the use of the bisphosphonate zoledronic acid in the treatment of osteolytic lesions. J Bone Miner Res. 16: 2027-2034.

Pollard M, Luckert PH. 1985. Effects of dichloromethylene diphosphonate on the osteolytic and osteoplastic effects of rat prostate adenocarcinoma cells. J Natl Cancer Inst. 75: 949-954.

Ramnath N, Creaven P. 2004. Matrix metalloproteinase inhibitors. Curr Oncol Rep. 6: 96–102.

Rao A, Luo C, Hogan PG. 1997. Transcription factors of the NFAT family: regulation and function. Annu Rev Immunol. 15: 707-747.

Rodriguez MS, Dargemont C, Hay RT. 2001. SUMO-1 conjugation in vivo requires both a consensus modification motif and nuclear targeting. J. Biol. Chem. 276: 12654–12659.

Rogers MJ. 2003. New insights into the molecular mechanisms of action of bisphosphonates. Curr Pharm Design. 9: 2643–2658.

Rubinfeld B, Albert I, Porfiri E, Fiol C, Munemitsu S, Polakis P. 1996. Binding of GSK3β to the APC-β-catenin complex and regulation of complex assembly. Science. 272: 1023–1026.

Santini D, Vincenzi B, Dicuonzo G, Avvisati G, Massacesi C, Battistoni F, Gavasci M, Rocci L, Tirindelli MC, Altomare V, Tocchini M, Bonsignori M, Tonini G. 2003. Zoledronic acid induces significant and long-lasting modifications of circulating angiogenic factors in cancer patients. Clin Cancer Res. 9: 2893-2897.

Sasaki A, Boyce BF, Story B. 1995. Bisphosphonate risedronate reduces metastatic human breast cancer burden in bone in nude mice. Cancer Res. 55: 3551-3557.

Sato M, Grasser W, Endo N. 1991. Bisphosphonate action. Alendronate localization in rat bone and effects on osteoclast ultrastructure. J Clin Invest. 88: 2095-2105.

Savage AD, Belson DJ, Vescio RA, Lichtenstein AK, Berenson JR. 1996. Pamidronate reduces IL-6 production by bone marrow stroma from muliple myeloma patients. Blood. 88:105.

Seidensticker MJ, Behrens J. 2000. Biochemical interactions in the wnt pathway. Biochim Biophys Acta 495: 168–182.

Senaratne SG, Pirianov G, Mansi JL, Arnett TR, Colston KW. 2000. Bisphosphonates induce apoptosis in human breast cancer cell lines. Br. J. Cancer. 82:1459–1468.

Senaratne SG, Pirianov G, Mansi JL, Arnett TR, Colston KW. 2000. Bisphosphonates induce apoptosis in human breast cancer cells. Br J Cancer. 82: 1459-1468.

Seufert W, Futcher B, Jentsch S. 1995. Role of a ubiquitin-conjugating enzyme in degradation of S- and M-phase cyclins. Nature. 373: 78-81

Sewing L, Steinberg F, Schmidt H, Göke R. 2008. The bisphosphonate zoledronic acid inhibits the growth of HCT-116 colon carcinoma cells and induces tumor cell apoptosis. Apoptosis. 13: 782-789

Shibasaki F, Price ER, Milan D, McKeon F. 1996. Role of kinases and the phosphatase calcineurin in the nuclear shuttling of transcription factor NF-AT4 382: 370-3.

Shipman CM, Croucher PI, Russell RGG, Helfrich MH, Rogers MJ. 1998. The bisphosphonate incadronate (YM175) causes apoptosis of human myeloma cells in vitro by inhibiting the mevalonate pathway. Cancer Res. 58: 5294-5297.

Shipman CM, Rogers MJ, Apperley JF, Russell RGG, Croucher PI. 1997. Bisphosphonates induce apoptosis in human myeloma cell lines: a novel anti-tumor activity. Br J Haematol. 98: 665-672.

Stearns ME, Wang M. 1996. Effects of alendronate and taxol on PC-3ML cell bone metastases in SCID mice. Invas Metastasis. 16: 116-131.

Stearns ME, Wang M. 1996. Effects of alendronate and taxol on PC-3 ML cell bone metastases in SCID mice. Invasion Metastasis 16: 116–131.

Takahashi R, Shimazaki C, Inaba T. 2001. A newly developed bisphosphonate, YM529, is a potent apoptosis inducer of human myeloma cells. Leukemia Res. 25: 77-83.

Tassone P, Forciniti S, Galea E. 2000. Growth inhibition and synergistic induction of apoptosis by zoledronate and dexamethasone in human myeloma cell lines. Leukemia. 14: 841-844.

Tassone P, Tagliaferri P, Galea E, Palmieri C, Viscomi C, Venuta S. 2002. Growth inhibition and apoptosis are induced by zoledronic acid on human pancreatic cancer cell lines. Proc Am Ass Cancer Res. 43: 956-957.

Tassone P, Tagliaferri P, Viscomi C, Palmieri C, Caraglia M, Alessandro AD, Galea E, Goel A, Abbruzzese A, Boland CR, Venuta S. 2003. Zoledronic acid induces antiproliferative and apoptotic effects in human pancreatic cancer cells in vitro. Br J Cancer. 88: 1971–1978.

Terui Y, Saad N, Jia S, McKeon F, Yuan J. 2004. Dual role of sumoylation in the nuclear localization and transcriptional activation of NFAT1. J Biol Chem. 279: 28257-65.

Ullen A, Lennartsson L, Hjelm-Eriksson M, Kalkner KM, Lennernas B, Nilsson S. 2003. Additive/synergistic anti-tumoral effects on prostate cancer cells in vitro following treatment with a combination of gemcitabine and zoledronic acid. Proc Am Soc Clin Oncol. 22: 432

van Beek E, Pieterman E, Cohen L, Lowik C, Papoulos C. 1999. Nitrogen-containing bisphosphonates inhibit isopentyl pyrophosphate

isomerase/farnesyl pyrophosphate synthase activity with relative potencies corresponding to their antiresorptive potencies in vitro and in vivo. Biochem. Biophys. Res. Commun. 255 : 491–494.

van der Pluijm G, Vloedgraven H, van Beek E, van der Wee-Pals L, Löwik C, Papapoulos S. 1996. Bisphosphonates inhibit the adhesion of breast cancer cells to bone matrices in vitro. J Clin Invest. 98: 698-705.

van der Pluijm G, Vloedgraven H, van Beek E, van der Wee-Pals L, Löwik C, Papapoulos S. 1996. Bisphosphonates inhibit the adhesion of breast cancer cells to bone matrices in vitro. J Clin Invest. 98: 698-705.

Verdidk R, Franke HR, Wolbers FR, Vermes I. 2007. Differential effects of bisphosphonates on breast cancer cell lines. Cancer Lett. 246: 308-312.

Virtanen SS, Väänänen HK, Härkönen PL, Lakkakorpi PT. 2002. Alendronate inhibits invasion of PC-3 prostate cancer cells by affecting the mevalonate pathway. Cancer Res. 62: 2708-2714.

Vogelstein B, Lane D, Levine AJ. 2000. Surfing the p53 network. Nature 408: 307-10.

Vogt U, Bielawski KP, Bosse U, Schlotter CM. 2004. Breast tumor growth inhibition in vitro through the combination of cyclophosphamide/ metotrexate/ 5-fluorouracil, epirubicin/ cyclophosphamide, epirubicin/ paclitaxel, and epirubicin/docetaxel with the bisphosphonates ibandronate and zoledronic acid. Oncol Rep. 12: 1109–1114.

Wang QM, Fiol CJ, DePaoli-Roach AA, Roach PJ. 1994. Glycogen synthase kinase-3 β is a dual specificity kinase differentially regulated by tyrosine and serine/threonine phosphorylation. J Biol Chem 269: 14566–14574.

Yaccoby S, Pearse RN, Johnson CL, Barlogie B, Choi Y, Epstein J. 2002. Myeloma interacts with the bone microenvironment to induce osteoclastogenesis and is dependent on osteoclast activity. Br J Haematol. 116: 278-290.

Yu-Cheng S, Geldof AA, Newling DW, Rao BR. 1992. Progression delay of prostate tumor skeletal metastasis effects by bisphosphonates. J Urol. 148: 1270-1273

Zeng X, Huang H, Tamai K, Zhang X, Harada Y, Yokota C. 2008. Initiation of Wnt signaling: control of Wnt coreceptor Lrp6 phosphorylation/activation via frizzled, dishevelled and axin functions. Development 135: 367–375.

7 ABBREVIATIONS

aa	Amino acid
Ab	Antibody
AP1	Activating protein-1
APS	Ammonium per sulfate
ATCC	American type culture collection
bp	Base pair
BPs	Bisphosphonates
BSA	Bovine serum albumine
CaCl2	Calcium chloride
c.a.	Constitutive active
CBP	CREB binding protein
CDK	Cyclin dependent kinase
CK-1	Casein kinase-1
CsA	Cyclosporin A
DAPI	4’,6-Diamidino-2-phenylindole
DBD	DNA binding domain
DMEM	Dulbecco´s Modified Eagle Medium
DMSO	Dimethylsulfoxide
DNA	Deoxyribonucleic acid
Dnase	Deoxyribonuclease
DTT	1,4 Dithiothreitol
E1	SUMO or ubiquitin activating enzyme
E2	SUMO or ubiquitin conjugating enzyme
E3	SUMO or ubiquitin ligase
E.coli	Escherichia coli
EDTA	Ethylene-diamine-tetra-acetic

E2F	Electro-acoustic 2 Factor
FCS	Fetal calf serum
G1	Gap1
GFP	Green fluorescent protein
GSK3	Glycogen synthase kinase 3
GTP	Guanosine tri-phosphate
HA	Hemagglutinin
HDAC	Histone deacetylase
HEPES	Hydroxyethyl-piperazineethanesulfonic acid
HRP	Horse readish peroxidase
IB	Immunoblot
IgG	Immunoglobulin G
IkB	Inhibitor of NFkB
IP	Immunoprecipitation
IL	Interleukin
JNK	Junc-Kinase
K	Lysin
kb	kilobases
kD	kilo dalton
LB-medium	Luria-Bertani medium
LiCl	Lithium chloride
$MgCl_2$	Magnesium chloride
MAPK	Mitogen activated protein kinase
MMP	Matrix metalloprotease
NaCl	Sodium chloride
N-BPs	Nitrogen contaning-bisphosphonates
NES	Nuclear export signal
NFAT	Nuclear factor of activated T-cell
NLS	Nuclear localization signal

NEM	N-ethylmaleimide
PCR	Polymerase chain reaction
Pi3K	Phosphoinositol 3 kinase
PML	Promyelocytic Leukemia protein
PMSF	Phenylmethylsulfonylfluorid
Rb	Retinoblastoma protein
RLU	Relative luciferase unit
rpm	Rounds per minute
RNA	Ribonuclic acid
RT	Room temperature
S-phase	Synthesis phase
SDS	Sodium dodecyl sulphate
SUMO	Small ubiquitin like modifier
TE	Tris-EDTA
TEMED	N, N, N', N'-tetramethylethylenediamine
Ub	Ubiquitin
ZOL	Zoledronic acid

8 ACKNOWLEDGMENTS

I take this opportunity to thank all those people who helped me directly or indirectly during the journey of completing my dissertation. I feel obliged and indebted to so many people, who influenced and shaped my present. This long venture was possible only because of the love, affection and guidance of the people who were with me all throughout the study.

I take this opportunity to acknowledge my mentor, my supervisor PD. Dr. Volker Ellenrieder, who has been an ideal since the day I joined in the Department of Gastroenterology and Endocrinology for my PhD. I express my sincere gratitude and regards to him for his ingenious advice, deep concern, obtrusive criticism and intelligence throughout the tenure of this study. I always appreciated his intelligence and ability to handle the most difficult situations in a very patient manner. His serene behavior and his thoughtful provoking discussions were always used to leave me encouraged and mesmerized. He has been a guide in every sense. I wish to thank him for providing excellent lab facilities, good working atmosphere and valuable guidance in time of need.

I would like to thank Prof. Dr. Thomas Gress for the permanent encouragements and stimulative scientific discussions.

Here I wish to express my gratefulness to Prof. Dr. Lorenz C. Hofbauer for supporting me constantly ever since we met and for his confidence in all my actions.

I sincerely acknowledge Mrs. Flügel Michel for her affection and hearty co-operation during this study. I would like to profoundly thank for her unconditional help.

I would like to say a sincere thank to my lab colleagues, Jehona Dittrich, Benjamin Kühnemuth, Eva Bug and Thomas Linhart for the nice and friendly atmosphere given during my PhD work.

I would like to say “Dankeschön”, to Elisabeth Glesel and Leonie Hofmann for correcting my thesis and helping me in the lab.

I also want to give my sincere thank to Dr. Malte Buchholz and Harald Schmidt for being always beside me, with small tips and tricks, which made the life in the lab agreeable.

I am also deeply appreciative to Kristina Reutlinger for her kind-heartedness and constant technical support in the lab, which was very helpful for me to complete my thesis.

How can I forget to acknowledge and thank Sandra Dobes, for her timely help during my research work.

My special thanks to Dr. Alex König and Dr. Ute König for correcting my thesis and their support and help was always there throughout my PhD work.

My truthful appreciation to some of my friends, Till Adhikary, Srikanth Karnati, Manvi Porwal, Sachin Kumar, Vijay Renigunta and Tilmann Rachner, for all those scientific discussions about my project.

My bottomless gratitude belong to Dr. Uday Kishore, who always encouraged me and offered me his tireless care throughout my scientific journey.

I want to express my gratitude and regards to my parents-in-law for their support and words of encouragement and appreciation, throughout my research work. I want to acknowledge my brother in law, Gaurav for his support and refreshing sense of humour.

Words are not enough to express my grateful appreciation for my parents. It is their endless support, love, patience, inspiration, affection and encouragement that have made this possible. My mother's confidence in me shaped my dreams and aspiration into reality. I want to affectionately acknowledge the immense help of my younger brothers, Amit and Ajit throughout this long tenure of study.

I want to acknowledge with great appreciation my loving and caring wife, Garima, for her positive energy and outlook. Her temperament, ideas, patience, unique ways of concern, sensitivity, unusual ways of appreciation and her dependence on me made me strong in the endeavors of research. I also want to thank her for her efforts in compiling and proof reading during the final phase of study work.

9 CURRICULUM VITAE

Mr. Shiv Kishor Singh

Signal Transduction & Transcription Laboratory

Dept. of Gastroenterology & Endocrinology,

Philipps-University,

Baldingerstrasse

D-35043 Marburg,

Germany

Tel.: +49 6421 5862782

Fax: +49 6421 5868922

Email: singhsh@staff.uni-marburg.de

Education:

Master of Science in Biochemistry from Bundelkhand University, Jhansi (India), in year 2004.

Bachelor of Science from St. Andrews College, Deen Dayal Upadhyay Gorakhpur University, Gorakhpur (India), 2000 .

Awards and Honors:

Travel award by **"Salk Institute"** for participation in the 2nd Salk Institute Mechanisms & Model of Cancer meeting held at Salk Institute for Biological Studies, La Jolla, CA, USA.

First poster prize at Bundelkhand University on "**National Science Day Functions**" Jhansi, India.

Oral and poster presentation:

SK Singh, E. Glesel, G. Singh, TM Gress and V. Ellenrieder. Nucleosomal Architecture of NFATc2 Mediated Repression. Accepted for Poster presentation in "*German Gastroenterology Meeting*" held at Hamburg, Germany from 30th September to 3rdOctober 2009.

SK Singh, G. Singh, A. König, K. Reutlinger, G. Suske, LC Hofbauer, TM Gress and V. Ellenrieder. The Antitumor Effects of Zoledronic acid Are Mediated by HDM2 Induced Proteasomal Degradation Of Oncogenic NFATc2. Accepted for poster presentation in *"2nd Salk Institute Mechanisms & Model of Cancer meeting"* held at Salk Institute for Biological Studies, La Jolla, CA, USA from 12th - 16th August 2009.

SK. Singh, G. Singh, A. König, E. Glesel, K. Reutlinger, G. Suske,TM Gress and V. Ellenrieder. Zoledronic Acid Exerts Anti-Tumerigenic Functions Through HDM2 Mediated Proteasomal Degradation of Oncogenic NFATc2. Accepted for poster presentation in *"Transcription and Cancer meeting"* held at Churchill College, University of Cambridge, UK from 8th - 10th July 2009.

SK Singh, G. Singh**,** A. König, K. Reutlinger, G. Suske, LC Hofbauer, TM Gress and V. Ellenrieder. The Antitumor Effects Of Zoledronic acid Are Mediated by HDM2 Induced Proteasomal Degradation of Oncogenic NFATc2. Accepted for poster presentation in *"The Ubiquitin Family"* meeting held at Cold Spring Harbor Laboratory, Cold Spring Harbor, NY, USA from 21st - 25th April 2009.

Accepted for oral presentation on the topic " Zoledronic acid inhibits cell proliferation and induces apoptosis in estrogen receptor-negative breast cancer cells" presented in *9th annual meeting YOUNG ACTIVE RESEARCH* held at Lübeck, Germany from 1st to 3rd October 2007.

G. Singh, **SK Singh**, A. König, K. Reutlinger, TM Gress and V. Ellenrieder. A novel NFAT-Smad3 interplay mediates TGF-β switch from a growth suppressor to a growth promoting pathway. Accepted for poster presentation in *"2nd Salk Institute Mechanisms & Model of Cancer meeting"* held at Salk Institute for Biological Studies, La Jolla, CA, USA from 12th - 16th August 2009.

G. Singh, **SK Singh**, A. König, K. Reutlinger, TM Gress and V. Ellenrieder. NFAT mediate TGF-β switch from a growth suppressor to a promoter of cell proliferation. Accepted for poster presentation in *"Transcription and Cancer meeting"* held at Churchill College Cambridge", UK from 8th - 10th July 2009.

G. Singh, **S.K. Singh**, A. König, K. Reutlinger, T.M. Gress, Martin E. Fernandez-zapico and V. Ellenrieder. NFAT and c-Myc at the core of TGF-β induced pancreatic cancer cell growth. Accepted for poster presentation in *"39th Annual meeting of American pancreatic association"* Chicago, USA from 3rd - 7th November 2008.

List of publications

Tilman D. Rachner, **Singh SK**, Michael Schoppet, Volker Ellenrieder, Regina Ebert, Franz J. Jakob and Lorenz C. Hofbauer. 2009. Zoledronic Acid Induces Apoptosis and Changes the TRAIL/OPG Ratio in Breast Cancer Cells. (In Press in Cancer Letters). Note: Tilman D. Rachner, **Singh SK** contributed equally.

Tilman D. Rachner, Peggy Benad, Martina Rauner, Claudia Goettsch, **Singh SK**, Michael Schoppet and Lorenz C. Hofbauer. 2009. Osteoprotegerin production by breast cancer cells is suppressed by dexamethasone and confers resistance against TRAIL-induced apoptosis. J Cell Biochem.108: 106-16

Mamta Singh, Taruna Madan, PatrickWaters, Sanchaita Sonar, **Singh SK**, Mohammad F. Kamran, Andrés López Bernal, P. Usha Sarma, Vijay K. Singh, Erika C. Crouch, Uday Kishore. 2009. Protective effects of recombinant forms of full-length and truncated human surfactant protein D inmurine model of invasive pulmonary aspergilllosis. Mol Immunol. 46: 2363-9.

Hofbauer LC, Rachner T, **Singh SK**. 2008. Fatal attraction: why breast cancer cells home to bone. Breast Cancer Res.10: 101.

Muyal JP, **Singh SK**, Fehrenbach H. 2008. DNA-microarray technology: comparison of methodological factors of recent technique towards gene expression profiling. Crit Rev Biotechnol. 28: 239-51

Hofbauer LC, Brueck CC, **Singh SK**, Dobnig H. 2007. Osteoporosis in patients with diabetes mellitus. J Bone Miner Res. 22: 1317-28

Manuscripts under preparation:

Singh SK, S. Dobes, G. Singh, A. König, J. Diettrich, K. Reutlinger, G. Suske, L. Hofbauer, T.M. Gress, M. Fernandez-Zapico, R. Urrutia and V. Ellenrieder. Zoledronic acid targets a phospho-depndent NFATc2 stabilization pathway to supress cancer growth. (*Submitted*)

G. Singh, **Singh SK**, A. König, K. Reutlinger, Martin Eilers, T.M. Gress, Martin E. Fernandez-zapico and V. Ellenrieder. A novel NFAT-Smad interplay mediates TGF-β switch from a suppressor to a growth promoting pathway. (*Revision under JBC*) **Note:** G. Singh, **Singh SK** contributed equally.

Ehrenwörtliche Erklärung

Ich erkläre ehrenwörtlich, dass ich die dem Fachbereich Medizin Marburg zur Promotionsprüfung eingereichte Arbeit mit dem Titel **„Molecular Characterization of Zoledronic acid Induced Growth Inhibition in Cancer “** in der Klinik für Innere Medizin unter Leitung von Herrn Prof. Dr. Thomas Mathias Gress mit Unterstützung durch Prof. Dr. Volker Ellenrieder ohne sonstige Hilfe selbst durchgeführt habe. Bei der Abfassung der Arbeit habe ich keine anderen als die in der Dissertation angeführten Quellen und Hilfsmittel benutzt und vollständig oder sinngemäß übernommene Zitate entsprechend gekennzeichnet. Ich habe bisher weder an einem in- und ausländischen Medizinischen Fachbereich ein Gesuch um Zulassung zur Promotion eingereicht noch eine andere Arbeit als Dissertation oder die vorliegende zu anderen Prüfungszwecken vorgelegt.

Shiv Kishor Singh

Date: 15.04.10

Marburg